DOKUZ EYLÜL UNIVERSITY

GRADUATE SCHOOL OF NATURAL AND APPLIED SCIENCES

INVESTIGATION OF GRANULAR MATERIALS BY ULTRASONIC VELOCITIES

by

Asif ZEB

August, 2017

İZMİR

INVESTIGATION OF GRANULAR MATERIALS BY ULTRASONIC VELOCITIES

A Thesis Submitted to the
Graduate School of Natural and Applied Sciences of Dokuz Eylül University in
Partial Fulfilment of the Requirements for the Masters of Science Degree in
Geological Engineering, Applied Geology Program

by

Asif ZEB

August, 2017

İZMİR

THESIS EXAMINATION RESULT FORM

We have read the thesis entitled **"INVESTIGATION OF GRANULAR MATERIALS BY ULTRASONIC VELOCITIES"** completed by **ASIF ZEB** under supervision of **PROF. DR. NECDET TÜRK** and we can certify that in our opinion it is fully adequate, in scope and in quality, as a thesis for the degree of Master of Science.

.....

Prof. Dr. Necdet TÜRK

Supervisor

Prof. Dr. Halil KUMSAR

(Jury Member)

Prof. Dr. A. Bahadır Yavuz

(Jury Member)

Prof. Dr. Emine İlknur CÖCEN

Director

ACKNOWLEDGEMENTS

I am grateful to my advisor, Prof. Dr Necdet TÜRK for considering my thesis topic and providing me all the support I needed during my research. My growth as a researcher is direct result of his mentorship and support. As a Masters student in Dokuz Eylül Univeristy, I had the opportunity to work in fully equipped laboratories to conduct my thesis work. The experiences I gain during my study groomed my problem-solving skills and helped me in decision making. I am also thankful to my friends and family for their motivation and prayers throughout my study.

I thank Dr. Hakan ELÇİ for giving me useful suggestions and all the help I needed during my research. I am grateful for discussions with Tümay KADAKÇI KOCA who was always willing to listen to my questions.

My time in Turkey was memorable and I want to thank the Government of Turkey for providing me scholarship for Masters study at Dokuz Eylül Univeristy.

Asif ZEB

INVESTIGATION OF GRANULAR MATERIALS BY ULTRASONIC VELOCITIES

ABSTRACT

In this study, measurements of sound velocity of selected granular materials was measured. For this purpose, five different lithologic rocks (andesite, granite, limestone, sandstone and tuff) were studied. Compressional wave velocities (Vp) were measured for both core specimens prepared from the selected rocks and also in aggregates of different sizes produced from the same rocks.

Vp measurements were made directly on the core and cube samples while Vp measurements for aggregates were only read by the ultrasonic instrument under compression. Measurements of Vp, both in rock and in aggregates, were compared with their physical and mechanical properties. It has been found that Vp increases with the increase in size of aggregates.

Keywords: Ultrasonic velocity, compressional wave velocity (Vp), unit weight, density, porosity and void ratio

TANELI CİSİMLERİN ZEMİN ÖZELLİKLERİNİN ULTRASONİK HIZ DEĞERLERİ İLE ARAŞTIRILMASI

ÖZ

Bu çalışmada daneler malzemelerin sıkışma ses hız ilerlemesi ölçümleri (Vp) yapılmıştır. Bu ama için beş farklı litolojide kayaç (andezit, granit, kireçtaşı, kumtaşı ve tüf) ile çalışılmıştır. Vp ölçümleri seçilen kayaçlardan hazırlanan hem karot ve küp örnekleri üzerinde hem de aynı kayalardan üretilen farklı çaplardaki agregalar üzerinde gerçekleştirilmiştir.

Karot ve küp örnekleri ile Vp ölçümleri kolaylıkla yapılabilirken, agrega örnekleri ancak belirli bir yük altında sıkıştırıldığı zaman Vp ölçümleri yapılabilmiştir. Hem kayada hem de agregalarda yapılan Vp ölçümleri onların fiziksel ve mekanik özellikleri ile karşılaştırılmıştır. Agregaların dane çapı artıkça Vp artmaktadır.

Anahtar kelimeler: Ultrasonik hız, kompresyonel dalga hızı (Vp), Birim ağırlık, yoğunluk, porozite ve boşluk oranı

CONTENTS

Page

LIST OF FIGURES

Page

LIST OF TABLES

Page

CHAPTER ONE
INTRODUCTION

1.1 Purpose and Scope

The aim of this study is to measure the ultrasonic velocities in aggregates of different particle sizes produced from the same rock and to determine the parameters affecting the variation of these measurements. For this purpose, rocks with 5 different lithologies were selected. First, core and cube samples were prepared from these rocks for physico-mechanical tests and sound velocity measurements. Then aggregates were prepared at different sizes (0-2, 2-4, 4-8, and 8-10) from the selected rocks, and for both prepared rocks core and cube samples and the aggregates, the physico-mechanical properties and ultrasonic velocity tests were performed.

1.2 Methods of Study

First step involved study of literature about the speed of sound velocity in granular materials.

Second step involved the preparation of thin sections, core and granular samples for physico-mechanical tests, chemical analysis, and sound velocity measurements.

Third step involved petrographic and chemical analysis of rocks selected for the study.

Fourth step involved physico-mechanical and sound velocity progress tests for both core and aggregate specimens of different sizes.

In fifth step, the petrographic and chemical analysis results of the rocks selected for the study and different effects of the physico-mechanical properties of the cube and aggregate samples on the sound velocity progression were evaluated.

1.3 Previous Work

Many scientists worked on seismic wave propagation in the granular material in the past. Different experiments have been conducted in the past to determine the wave speed and wide range of wave speeds are reported.

Two mechanisms for the quarter-power scaling were observed at low pressure by Duffy & Mindlin (1957). This method was applied to a column made from small ball bearings packed into a cubic lattice. A rubber bag enclosed this packing which was evacuated to different degrees leading to isostatic confining pressures. They explained that different diameters of particles cause the variations in the scaling for lower pressures. Their theory is based on the particles of identical numbers. The same method was applied by Hardin & Richart (1963) to the Ottawa sands. They also explained the different effects of water saturation and void fraction on the wave speed. In their study, they found that the wave speed was scaled with confining pressure to the 1/4 power for both dry and wet sands.

Wyllie (1960) measured the effect of porosity of sandstones on the difference between dry and fully water-saturated sandstone velocities. The porosity was minimum when the velocity difference was maximum. Experiments showed that the velocities of dry sandstones and water-saturated sandstones increased with the decrease in porosity and as the amount of cementing material increases that caused decreased in porosity due to which the velocity in dry sandstone and water-saturated sandstone increased.

Fountain (1980) explained velocity difference between saturated and dry samples was very large for lower porosities but small for porosities more than 10 %. The Wyllie's time-average equation described the variation of Vp of basalt samples as a porosity function. This study demonstrated that in the oceanic crustal rocks, the porosities between 0-25 percent significantly reduced compressional wave velocities.

Han et al. (1986) studied 75 different samples of sandstone and concluded that porosities range from 2 - 30 percent and the clay contents from 1 - 50 percent were linearly related to water-saturated sandstones (shaly), compressional and shear velocity. The effects of clay content and porosity on the shear velocity were larger than on the compressional velocity. In sandstones, the pore fluid (water) increased the bulk modulus while decreased the shear modulus of clays. Water-saturated clays increased the stiffness of grain contacts in poorly consolidated sandstones.

Goddard (1990) explained the variations in the pressure scaling. Goddard tried to explain that the interaction between particles dominated by the conical asperities and the other explanation was based on macroscopic effects. For Hertzian effect, the wave speed scaling with pressure should be $c \sim p^{1/6}$ (coordination number is the scaling at differents pressures). According to Goddard, the pressure increase caused the increase in coordination number ($c \sim p^{1/6}$). The coordination number argument for the scaling of pressure transitions was supported by Makse et al. (1999).

Sun et al. (1991) investigated elastic wave velocity in liquid saturated porous rocks. They concluded that in liquid-saturated porous rocks, time-average equation is dependent on high porosity intervals. For different fluids, there were significant velocity changes which they observed by seismic response.

Liu & Nagel (1993) investigated vibrations at low-amplitude in dry unconsolidated granular media. They found that if the amplitude of the vibrations increased, the nonlinearity was observed near the point at which the hysteretic behavior first seen.

Ben-Dor et al. (1997) studied the granular bed and its interaction with shock wave. They took a long shock tube and created a granular bed at its end. They observed that their transmitted waves were very similar to the waves encountered but there were some doubts about their similarity. Different waves were generated by the impact of shock led. Pressure traces helped them to identify each wave such as compaction wave, transmitted wave and weak refraction wave. The data they collected can be doubtful because the air pressure did also interfere in the pressure measured by different sensors.

Jia et al. (1999) used ultrasonic waves to study wave propagation in stressed granular glass beads. They studied the phenomenon of wave propagation passing through the effective wavelength of granular media in a frequency range that was comparable to the size of grain. Based on their study, they identify two different waves which they named as E (P) and S waves. The effective wavelength of E (P) wave was larger than the particle size. The frequency of E wave was much lower than the S wave. The structure of S wave was irregular. This irregular structure of S wave caused the multiple scattering and interference in the granular media.

Bonner et al. (2002) used ultrasonic pulse transmission method (100-500 kHz) to measure Vp and Vs for synthetic soils. In their study, they determined the velocities by loading the sample under small uniaxial stress. For the 10% clay-sand sample, 3 waveforms plotted at the same scale (zero gauge units, 7.8 and 15.6 psi) are shown in Figure 1.1. With small uniaxial loads, dramatic increase occured in all velocities, indicating strong nonlinearity of the acoustic properties.

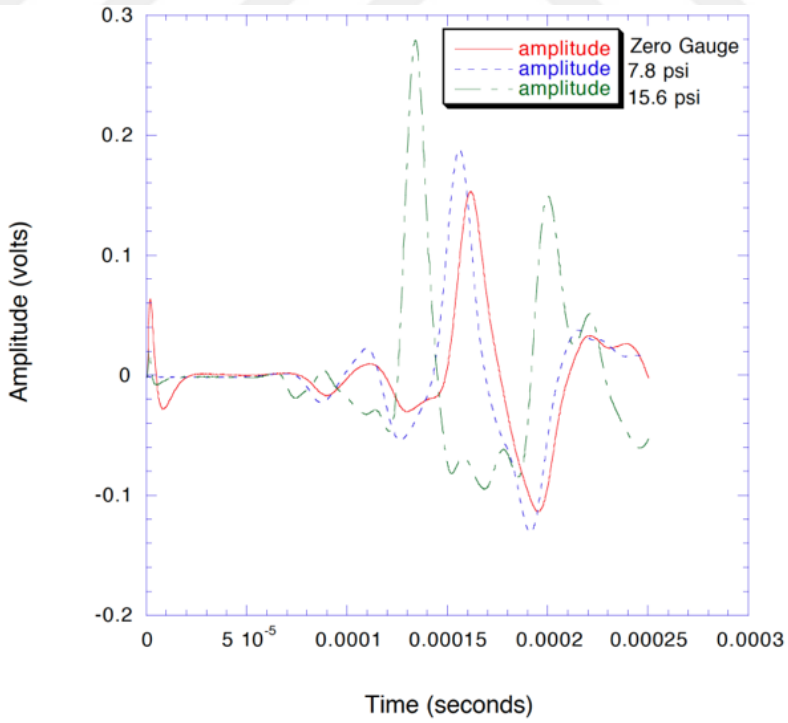

Figure 1.1 Waveforms for 10 % clay, 90 % sand sample for 3 different load values of F-50 Dry Ottawa Sand (Boner et al., 2002)

Tyler et al. (2004) used different approach by focusing on ultrasonic waves generated due to friction by granular materials. They also tried to provide alternatives real-time geotechnical ground condition monitoring applications to evaluate ultrasonic monitoring of drilling. The sound signal was used as a tool characterize the material properties of the friction pair. A simple arrangement for drilling was used in which rotating probe increased the friction at probe-tip-granular contact.

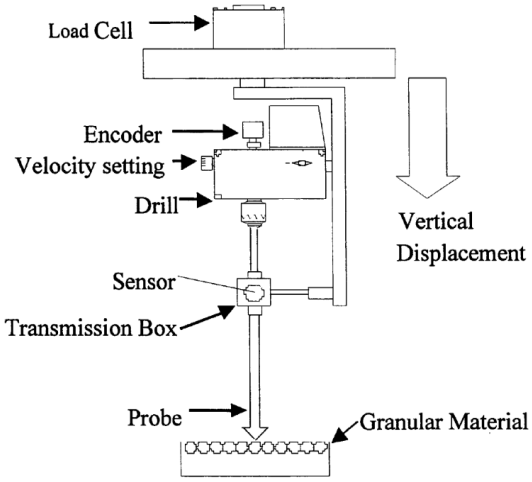

Figure 1.2 Schematic diagram of probing apparatus (Tyler et al., 2004)

From their research, Tyler et al. (2004) concluded that ultrasonic signals were sensitive to various parameters like sliding velocity, density, load, mineralogy and particle size.

Hamada (2004) found that the saturating fluid type had a great effect on compressional wave. To identify fluid type, the use of the ratio of Vp/Vs was a good tool. Due to the decrease of rock density of reservoir rocks, the compressional wave velocity also decreased.

Verwer & Braaksma (2009) suggested that for the carbonate samples, time average equation for velocity-porosity transform described observed trends of sound velocity but significantly underestimated velocity due to the presence of magmatic minerals in the matrix of carbonate- volcanoclastic sedimentary rocks. Their findings underlined that the acoustic behavior was more complex in mixed carbonate- volcanoclastic

sedimentary rocks than in pure carbonates and pure siliciclastic, where the observed relationships between porosity and acoustic velocity were explained by the rock texture and mineralogical composition.

Griffiths et al. (2010) observed the effect of interstitial fluid on acoustic propagation. Various velocity measurements and ultrasonic wave transmission were observed to be dependent on the type of interstitial fluid. The viscosity was increased by silicon oils to show that according to power law 1/6, there was no effect on wave velocity by increasing viscosity. The coefficient of transmission increased with the viscosity. Their experiment explained that in dry case, transmission coefficient increased strongly while velocity remained the same.

Sikora & Turkiewicz (2010) performed different experiments to get knowledge about the sound absorption readings of different granular materials. They took different materials for their experiment and one of them was high-silica sand. The bulk volume of that sand was 1440 kg/m^3, grain size was 1-2 mm and shape of the grain was oval and irregular. They concluded that the frequency bands in which the absorption of greatest sound occurred, in narrow and wide bands the granular materials may be divided.

Knuth et al. (2013) presented the results from ultrasonic wave propagation to study elastic properties during shear. Ultrasonic velocity and density increased by applying load.

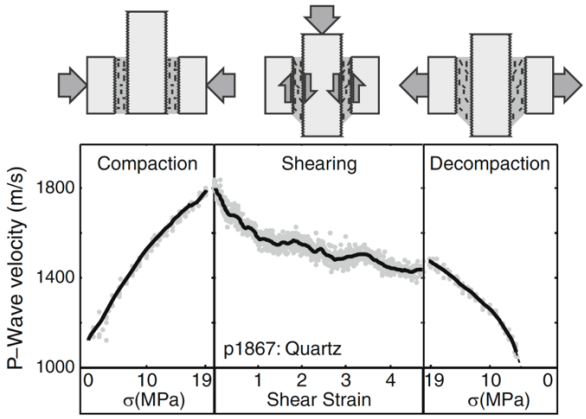

Figure 1.3 P-wave velocity measurement during a full shear experiment, showing application of normal load, shear, and removal of normal load (M. Knuth et al., 2013)

Mandal et al. (2014) studied cementitously stabilized materials (CSM) using ultrasonic pulse velocity techniques. These CSMs were clay-cement, sand-cement, gravel-cement and different types ashes. The Vp decreased with decreasing density of the sample, whereas Vp increased when the binder content and curing time increased which means more the proportion of cement (compaction) in the sample, more would be the Vp.

Wang et al (2015) explained the pore structure complexity, the relationship between porosity and P-wave velocity in carbonate rocks showed a great variability. This variability introduced high uncertainties to seismic inversion, amplitude variation with offset analysis, porosity estimation, and pore-pressure prediction based on velocity data.

Marwah (2017) calculated velocity and found out that Wyllie's time- average equation is directly proportional to the density and by linking the Newton-Laplace equation to Wyllie's equation, derived a new equation for elastic modulus. By new equation for elastic modulus, the inconsistency was clarified.

Mahdevari & Maarefvand (2017) evaluated the volumetric block proportion of block-in-matrix rocks (bimrocks). They also determined P wave and S wave velocity of the aggregate by using the Pundit Lab plus ultrasonic instrument. They concluded that velocity of P-wave for coarse aggregate samples was more than the fine aggregates and they did not observe any specific trend dominant for variation in P and S wave velocity against the maximum block size.

CHAPTER TWO
SAMPLE PREPARATION

2.1 Introduction

Five rock types have been studied in this thesis; Andesite, Granite, Limestone, Sandstone and Tuff. The samples have been tested in both intact and aggregate form.

2.2 Location of Samples

2.2.1 Andesite (A)

One of the five samples used in this study was Andesite located in Yunt mount, Karakılınçlı village, Manisa province. Karakılınçlı village is present in the Manisa province. The coordinates of the Karakılıçlı Village are 38 ° 36 '50.5188' 'North and 27 ° 25' 46.4232 'East.

2.2.2 Granite (G)

Many published work on the magmatic rocks or intrusive igneous rocks of the Western Anatolia had been done in the past but due to diverse views and models, they are commonly contradicting. Altunkaynak & Yılmaz (1998) published their work related to the Mount Kozak from where granite is taken for this study. The Mount Kozak is an igneous complex located close to the towns of Ayvalık, Bergama and Burhaniye in the Western Anatolia, Turkey. During the Late Oligocene–Early Miocene, magmatic activity occurred. According to Altunkaynak & Yılmaz (1998), the Kozak magmatic assemblage is composed of;

- Plutonic
- Hypabyssal
- Volcanic associations.

The geochemical and petrographic characteristics of granodiorite and mafic enclaves shows that the Kozak granodiorite is formed due to partial melting of basic magma and then its fractional crystallization (Akal & Helvaci, 1999).

2.2.3 Limestone (LS)

Limstone samples are from the Karaburun area in İzmir. Limestones present in Karaburun Peninsula have great potential to be a good block and crushed stone source for building purposes (Erdoğan, 1990).

2.2.4 Sandstone (SS)

The sandstone sample used in this study is located in Ordu region of Turkey. Terlemez & Yılmaz (1980) conducted detail study of the Ordu region and geological setting of sandstone sample is taken from their research work. In their study, they suggested that sandstone, which is the least visible rock formation in the Mesudiye Formation, is gray and greenish, medium-bedded and fine granular. A large proportion of the grains are of volcanic origin. Generally, granules are rounded, poorly sized, sometimes medium sized. Microscopically altered feldspar fragments are observed which are turned into volcanic rock fragments, augite, biotite, sandstone and trachyte fragments, calcite, iron hydroxide and ferrite opaque minerals.

2.2.5 Tuff (T)

The texture of tuff is generally similar to pumice and both are light in weight. The tuff sample used in this study is from Alaçatı in Izmir. Tuff is a weak rock and lost strength as it undergoes the process of weathering however most of the buildings in Alaçatı area are constructed from tuff because of its isolation properties (Yavuz, 2012).

The location of the above-mentioned samples are shown in Figure 2.1 except the from Ordu.

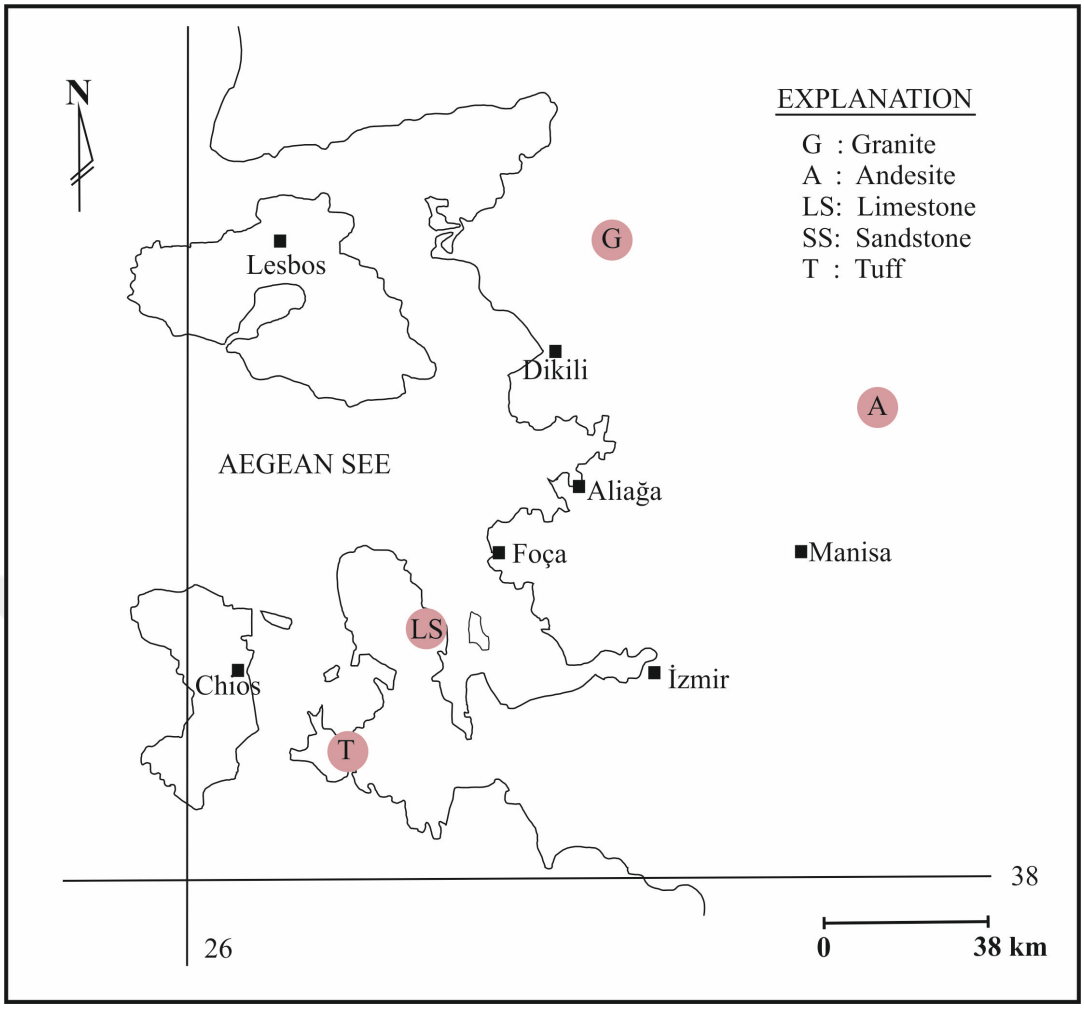

Figure 2.1 Samples Location Map. Sandstone (SS) was taken from Ordu province not located in the above map due to small scale

2.3 Preparation of Core Samples

The rocks for testing were obtained from natural stone factory of the D.E.Ü in Torbalı Vocational School, İzmir. In the laboratory, cores with a diameter of 50 mm were taken from the blocks with a core machine (Figure 2.2). Then, these cores were cut with a stone cutting saw to have a length to diameter ratio of 2 (Figure 2.3) and 5 samples of cores were prepared from each rock (Figure 2.4). Roughing caused by the cutting process was corrected with the help of abrasive disc. In addition, five cube samples were prepared from each rock, using a stone cutting machine, with one side of 70 mm (Figure 2.5).

Figure 2.2 Core samples drilling from block (Personal archive, 2017)

Figure 2.3 Cutting cores to desired diameter (Personal archive, 2017)

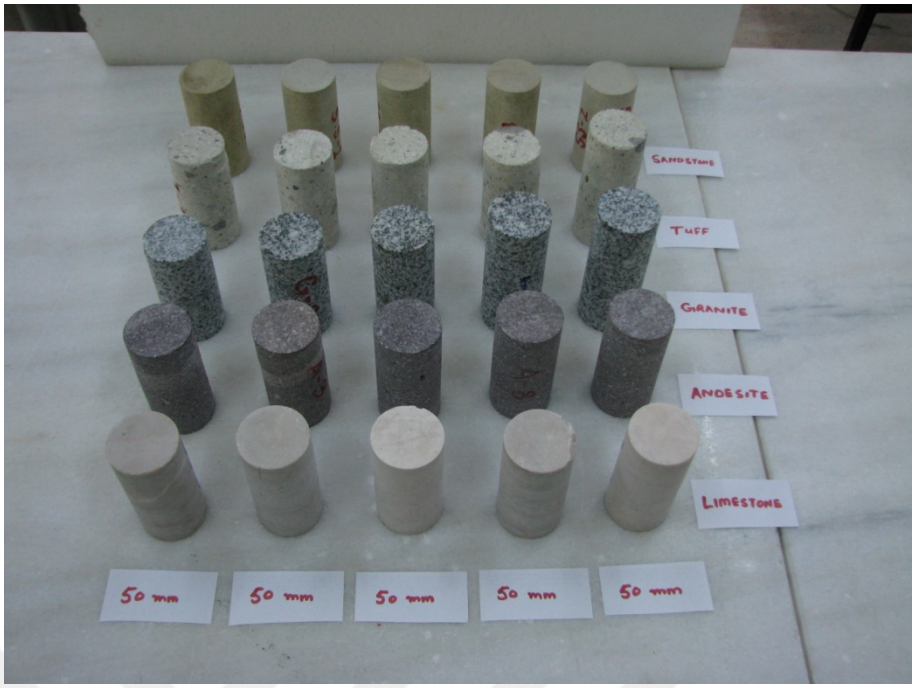

Figure 2.4 Prepared core samples (Personal archive, 2017)

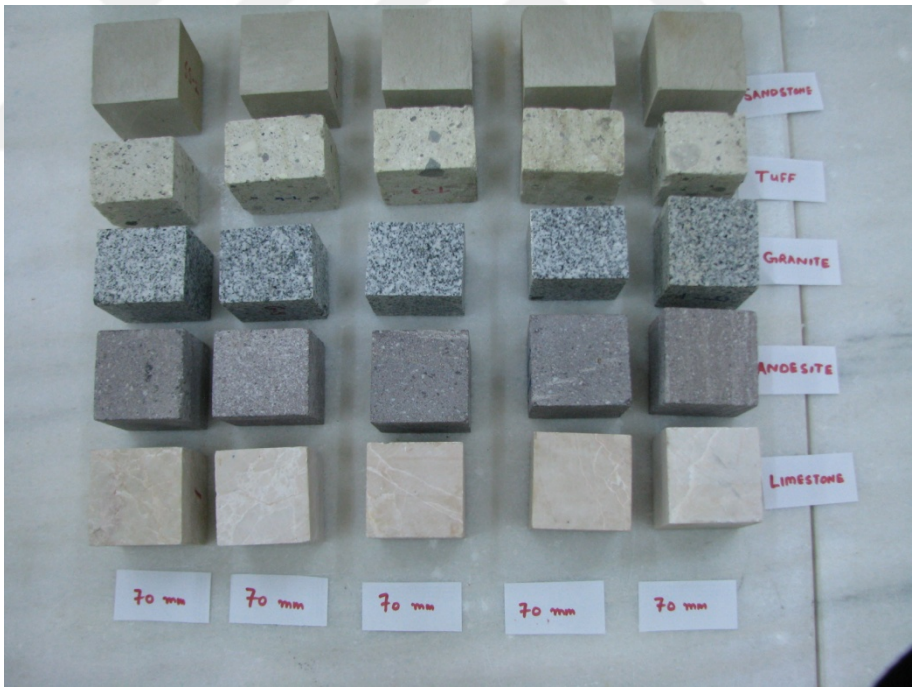

Figure 2.5 Prepared cube samples (Personal archive, 2017)

2.4 Preparation of Aggregate Samples

Block samples were first crushed by a hammer and crushed to 10 cm. 10 cm or smaller pieces were broken into aggregates of different size in the laboratory by jaw crusher (Figure 2.6). These aggregates were sieved by sieve analysis to prepare 5 kg for each samples as 0-2, 2-4, 4-8, 8-10 mm (Figure 2.7).

2.5 Preparation of Thin Section and Chemical Analysis of the Tested Samples

Atleast one thin section was prepared from each rock. Samples of 5x10x3 cm^3 were cut from the rocks for thin sections and a surface was made smooth using abrasive powder and water on the rotating disc. These rock samples were then dried on a hot plate. At the same time, the surface to be glued to the stone is also abraded with the help of water and an abrasive powder and an uneven surfaces still be removed. The dried rock samples were pasted to glass with the aid of araldite and allowed to remained for 2 hours at 60 °C. Then the rocks were cut with a circular saw and thinned to a few mm thickness. Finally, this glass pasted rock was thinned to 15 μm on the rotating disk with the help of water and abrasive powder, In addition, each sample of rock selected for work was 63 μm in size and weighed upto 50 grams for chemical analysis were carried out in ACME laboratories.

Figure 2.6 Preparation of aggregate samples (Personal archive, 2017)

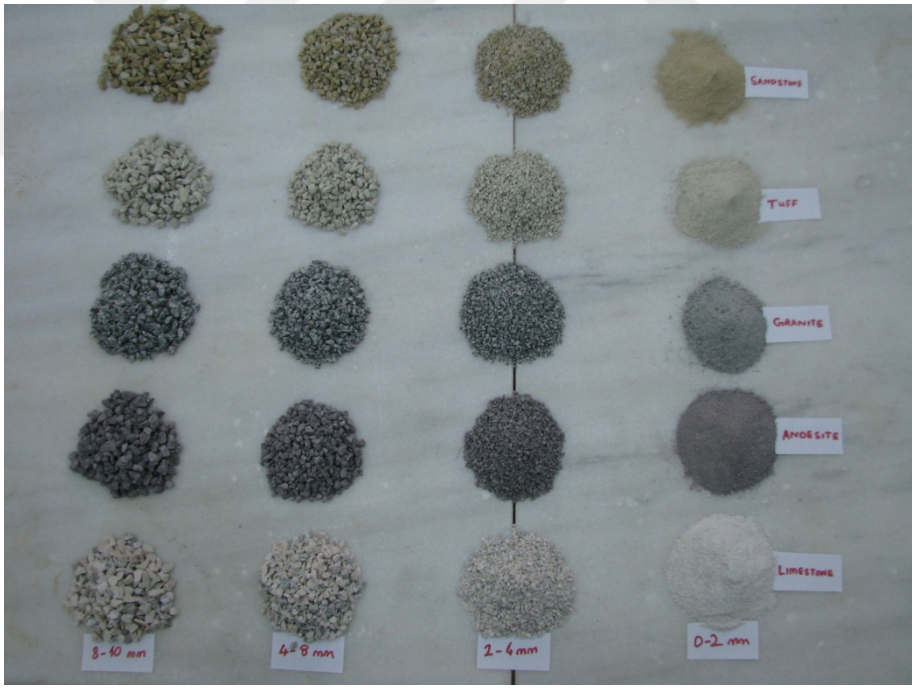

Figure 2.7 Samples of aggregates prepared at different diameters (Personal archive, 2017)

CHAPTER THREE
CHEMICAL AND PETROGRAPHIC PROPERTIES OF ROCK SAMPLES

The rock samples used in this study were investigated on polarized and non-polarized "Olympus BX41 and BX50" type research microscopes. By performing a modal analysis of each rock sample, the minerals forming the rock are presented as a percentage. In addition, each rock sample was subjected to chemical analysis and the major oxide element percentages of the rock are tabulated.

3.1 Andesite

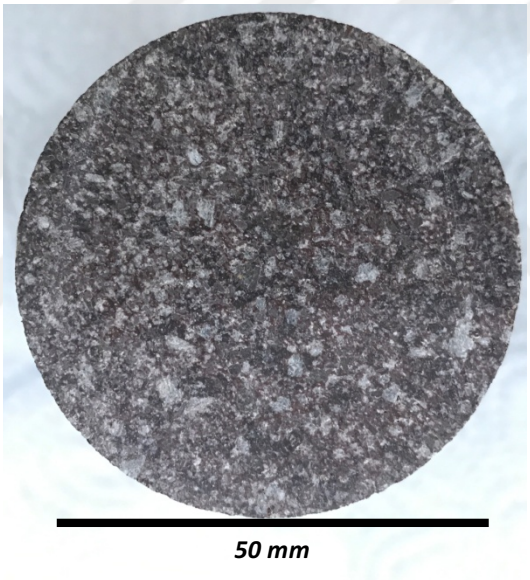

Figure 3.1 Andesite core view perpendicular to core axis (Personal archive, 2017)

Table 3.1 Chemical analysis of Andesite

Major element oxide %										
SiO_2	Al_2O_3	Fe_2O_3	MgO	CaO	Na_2O	K_2O	TiO_2	MnO	*LOI	Total
61.29	16.25	4.08	1.44	5.71	3.79	2.52	0.55	0.123	4.16	99.913

*LOI: Lost on ignition

Macroscopic study showed that the fresh surface colour was brownish red. In the visual appearance, medium-small sub-idiomorphic grains and flow-lava texture can be seen.

Figure 3.2 Macro photos display, a) lava-flow texture, b) fractured surface from the andesite sample

Microscopic study suggested that the rock consists of K-feldspar in high percentage, quartz and plagioclase grains of different sizes with smaller biotite grains. The stone displays a characteristic a hypocrystalline texture.

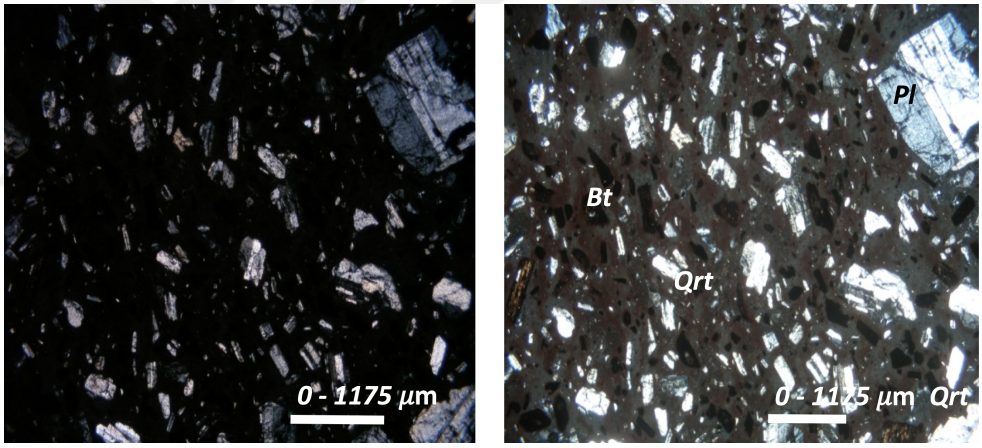

Figure 3.3 Thin section photos a) cross-polar view, b) parallel polar view represents typical hypocrystalline texture. Pl: Plagioclase, Qrt: Quartz. Bt: Biotite

Table 3.2 Mineral percentage in Andesite

Mineral	**%**
K-feldspar	23
Quartz	2
Plagioclase	47
Biotite	5
Others(Matrix)	23
Total	100

3.2 Granite

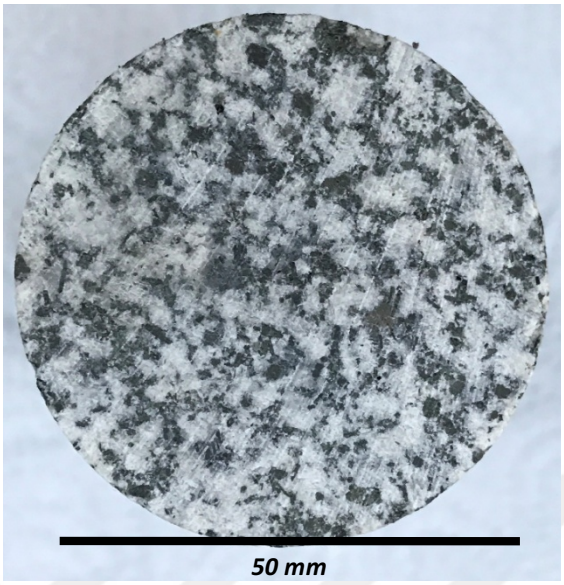

Figure 3.4 Granite core view perpendicular to core axis (Personal archive, 2017)

Table 3.3 Chemical analysis of Granite

Major element oxide %								
SiO_2	Al_2O_3	Fe_2O_3	MgO	CaO	Na_2O	K_2O	*LOI	Total
59.75	17.25	5.92	1.98	4.22	3.04	5.95	1.40	99.49

*LOI: Lost on ignition

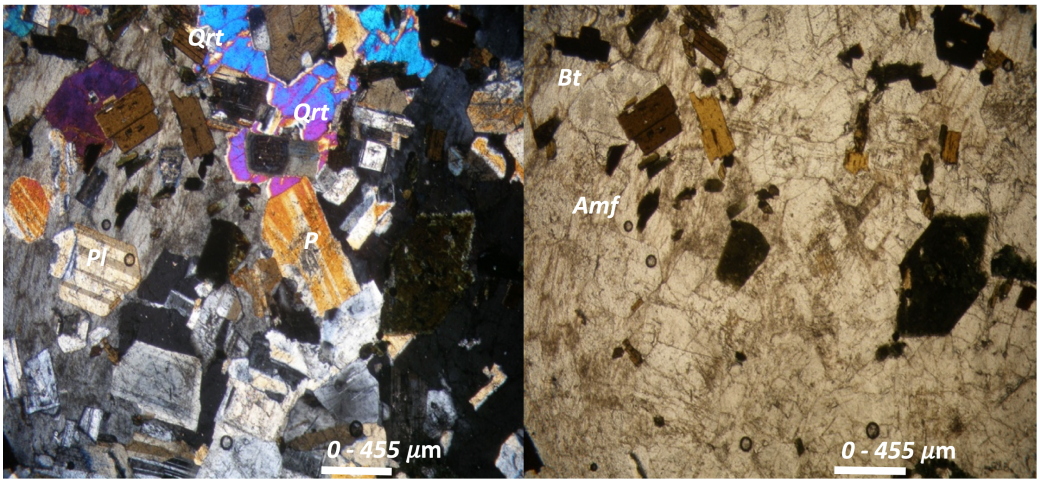

Figure 3.5 Thin section of Granite rock. Pl: Plagioclase, Qrt: Quartz. Bt: Biotite. Amf: Amphibole

Thin section of granite shows the presence of minerals such as quartz, hornblende, plagioclase, biotite and orthoclase.

Table 3.4 Mineral percentage in Granite rock

Mineral	**%**
Plagioclase	34-53
Feldspar	24-35
Quartz	21-29
Biotite	5-10
Amphibole	3-8
Total	100

3.3 Limestone

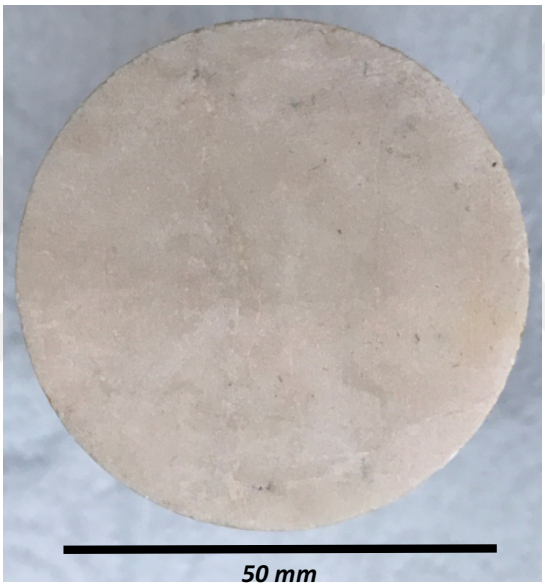

Figure 3.6 Limestone core view perpendicular to core axis (Personal archive, 2017)

Table 3.5 Chemical analysis of Limestone

Major element oxide %										
SiO_2	Al_2O_3	Fe_2O_3	MgO	CaO	Na_2O	K_2O	TiO_2	MnO	*LOI	Total
0.30	0.11	0.03	8.37	45.43	0.008	0.077	0.01<	0.008	45.19	99.533

*LOI: Lost on ignition

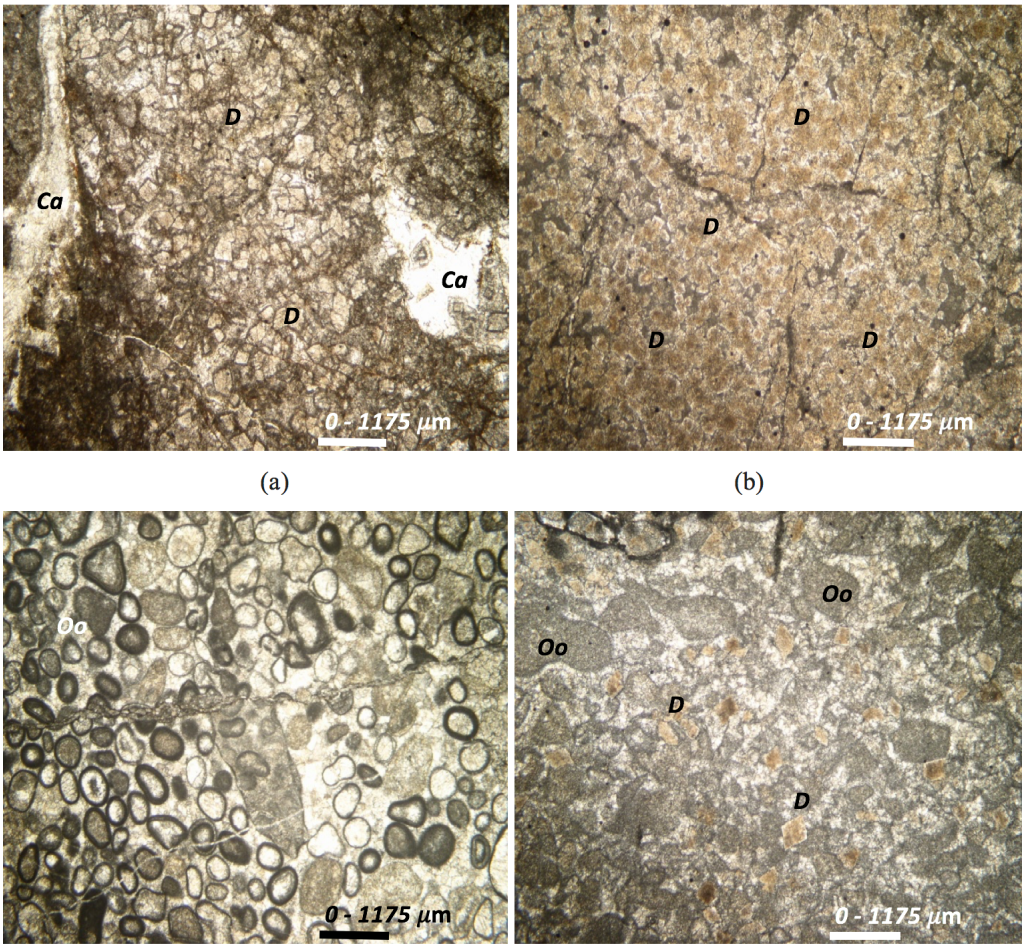

Figure 3.7 Thin section view shows light reddish pinkish color. Dolomitic grainstone, dolostone (a), dolomite (b), calcite dolostone, dolomitic grainstone and oolitic grainstone (c and d)

Table 3.6 Mineral content in Limestone

Mineral	**%**
Calcite	70-80
Dolomite	25-30
Total	100

Limestone is reddish pinkish beige in color. Limestone is generally pseudomicritic neomorphic carbonate sludge. Limestone is dolomitic in nature. Dolomites probably have dolomicrite and dolomicrosparitic texture. Recrystallization completely erased the initial texture. However, considering all the properties of the rock, this neomorphic facies may be thought to have been transformed from the primary oolitic granitic facies (Figure 3.7). Dolomitized oolite are bearing grainstone with dolosparitic cement and high energy oolites.

3.4 Sandstone

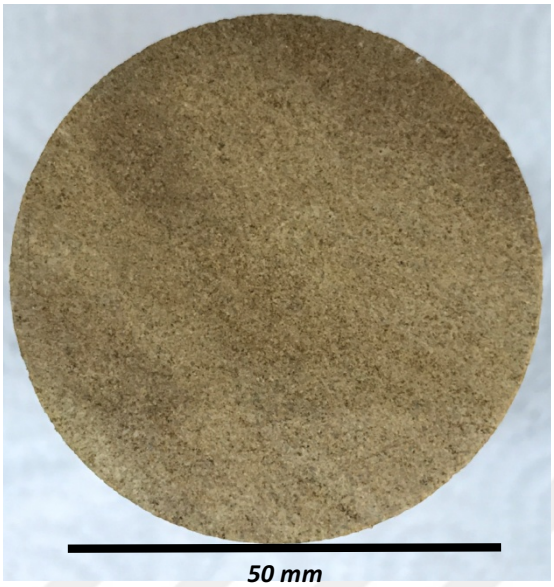

Figure 3.8 Sandstone core view perpendicular to core axis (Personal archive, 2017)

Table 3.7 Chemical analysis of Sandstone

Major element oxide %										
SiO_2	Al_2O_3	Fe_2O_3	MgO	CaO	Na_2O	K_2O	TiO_2	MnO	*LOI	Total
69.25	11.22	4.87	0.8	5.1	1.5	2.52	0.25	0.33	4.16	100

*LOI: Lost on ignition

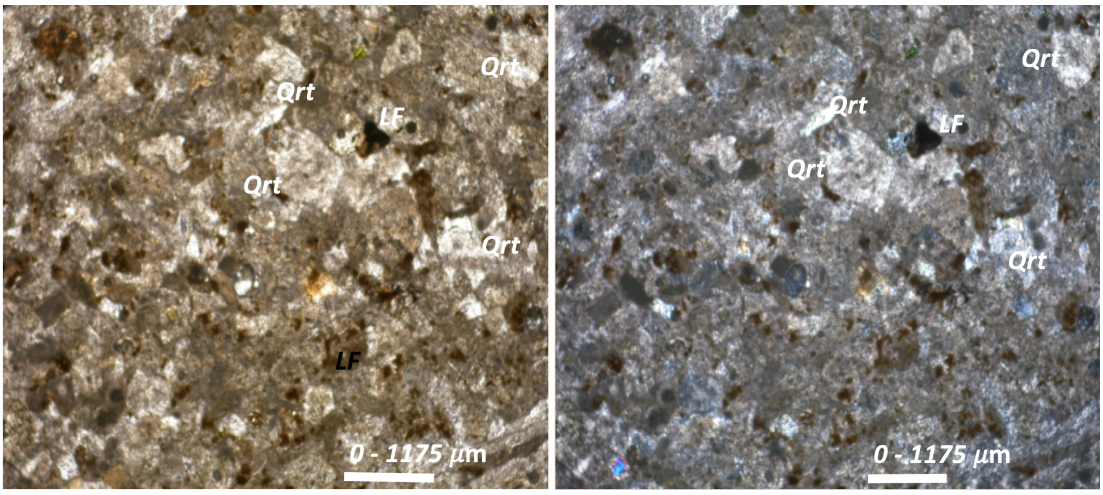

Figure 3.9 Thin section view of Sandstone Qtr: Quartz, LF: Lithic fragments

Table 3.8 Mineral pecentage in Sandstone

Mineral	**%**
Feldspar (F)	60
Quartz (Qrt)	30
Lithic fragments (LF)	10
Total	100

3.5 Tuff

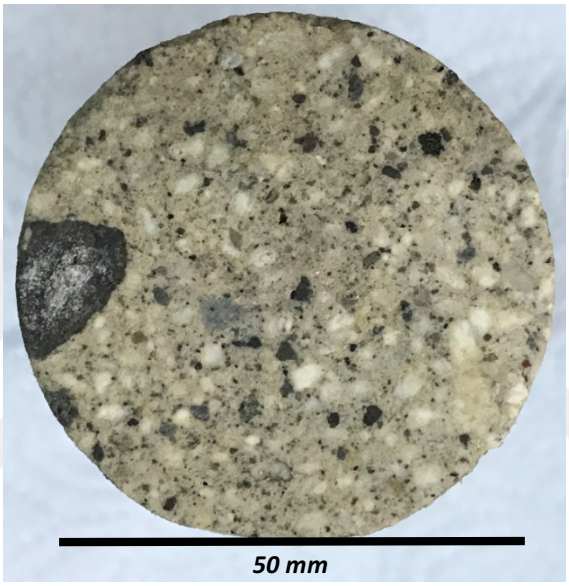

Figure 3.10 Tuff core view perpendicular to core axis (Personal archive, 2017)

Table 3.9 Chemical analysis of Tuff

Major element oxide %										
SiO_2	Al_2O_3	Fe_2O_3	MgO	CaO	Na_2O	K_2O	TiO_2	MnO	*LOI	Total
63.96	9.11	0.97	0.90	5.78	2.35	3.94	0.07	0.133	12.15	99.363

*LOI: Lost on ignition

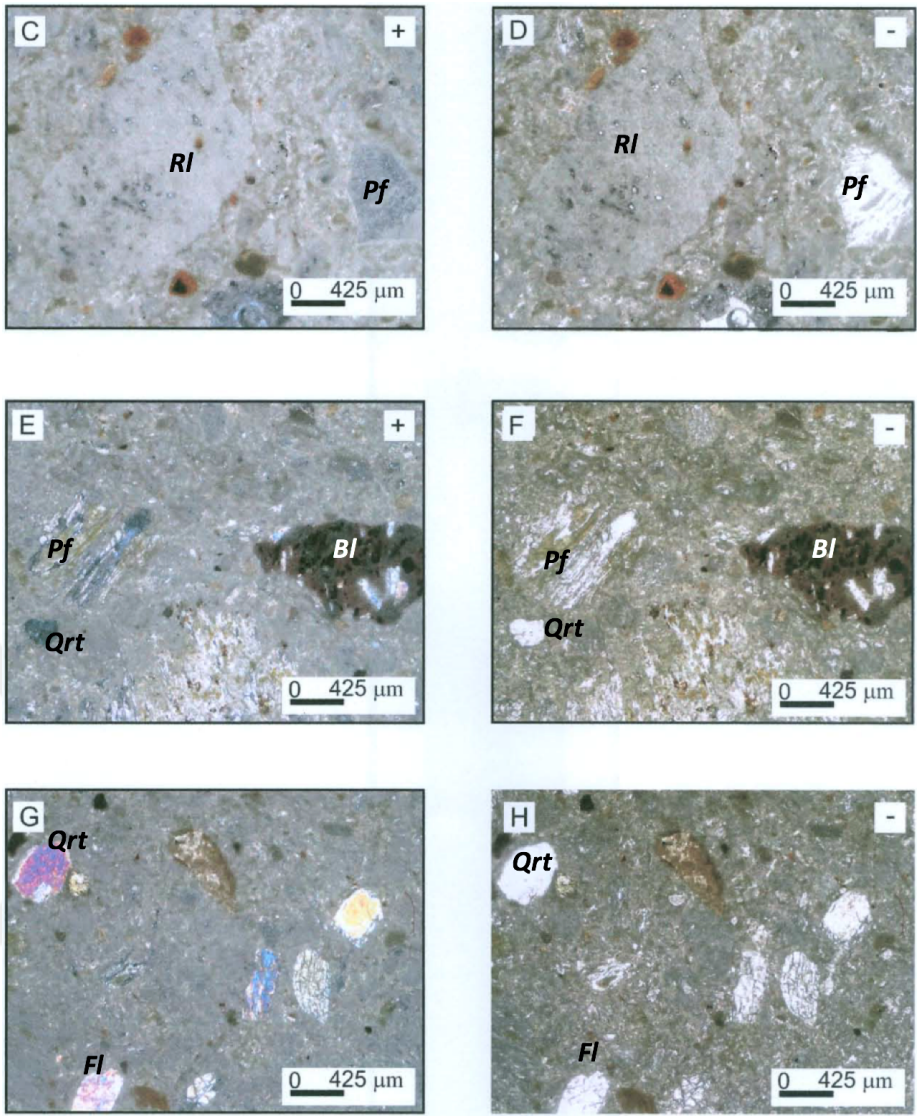

Figure 3.11 Thin section view of Tuff containing lithic components and crystal fragments.
Rl: Rhyolitic lava, Pf: Pumice fragments, Bl: Basalt lava, Qtr: Quartz, Fl: Feldspar

The angular rock fragments of andesite, rhyolite, basalt, claystone and lacustrine limestone are present in the tuff. These angular fragments vary in size.

Table 3.10 Mineral composition of Tuff

Mineral	**%**
Rhyolitic lava-glass fragments	10%
Basalt lava	5-10%
Pumice fragments	60-70%
Feldspar-quartz	3-5%
Amphibole-pyroxene	1-5%
Total	100

CHAPTER FOUR
PHYSICAL PROPERTIES OF CORE AND CUBE ROCK SAMPLES

For this study minimum five different cores and cubes were taken for each lithology. Each core and cube had corresponding physical parameters (diameter, height, mass before and after dehydration). Different properties of core and cubes samples were measured before and after dehydration.

4.1 Dry and Saturated Unit Weight of Core Samples

During the determination of the unit weight, core samples of 50 mm and 54 mm diameter. All the samples were put into the water for 24 hours and after 24 hours their saturated weights and saturated weights in water were measured (Figure 4.1). Samples were then placed in oven for 24 hours at 105 degrees Celsius and dry weights were measured.

Dry unit weight = dry weight / (saturated weight - saturated weight in water)

Saturated unit weight = saturated weight / (saturated weight – saturated weight in water)

Figure 4.1 Samples measurements by Archimedes Balance (Personal archive, 2017)

4.1.1 Porosity and Void Ratio

Same procedure used for the measurement of porosity and void ratio. First the weight of water saturated samples was determined and then they were dried for 24 hours at 105 degrees Celsius.

Porosity = (saturated weight (ms) – dry weight (md)) / (saturated weight (ms) – saturated weight in water (mh)) x 100

Void ratio = (saturated weight (ms) – dry weight (md)) / (dry weight (md) – saturated weight in water (mh)) x 100

Table 4.1 Dry unit weight (γ_{dry}), saturated unit weight (γ_{sat}), porosity (n) and void ratio (e) of all core samples

Lithology	**S. No**	**mh (g)**	**ms (g)**	**md (g)**	**γ_{dry} (g/cm^3)**	**γ_{sat} (g/cm^3)**	**n (%)**	**e (%)**
Andesite	A-1	274.86	462.64	457.51	2.436	2.464	2.732	2.809
	A-2	270.76	456.29	451.06	2.431	2.459	2.819	2.901
	A-3	274.5	461.44	456.31	2.441	2.468	2.744	2.822
	A-4	278.14	465.35	460.62	2.460	2.486	2.527	2.592
	A-5	278.85	466.33	461.97	2.464	2.487	2.326	2.381
A.Mean	**-**	**275.42**	**462.41**	**457.49**	**2.446**	**2.473**	**2.63**	**2.70**
STDEV	**-**	**3.242**	**3.952**	**4.260**	**0.015**	**0.013**	**0.201**	**0.212**
Granite	G-1	322.86	513.65	511.73	2.682	2.692	1.006	1.017
	G-2	323.79	515.12	513.13	2.682	2.692	1.040	1.051
	G-3	260.31	414.25	412.7	2.681	2.691	1.007	1.017
	G-4	384.52	612.24	609.52	2.677	2.689	1.194	1.209
	G-5	384.83	612.44	609.72	2.679	2.691	1.195	1.209
	G-6	426.12	678.11	675.42	2.680	2.691	1.068	1.079
	G-7	423.72	675.15	672.21	2.674	2.685	1.169	1.183
	G-8	424.62	676.41	673.6	2.675	2.686	1.116	1.129
	G-9	425.63	677.95	674.64	2.674	2.687	1.312	1.329
	G-10	424.67	676.24	673.36	2.677	2.688	1.145	1.158
	G-11	372.78	595.17	592.52	2.664	2.676	1.192	1.206
A.Mean	**-**	**379.44**	**604.25**	**601.69**	**2.677**	**2.688**	**1.13**	**1.14**
STDEV	**-**	**55.632**	**88.752**	**88.262**	**0.005**	**0.005**	**0.095**	**0.097**

Table 4.1 Continues

Limestone	LS-1	331.04	515.71	514.21	2.784	2.793	0.812	0.819
	LS-2	331.75	516.37	515.01	2.790	2.797	0.737	0.742
	LS-3	315.16	499.51	499.32	2.709	2.710	0.103	0.103
	LS-4	332.74	517.79	517.04	2.794	2.798	0.405	0.407
	LS-5	413.52	655.16	654.56	2.709	2.711	0.248	0.249
	LS-6	416.64	656.37	655.99	2.736	2.738	0.159	0.159
	LS-7	416.18	658.22	657.48	2.716	2.719	0.306	0.307
	LS-8	419.68	662.32	661.41	2.726	2.730	0.375	0.376
A.Mean	**-**	**372.09**	**585.18**	**584.38**	**2.746**	**2.75**	**0.39**	**0.40**
STDEV	**-**	**47.827**	**78.095**	**78.227**	**0.037**	**0.040**	**0.257**	**0.259**
Sandstone	SS-1	262.77	451.08	430.79	2.288	2.395	10.775	12.076
	SS-2	264.32	452.87	433.35	2.298	2.402	10.353	11.548
	SS-3	254.69	442.86	419.37	2.229	2.354	12.483	14.264
	SS-4	257.16	445.16	423.64	2.253	2.368	11.447	12.926
	SS-5	255.75	444.66	422.29	2.235	2.354	11.842	13.432
	SS-6	353.4	604.55	579.49	2.307	2.407	9.978	11.084
	SS-7	355.55	606.78	582.67	2.319	2.415	9.597	10.616
	SS-8	356.03	607.35	583.7	2.323	2.417	9.410	10.388
	SS-9	357.26	608.45	585.19	2.330	2.422	9.260	10.205
	SS-10	360.07	611.24	588.92	2.345	2.434	8.886	9.753
A.Mean	**-**	**307.70**	**527.50**	**504.94**	**2.293**	**2.40**	**10.40**	**11.63**
STDEV	**-**	**51.507**	**84.577**	**83.454**	**0.041**	**0.029**	**1.204**	**1.509**
Tuff	T-1	146.25	335.09	280.61	1.486	1.774	28.850	40.548
	T-2	160.57	349.42	311.14	1.648	1.850	20.270	25.423
	T-3	183.6	433.88	365.45	1.460	1.734	27.341	37.630
	T-4	143.41	332.31	279.04	1.477	1.759	28.200	39.276
	T-5	130.84	316.22	274.4	1.480	1.706	22.559	29.131
	T-6	183.99	433.2	365.64	1.467	1.738	27.110	37.192
	T-7	157.33	407.7	344.42	1.376	1.628	25.275	33.823
	T-8	153.76	399.25	338.44	1.379	1.626	24.771	32.927
	T-9	144.2	389.65	330.74	1.347	1.587	24.001	31.580
	T-10	175.9	425.95	360.74	1.443	1.703	26.079	35.279
	T-11	156.71	401.83	342.82	1.399	1.639	24.074	31.707
A.Mean	**-**	**157.87**	**384.05**	**326.68**	**1.451**	**1.704**	**25.32**	**34.05**
STDEV	**-**	**17.195**	**43.205**	**35.040**	**0.081**	**0.078**	**2.556**	**4.531**

4.2 Dry and Saturated Unit Weight, Porosity and Void Ratio of Cube Samples

The 70 x 70 x 70 mm sized cube samples were used in this study to find their saturated and dry unit weight, porosity and void ratio. To find these properties of cube samples same procedure was done as did before for the core samples.

Table 4.2 Dry unit weight, saturated unit weight, porosity and void ratio of all cube samples

Lithology	**S. No**	**mh (g)**	**ms (g)**	**md (g)**	**γ_{dry} (g/cm^3)**	**γ_{sat} (g/cm^3)**	**n (%)**	**e (%)**
Andesite	A-1	500.9	845.9	836.31	2.424	2.452	2.780	2.859
	A-2	541.3	905.35	895.81	2.461	2.487	2.621	2.691
	A-3	530.72	888.27	879.02	2.458	2.484	2.587	2.656
	A-4	489.75	828.61	819.08	2.417	2.445	2.812	2.894
	A-5	478.78	815.36	806.54	2.396	2.422	2.620	2.691
	A-6	500.13	843.23	834.74	2.433	2.458	2.474	2.537
	A-7	489.56	831.16	822.51	2.408	2.433	2.532	2.598
	A-8	487.83	822.58	813.56	2.430	2.457	2.695	2.769
	A-9	502.01	843.7	834.85	2.443	2.469	2.590	2.659
A.Mean	**-**	**502.33**	**847.13**	**838.05**	**2.430**	**2.456**	**2.66**	**2.71**
STDEV	**-**	**20.67**	**30.25**	**30.07**	**0.022**	**0.022**	**0.110**	**0.116**
Granite	G-1	496.63	791.39	788.64	2.676	2.685	0.933	0.942
	G-2	526.33	838.62	835.84	2.676	2.685	0.890	0.898
	G-3	519.25	827.48	824.64	2.675	2.685	0.921	0.930
	G-4	577.66	920.75	918.84	2.678	2.684	0.557	0.560
	G-5	610.73	973.27	970.93	2.678	2.686	0.645	0.650
	G-6	588.86	938	935.82	2.680	2.687	0.624	0.628
A.Mean	**-**	**533.24**	**881.59**	**879.12**	**2.677**	**2.685**	**0.76**	**0.77**
STDEV	**-**	**45.287**	**72.154**	**72.456**	**0.002**	**0.001**	**0.171**	**0.173**
Limestone	LS-1	637.95	1006.77	1005.37	2.726	2.730	0.380	0.381
	LS-2	613.81	959.59	958.89	2.773	2.775	0.202	0.203
	LS-3	579.15	910.85	909.72	2.743	2.746	0.341	0.342
	LS-4	601.99	944.64	944.01	2.755	2.757	0.184	0.184
	LS-5	625.17	985.72	984.65	2.731	2.734	0.297	0.298

Table 4.2 Continues

A.Mean	**-**	**611.16**	**961.51**	**960.53**	**2.746**	**2.748**	**0.28**	**0.28**
STDEV	**-**	**22.521**	**37.045**	**36.911**	**0.019**	**0.018**	**0.086**	**0.086**
Sandstone	SS-1	545.2	928.27	885.51	2.312	2.423	11.162	12.565
	SS-2	540.26	916.44	877.54	2.333	2.436	10.341	11.533
	SS-3	521.31	886.11	844.46	2.315	2.429	11.417	12.889
	SS-4	540.98	917.1	878.47	2.336	2.438	10.271	11.446
	SS-5	536.87	910.34	871.79	2.334	2.438	10.322	11.510
A.Mean	**-**	**536.92**	**911.65**	**871.55**	**2.326**	**2.433**	**10.70**	**11.99**
STDEV	**-**	**9.218**	**15.675**	**15.910**	**0.012**	**0.007**	**0.544**	**0.684**
Tuff	T-1	163.28	379.97	319.26	1.473	1.754	28.017	38.922
	T-2	240.06	566.94	490.68	1.501	1.734	23.330	30.429
	T-3	185.03	440.17	378.3	1.483	1.725	24.249	32.012
	T-4	172.96	432.41	367.77	1.417	1.667	24.914	33.181
	T-5	247.8	573.73	502.75	1.543	1.760	21.778	27.841
	T-6	179.63	449.38	380.44	1.410	1.666	25.557	34.331
	T-7	156.52	362.43	315.04	1.530	1.760	23.015	29.895
	T-8	260.16	586.72	521.06	1.596	1.797	20.107	25.167
	T-9	367.42	840.48	730.23	1.544	1.777	23.306	30.388
A.Mean	**-**	**219.21**	**514.69**	**445.06**	**1.500**	**1.738**	**23.81**	**31.352**
STDEV	**-**	**67.848**	**148.098**	**132.214**	**0.061**	**0.046**	**2.267**	**3.944**

4.3 Determination of P-wave Velocity in Core and Cube Samples

The system used throughout this research work was Pundit Lab which is an ultrasonic pulse velocity (UPV) test instrument. It features transit time, measurement of pulse velocity, path length measurement and also measurement of surface velocity. Pundit Lab$^+$ instrument was used to determine the compressional wave velocities (Vp) of core samples, block samples and granular materials. First the length of specimen was measured and then arrival time was recorded by the Pundit Lab$^+$. Two probes, one act as a transducer and other as a receiver, used to pass the P-waves through the sample. The formula to calculate the P-wave velocity is,

$$Vp=h/t \tag{4.1}$$

Where, “Vp” is P-wave velocity

“h” is length of the specimen

“t” is arrival time

At least five core and bock samples of five different lithology were used to determine their Vp. The diameter of all the core samples was 50 mm. First the Vp of both dry and water saturated samples was measured.

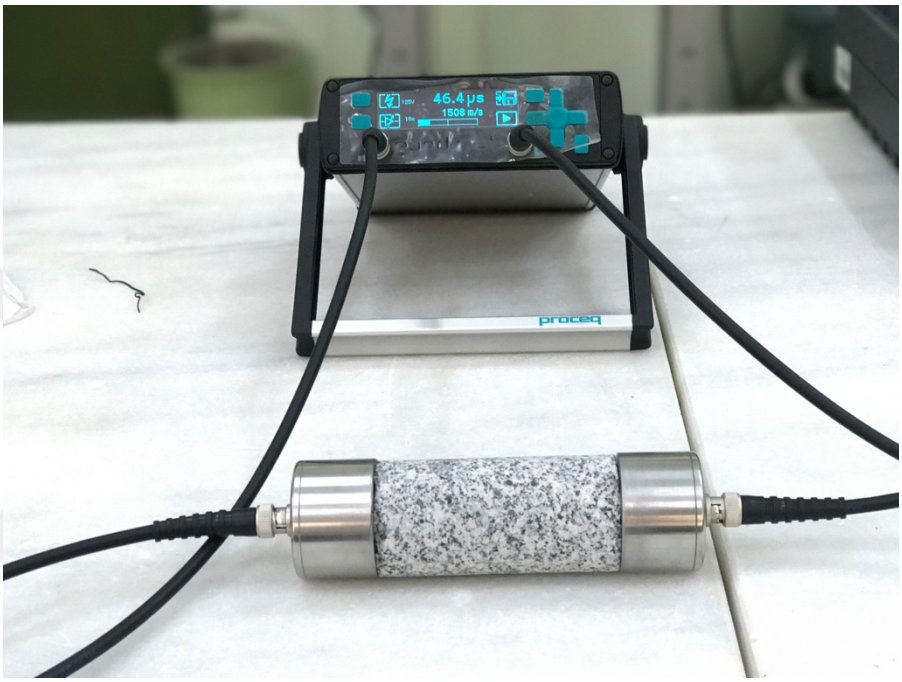

Figure 4.2 Ultrasonic waves testing instrument (Personal archive, 2017)

Table 4.3 P-wave velocity values of core samples

Lithology	S. No	h (mm)	t_{dry} (µs)	t_{sat} (µs)	$Vp_{(dry)}$ (m/sec)	$Vp_{(sat)}$ (m/sec)
Andesite	A-1	101.5	25.5	25	3980.39	4060.00
	A-2	100.52	25.2	25	3988.89	4020.80
	A-3	101.06	25	24.5	4042.40	4124.90
	A-4	101.84	24.5	24.5	4156.73	4156.73
	A-5	101.47	24.5	24.5	4141.63	4141.63
A.Mean	**-**	**101.28**	**24.94**	**24.7**	**4062.01**	**4100.81**
STDEV	**-**	**0.51**	**0.44**	**0.27**	**83.22**	**57.97**

Table 4.3 Continues

Granite	G-1	105.62	25.4	22.9	4158.27	4612.23
	G-2	104.16	25.9	23	4021.62	4528.70
	G-3	124.11	31.4	27.9	3952.55	4448.39
	G-4	120.76	31.1	27.4	3882.96	4407.30
	G-5	123.96	31.5	27.9	3935.24	4443.01
A.Mean	**-**	**115.72**	**29.06**	**25.82**	**3990.13**	**4487.93**
STDEV	**-**	**9.99**	**3.12**	**2.63**	**106.27**	**82.45**
Limestone	LS-1	101.43	19.5	19.5	5201.54	5201.54
	LS-2	101.26	19.5	19.5	5192.82	5192.82
	LS-3	100.83	21.5	20	4689.77	5041.50
	LS-4	100.88	21	20	4803.81	5044.00
	LS-5	101.05	20	19.5	5052.50	5182.05
	LS-6	102.7	19.5	19.5	5266.67	5266.67
A.Mean	**-**	**101.36**	**20.17**	**19.67**	**5034.52**	**5154.76**
STDEV	-	**0.70**	**0.88**	**0.26**	**236.33**	**91.65**
Sandstone	SS-1	104.29	31.4	30.9	3321.34	3375.08
	SS-2	103.21	31	30.3	3329.35	3406.27
	SS-3	103.33	31.9	31.9	3239.18	3239.18
	SS-4	103.61	33.8	31.1	3065.38	3331.51
	SS-5	103.53	33.4	33.1	3099.70	3127.79
A.Mean	-	**103.59**	**32.3**	**31.5**	**3210.99**	**3295.98**
STDEV	-	**0.42**	**1.24**	**1.08**	**123.05**	**113.13**
Tuff	T-1	103.93	48.3	79.5	2151.76	1307.30
	T-2	102.73	46.6	71	2204.51	1446.90
	T-3	103.2	55	88.8	1876.36	1162.16
	T-4	103.16	54.3	65.8	1899.82	1567.78
	T-5	123.5	59	68.9	2093.22	1792.45
A.Mean	-	**107.3**	**52.64**	**74.8**	**2045.13**	**1455.32**
STDEV	-	**9.06**	**5.10**	**9.33**	**148.90**	**241.99**

Table 4.4 P-wave velocity values of cube samples

Lithology	S. No	h (mm)	t_{dry} (µs)	t_{sat} (µs)	$Vp_{(dry)}$ (m/sec)	$Vp_{(sat)}$ (m/sec)
Andesite	A-1	71.94	20	20	3597.00	3597.00
	A-2	69.76	18.5	19.5	3770.81	3577.44
	A-3	69.99	19	18.5	3683.68	3783.24
	A-4	66.71	18.9	19	3529.63	3511.05
	A-5	74.15	21	20.9	3530.95	3547.85
A.Mean	-	**70.51**	**19.48**	**19.58**	**3622.41**	**3603.32**
STDEV	-	**2.76**	**1.01**	**0.93**	**104.16**	**105.68**
Granite	G-1	73.57	21.2	18	3470.28	4087.22
	G-2	73.88	21.5	18	3436.28	4104.44
	G-3	73.56	21.5	18	3421.40	4086.67
	G-4	73.52	21	18	3500.95	4084.44
	G-5	70.84	17.5	16.5	4048.00	4293.33
A.Mean	-	**73.07**	**20.54**	**17.7**	**3575.38**	**4131.22**
STDEV	-	**1.26**	**1.71**	**0.67**	**266**	**90.98**
Limestone	LS-1	72.7	16	15	4543.75	4846.67
	LS-2	70.98	14.5	14.5	4895.17	4895.17
	LS-3	70.04	14.5	14.5	4830.34	4830.34
	LS-4	70.95	14.5	14.5	4893.10	4893.10
	LS-5	72.36	15.5	15	4668.39	4824.00
A.Mean	-	**71.41**	**15**	**14.7**	**4766.15**	**4857.86**
STDEV	-	**1.10**	**0.71**	**0.27**	**154.84**	**34.14**
Sandstone	SS-1	71.99	25.4	24.3	2834.25	2962.55
	SS-2	72.61	23	22.9	3156.96	3170.74
	SS-3	69.81	23.5	23	2970.64	3035.22
	SS-4	73.44	22.5	23.3	3264.00	3151.93
	SS-5	73.86	22	22.5	3357.27	3282.67
A.Mean	-	**72.34**	**23.28**	**23.2**	**3116.62**	**3120.62**
STDEV	-	**1.59**	**1.31**	**0.68**	**213.49**	**124.53**
Tuff	T-1	79.14	40.3	47.9	1963.77	1652.19
	T-2	79.52	39.8	48.3	1997.99	1646.38
	T-3	71.22	36.3	44.3	1961.98	1607.67
	T-4	72.96	37.8	47.5	1930.16	1536.00
	T-5	79.4	36.3	40.5	2187.33	1960.49
A.Mean	-	**76.45**	**38.1**	**45.7**	**2008.25**	**1680.55**
STDEV	-	**4.03**	**1.89**	**3.31**	**102.95**	**163.21**

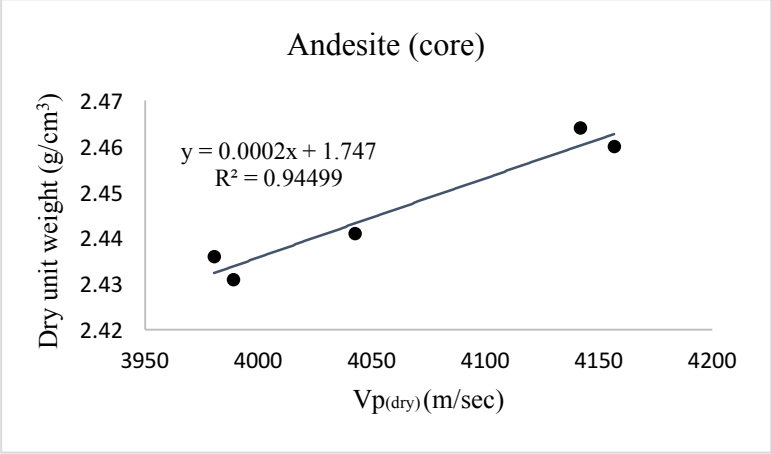

Figure 4.3 Graphical representation of dry Vp to dry unit weight for Andesite (core)

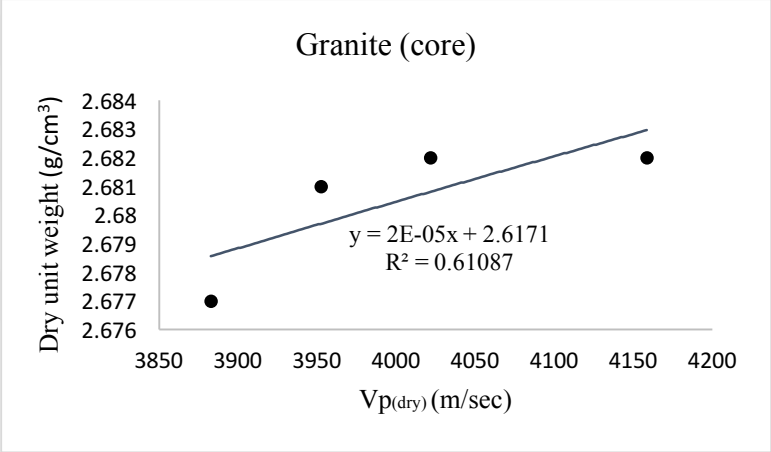

Figure 4.4 Graphical representation of dry Vp to dry unit weight for Granite (core)

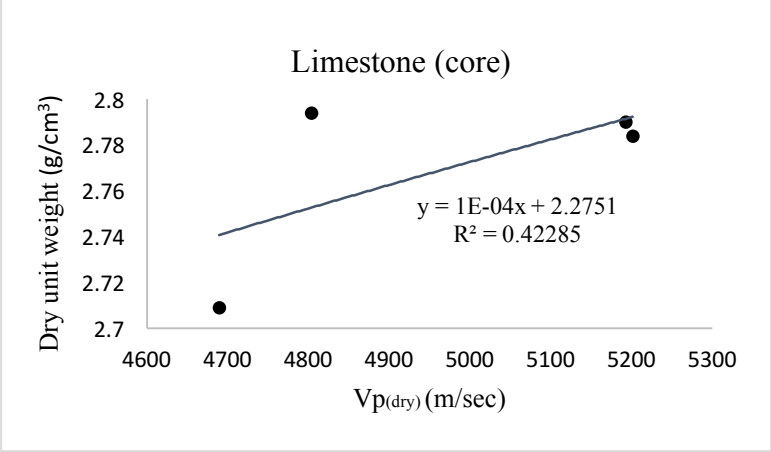

Figure 4.5 Graphical representation of dry Vp to dry unit weight for Limestone (core)

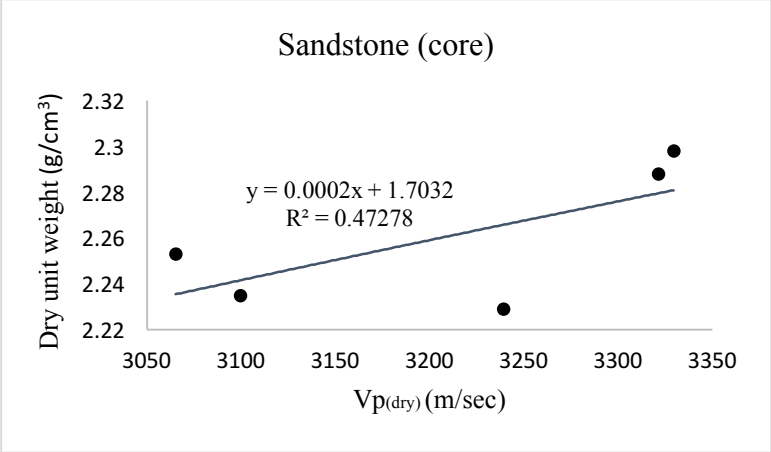

Figure 4.6 Graphical representation of dry Vp to dry unit weight for Sandstone (core)

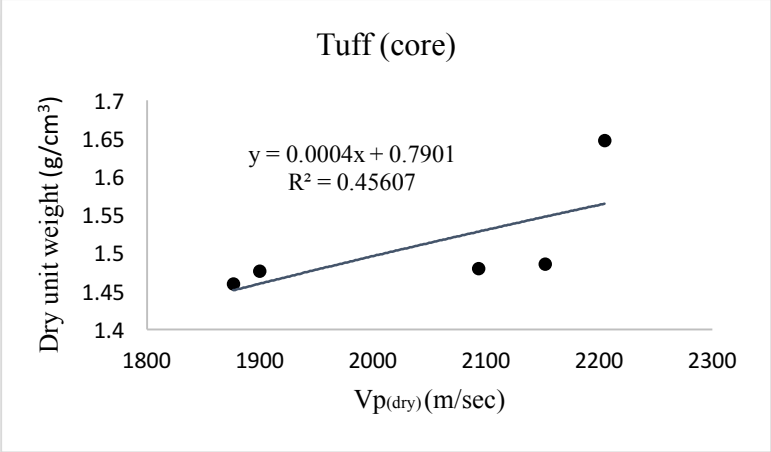

Figure 4.7 Graphical representation of dry Vp to dry unit weight for Tuff (core)

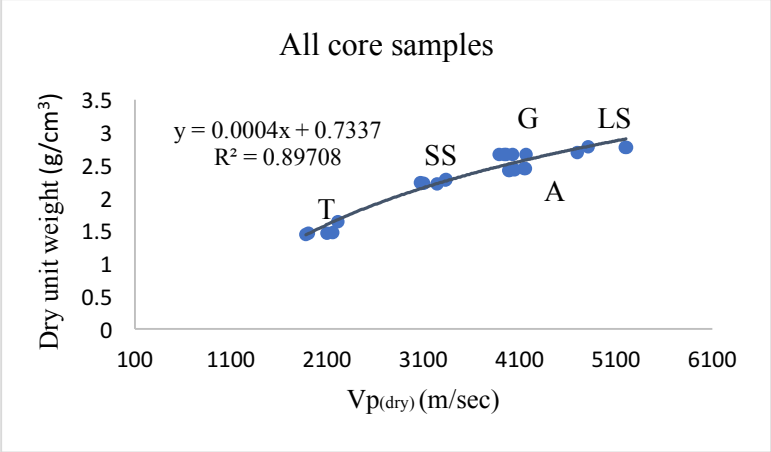

Figure 4.8 Graphical representation of dry Vp to dry unit weight trend for all core samples

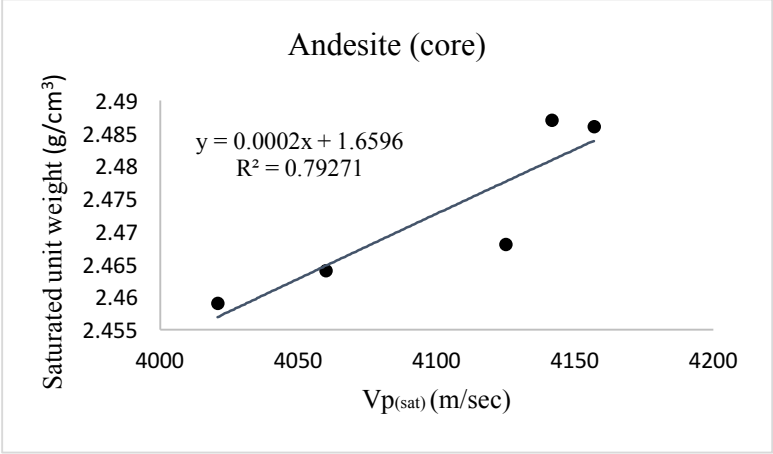

Figure 4.9 Graphical representation of saturated Vp to saturated unit weight for Andesite (core)

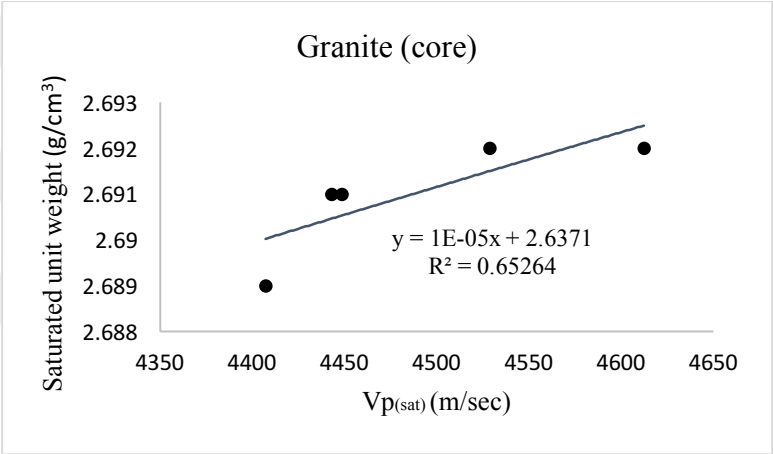

Figure 4.10 Graphical representation of saturated Vp to saturated unit weight for Granite (core)

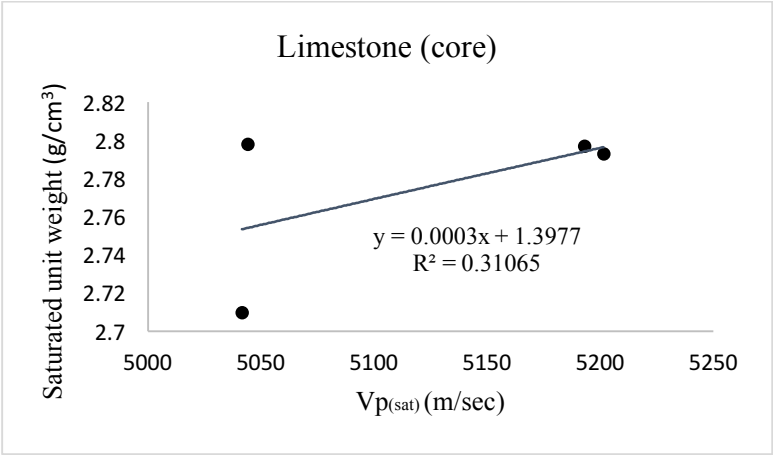

Figure 4.11 Graphical representation of saturated Vp to saturated unit weight for Limestone (core)

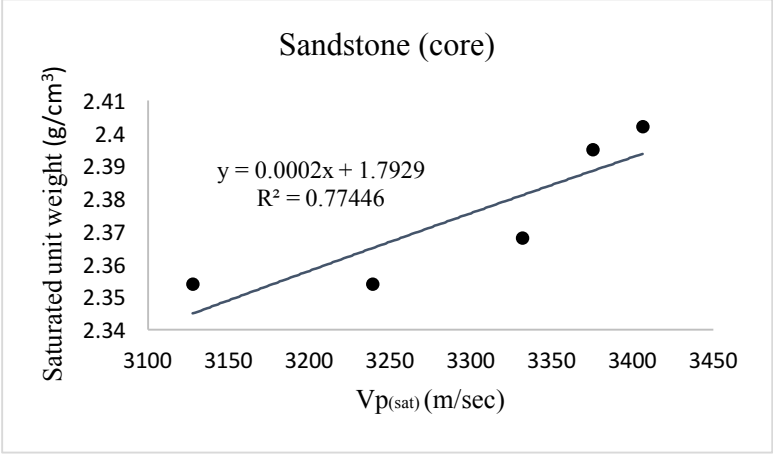

Figure 4.12 Graphical representation of saturated Vp to saturated unit weight for Sandstone (core)

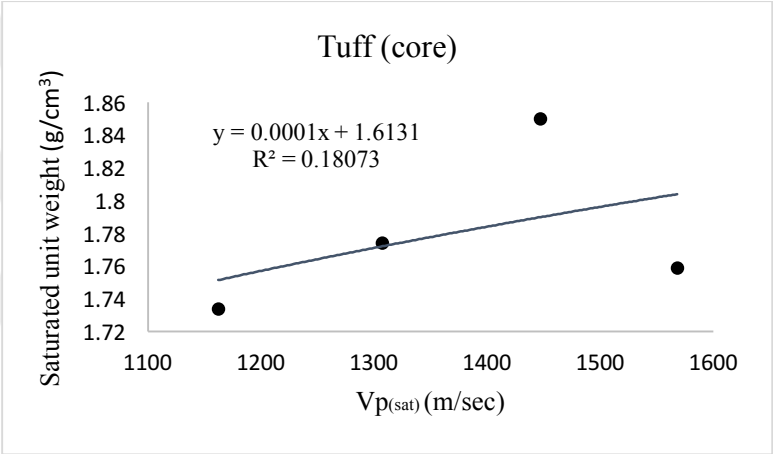

Figure 4.13 Graphical representation of saturated Vp to saturated unit weight for Tuff (core)

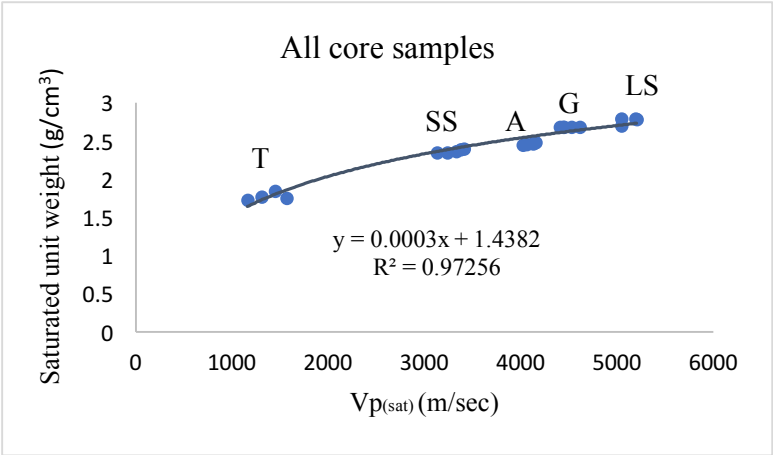

Figure 4.14 Graphical representation of saturated Vp to saturated unit weight trend for all core samples

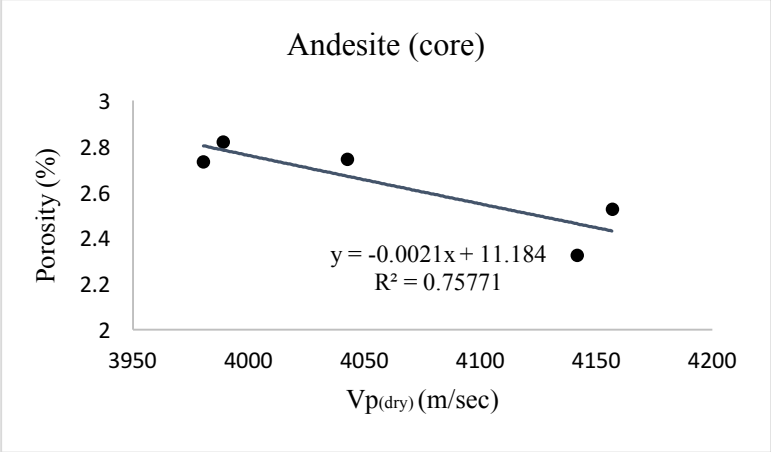

Figure 4.15 Graphical representation of dry Vp to porosity for Andesite (core)

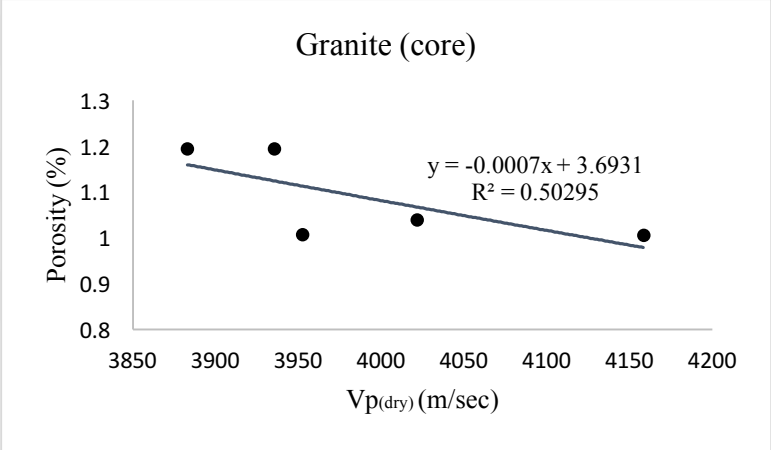

Figure 4.16 Graphical representation of dry Vp to porosity for Granite (core)

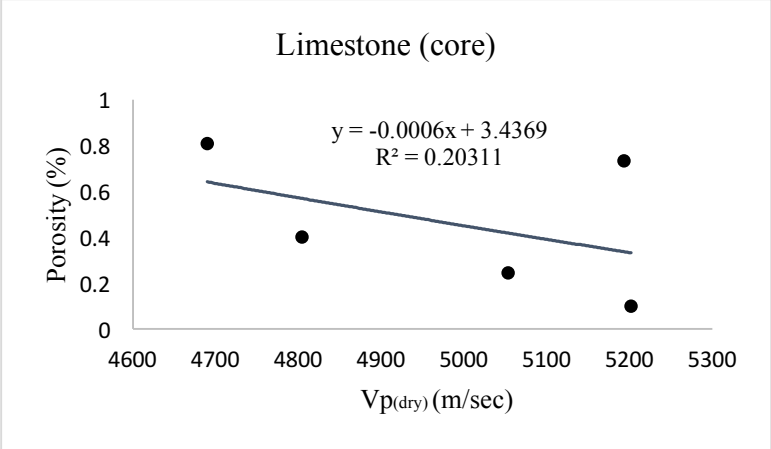

Figure 4.17 Graphical representation of dry Vp to porosity for Limestone (core)

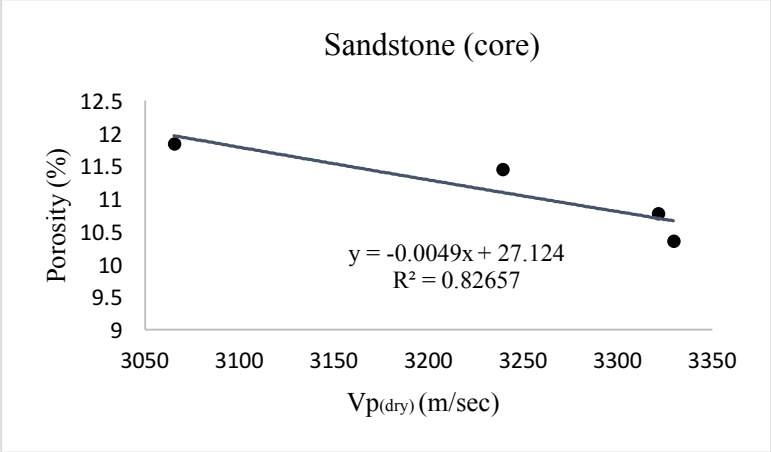

Figure 4.18 Graphical representation of dry Vp to porosity for Sandstone (core)

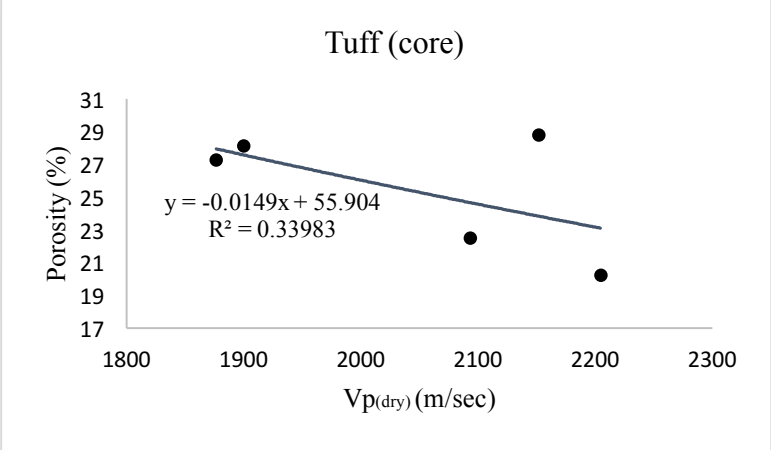

Figure 4.19 Graphical representation of dry Vp to porosity for Tuff (core)

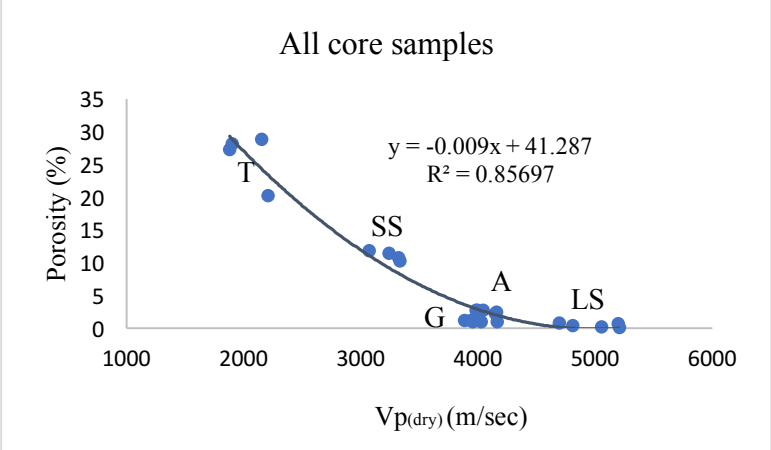

Figure 4.20 Graphical representation of dry Vp to porosity trend for all core samples

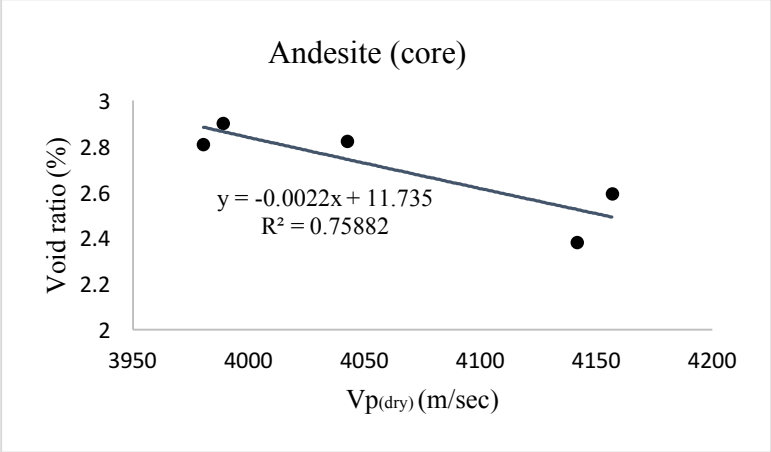

Figure 4.21 Graphical representation of dry Vp to void ratio for Andesite (core)

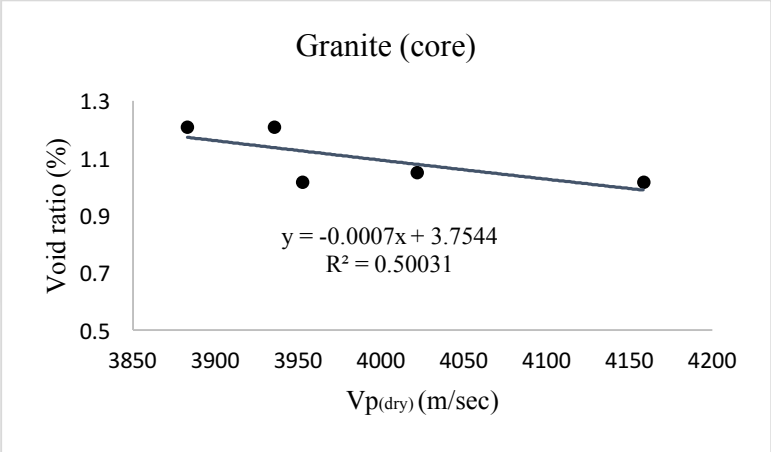

Figure 4.22 Graphical representation of dry Vp to void ratio for Granite (core)

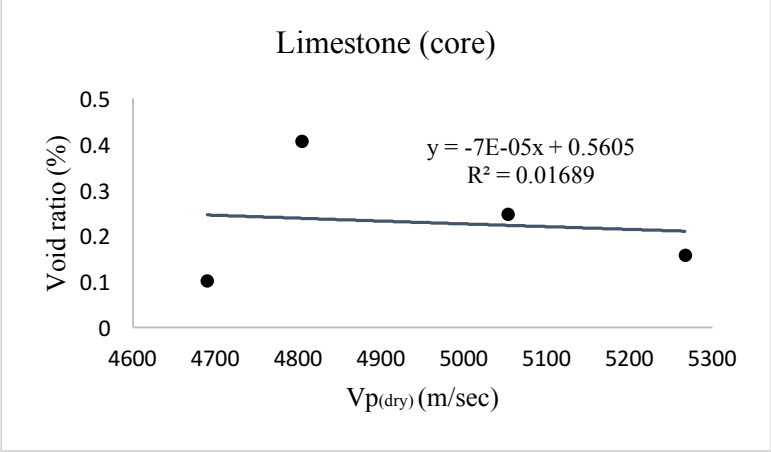

Figure 4.23 Graphical representation of dry Vp to void ratio for Limestone (core)

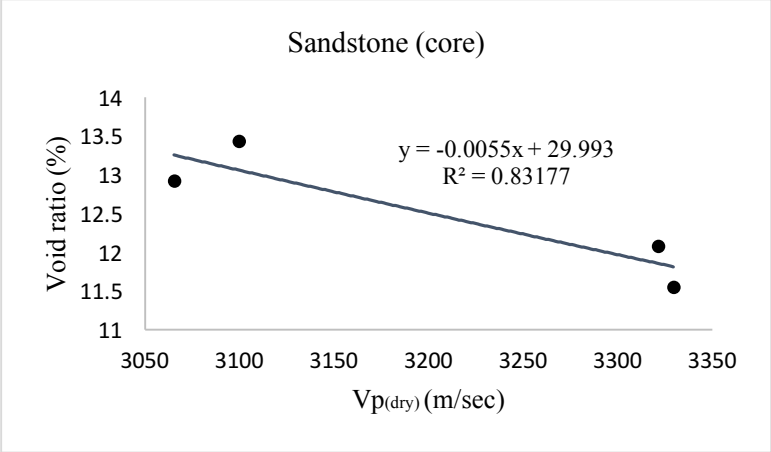

Figure 4.24 Graphical representation of dry Vp to void ratio for Sandstone (core)

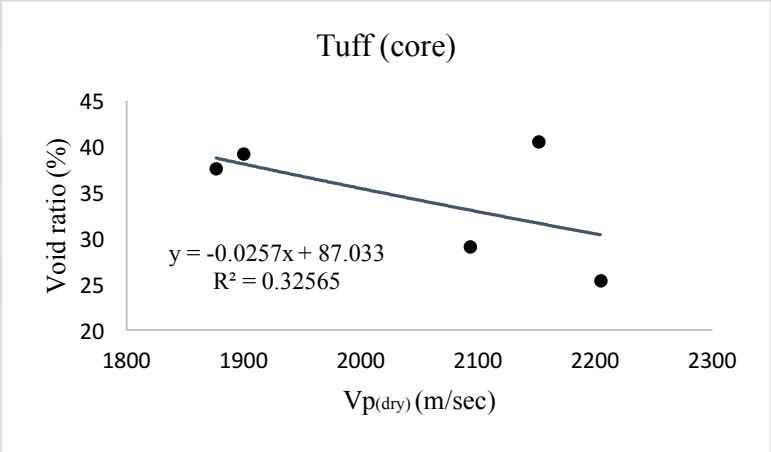

Figure 4.25 Graphical representation of dry Vp to void ratio for Tuff (core)

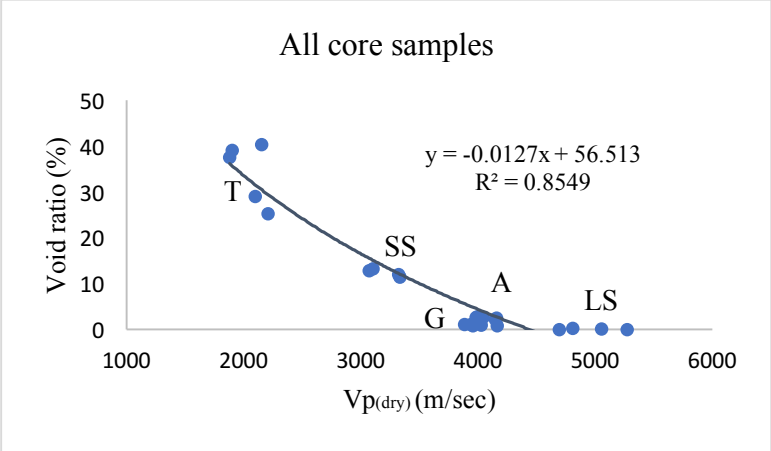

Figure 4.26 Graphical representation of dry Vp to void ratio trend for all core samples

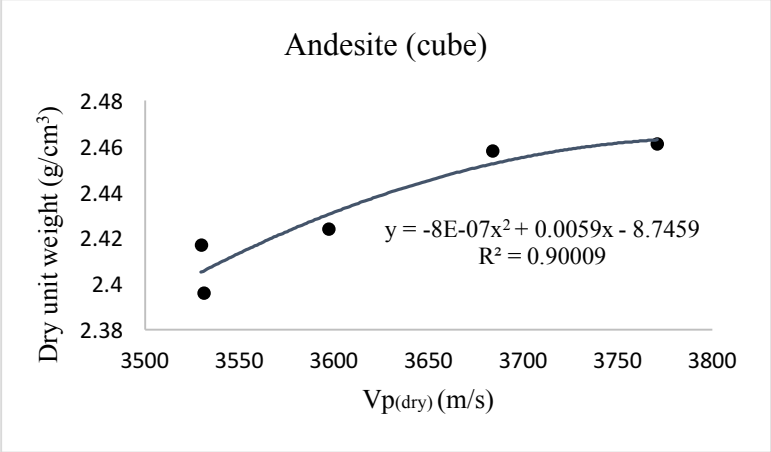

Figure 4.27 Graphical representation of dry Vp to dry unit weight for Andesite (cube)

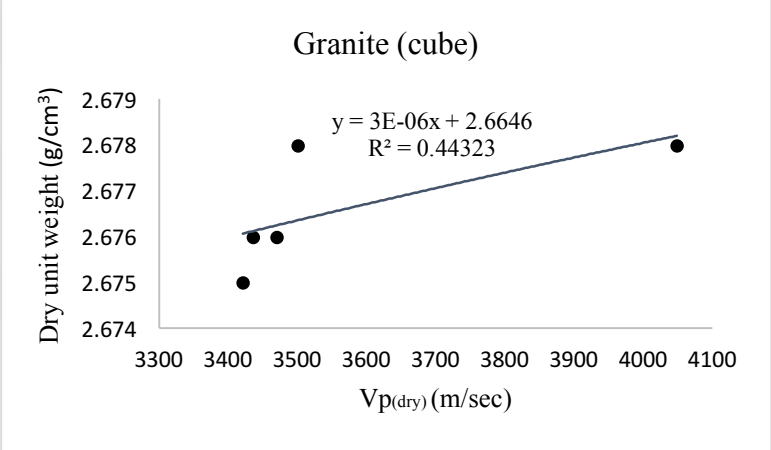

Figure 4.28 Graphical representation of dry Vp to dry unit weight for Granite (cube)

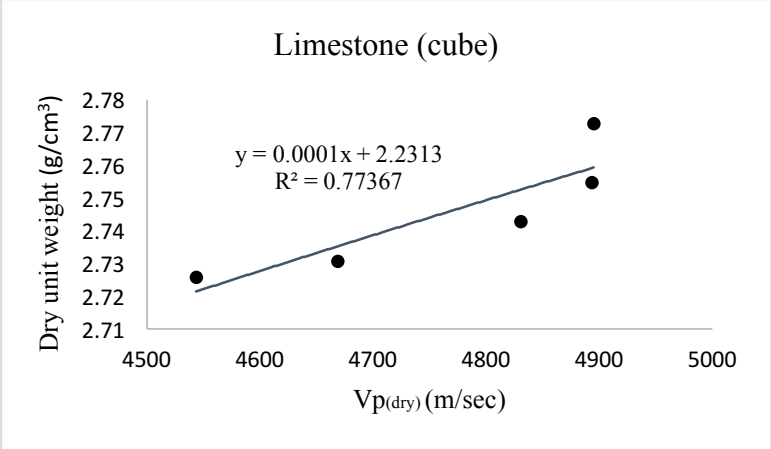

Figure 4.29 Graphical representation of dry Vp to dry unit weight for limestone (cube)

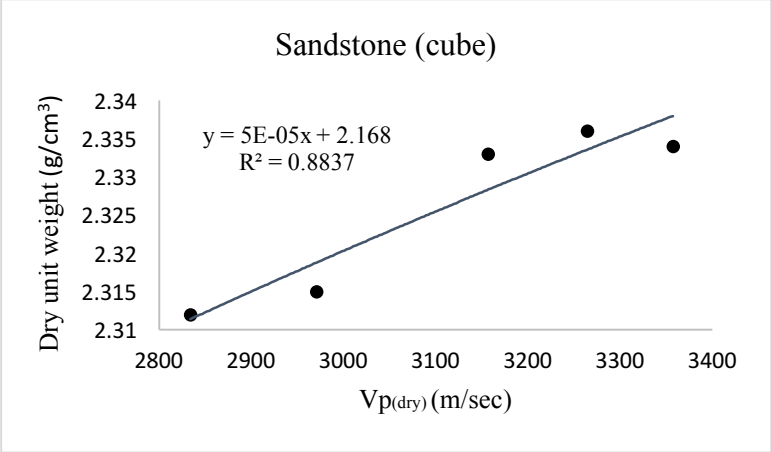

Figure 4.30 Graphical representation of dry Vp to dry unit weight for Sandstone (cube)

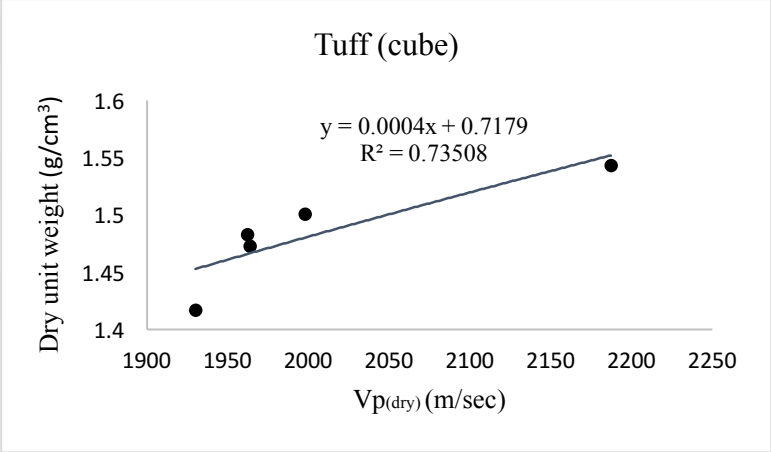

Figure 4.31 Graphical representation of dry Vp to dry unit weight for Tuff (cube)

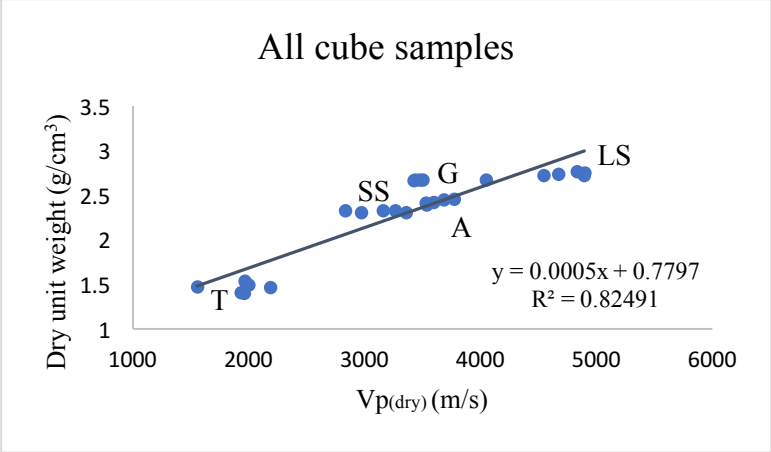

Figure 4.32 Graphical representation of dry Vp to dry unit weight trend for all cube samples

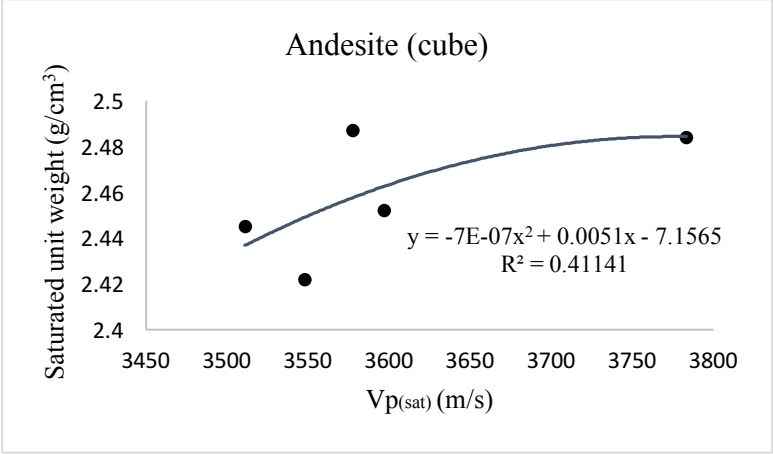

Figure 4.32 Graphical representation of saturated Vp to saturated unit weight for Andesite (cube)

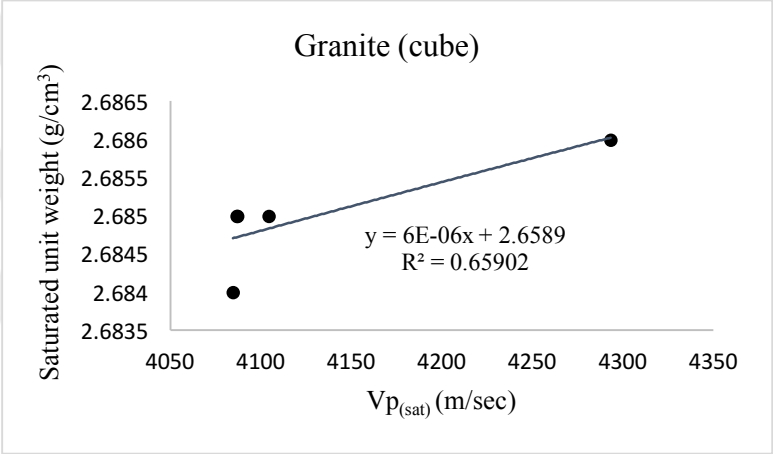

Figure 4.34 Graphical representation of saturated Vp to saturated unit weight for Granite (cube)

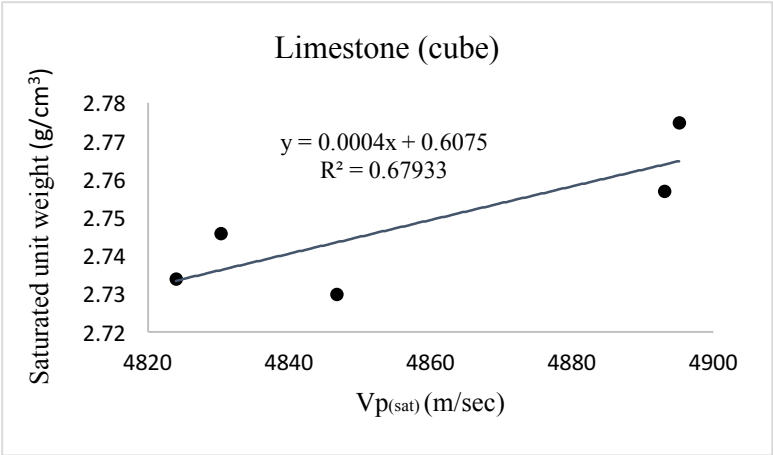

Figure 4.35 Graphical representation of saturated Vp to saturated unit weight for Limestone (cube)

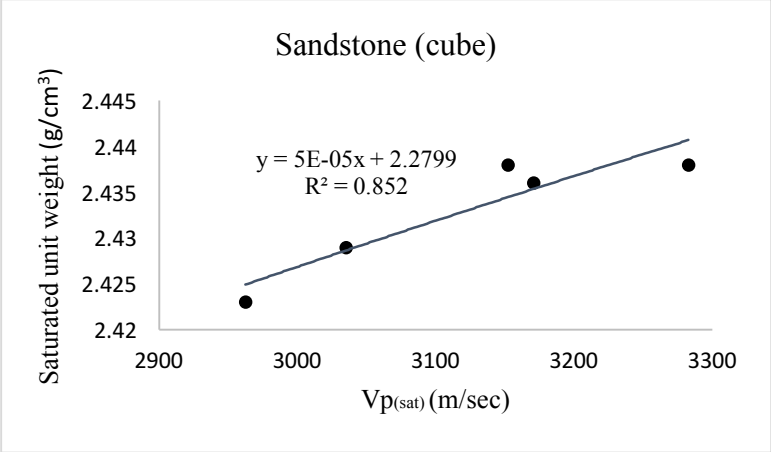

Figure 4.36 Graphical representation of saturated Vp to saturated unit weight for sandstone (cube)

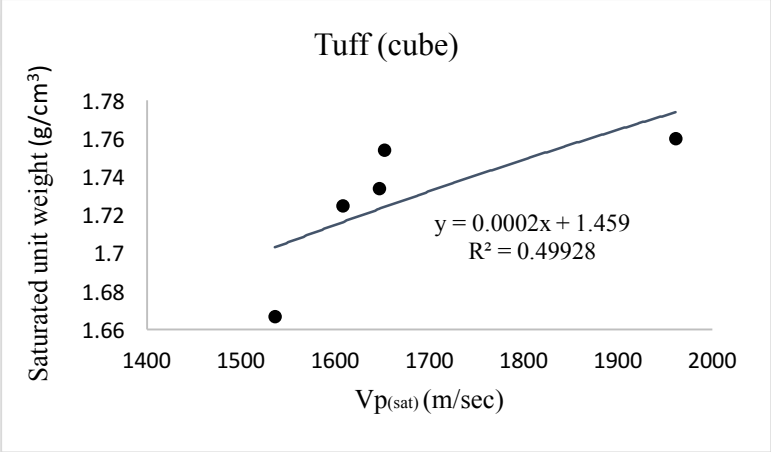

Figure 4.37 Graphical representation of saturated Vp to saturated unit weight for Tuff (cube)

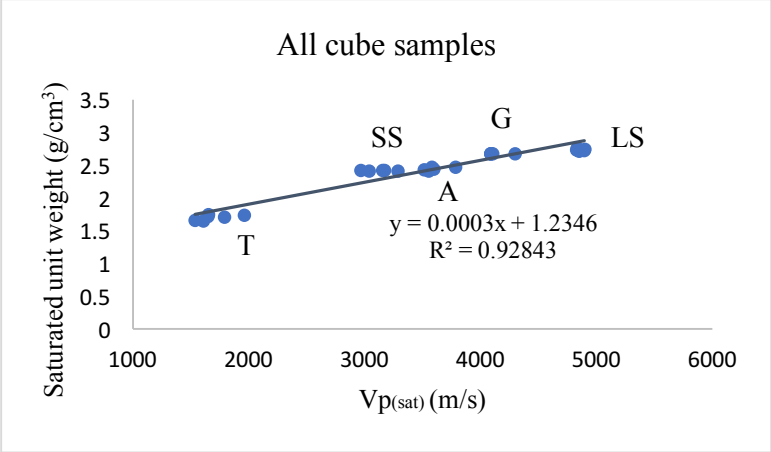

Figure 4.38 Graphical representation of saturated Vp to saturated unit weight trend for all cube samples

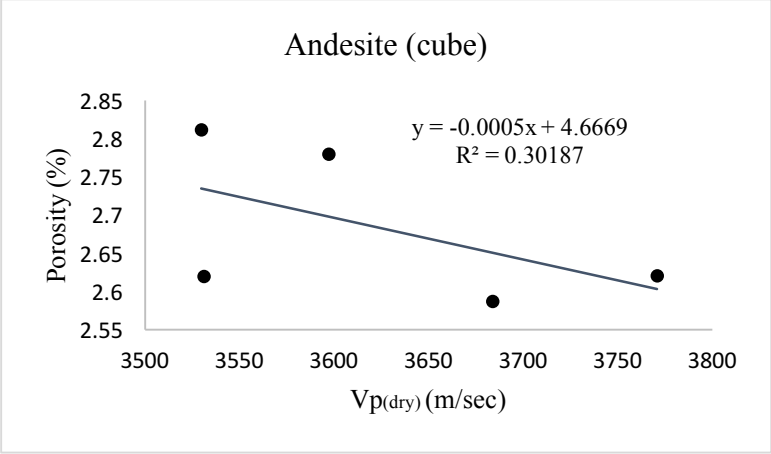

Figure 4.39 Graphical representation of dry Vp to porosity for Andesite (cube)

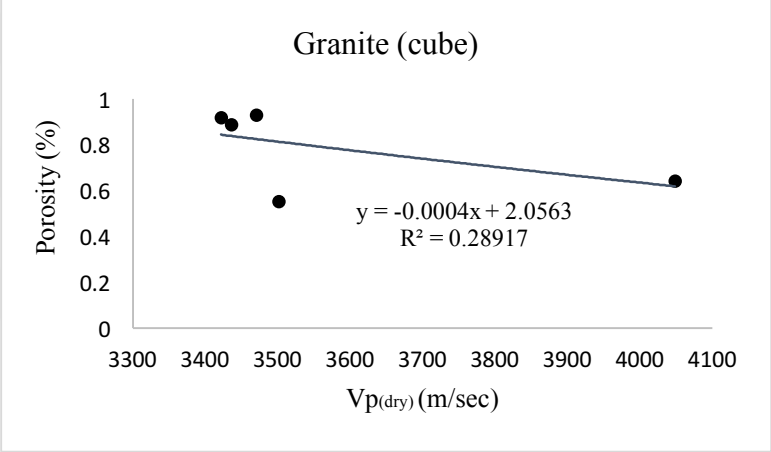

Figure 4.40 Graphical representation of dry Vp to porosity for Granite (cube)

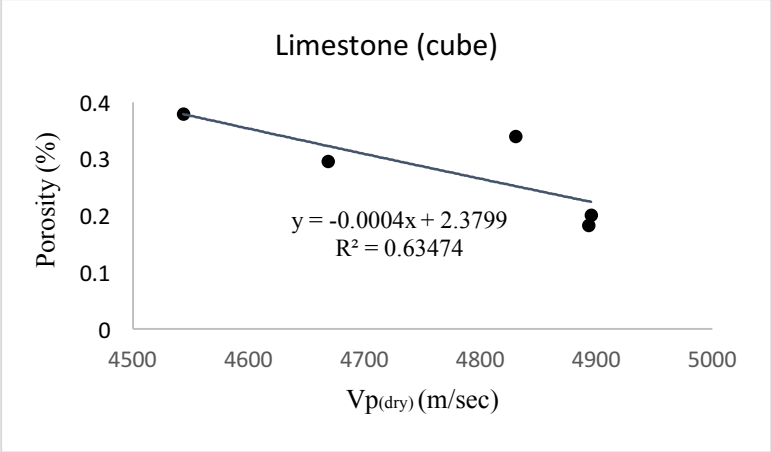

Figure 4.41 Graphical representation of dry Vp to porosity for Limestone (cube)

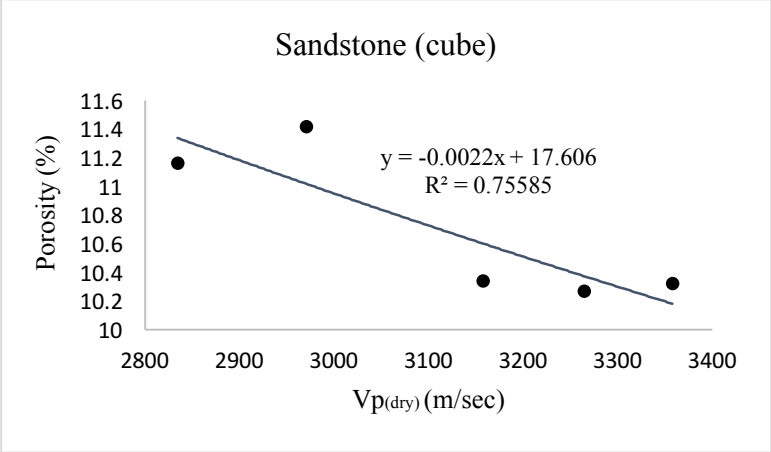

Figure 4.42 Graphical representation of dry Vp to porosity for Sandstone (cube)

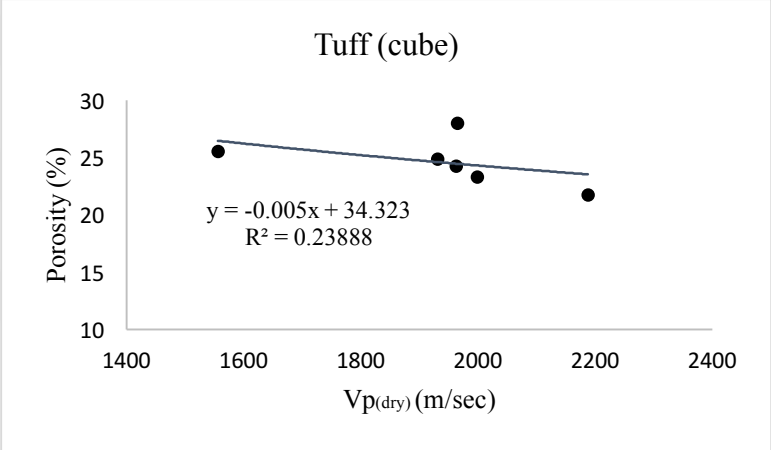

Figure 4.43 Graphical representation of dry Vp to porosity for Tuff (cube)

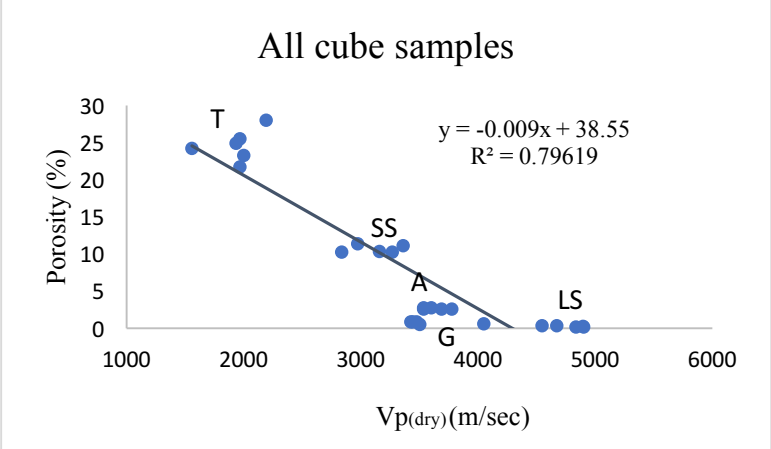

Figure 4.44 Graphical representation of dry Vp to porosity trend for all cube samples

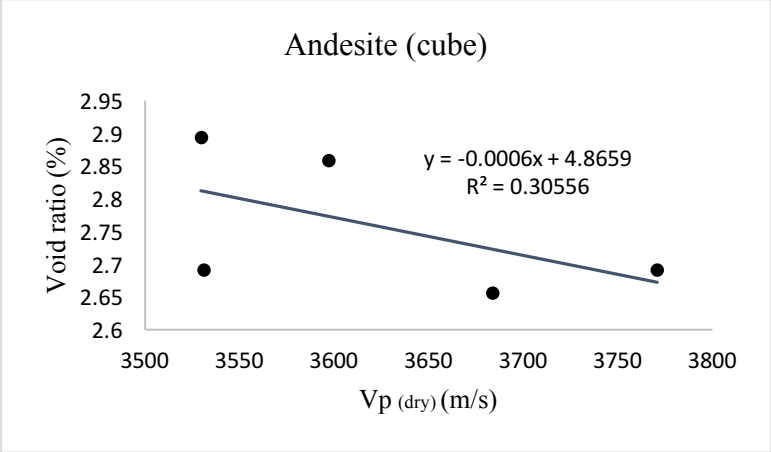

Figure 4.45 Graphical representation of dry Vp to void ratio for Andesite (cube)

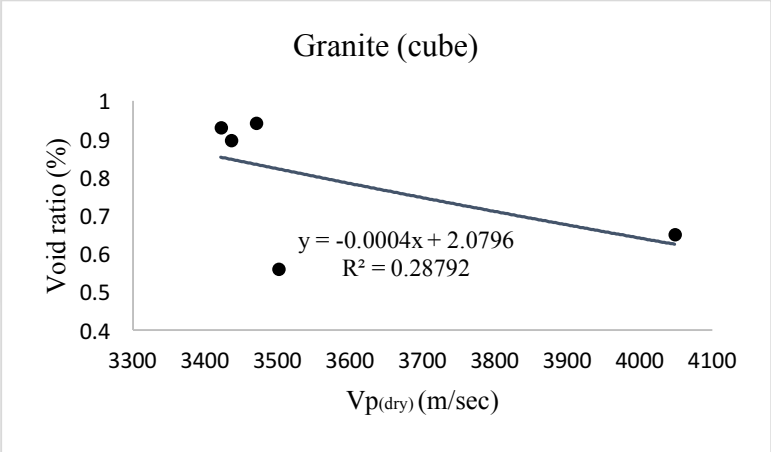

Figure 4.46 Graphical representation of dry Vp to void ratio for Granite (cube)

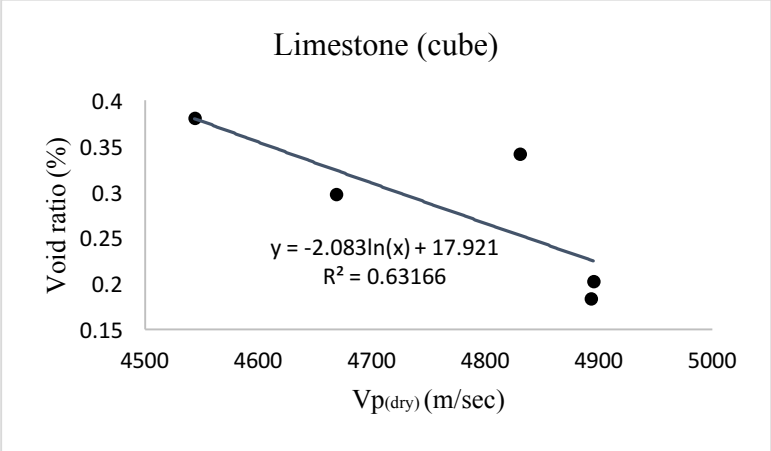

Figure 4.47 Graphical representation of dry Vp to void ratio for Limestone (cube)

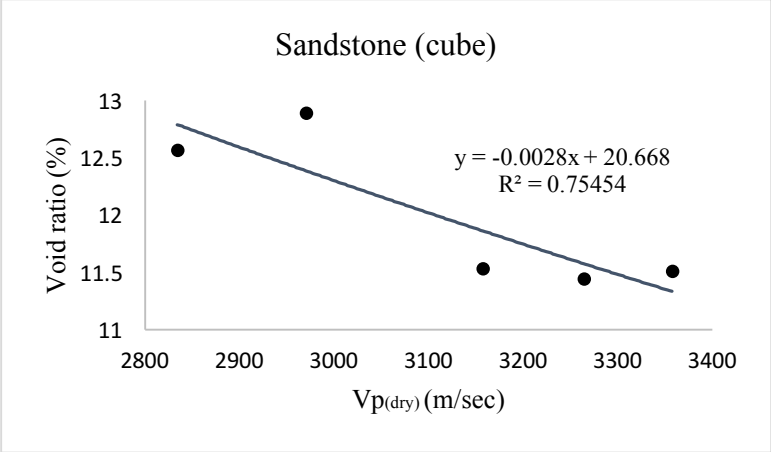

Figure 4.48 Graphical representation of dry Vp to void ratio for Sandstone (cube)

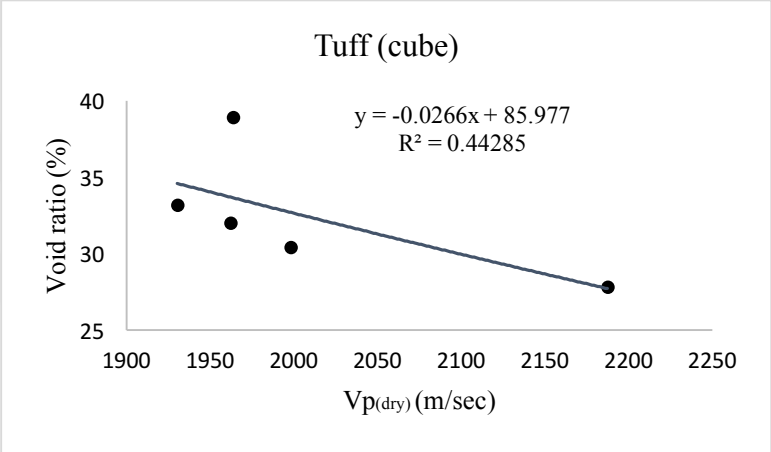

Figure 4.49 Graphical representation of dry Vp to void ratio for Tuff (cube)

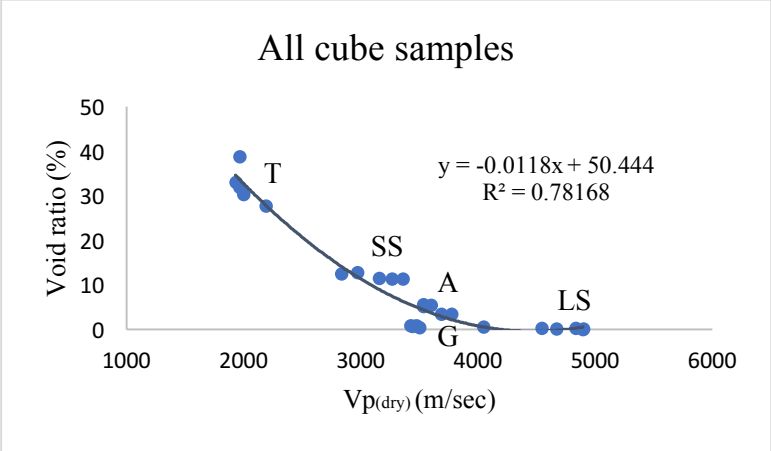

Figure 4.50 Graphical representation of dry Vp to void ratio trend for all cube samples

Table 4.5 Mean values of dry unit weight, saturated unit weight, porosity and void ratio of combine core and cube samples

Lithology		γ_{dry} (g/cm^3)	γ_{sat} (g/cm^3)	n (%)	e (%)	$Vp_{(dry)}$ (m/sec)	$Vp_{(sat)}$ (m/sec)
Andesite	**A.Mean**	2.435	2.462	2.636	2.708	3842.21	3852.06
	STDEV	0.021	0.021	0.146	0.155	248.15	274.24
Granite	**A.Mean**	2.677	2.687	1.001	1.011	3782.76	4309.57
	STDEV	0.004	0.004	0.219	0.223	290.25	205.05
Limestone	**A.Mean**	2.746	2.749	0.350	0.352	4912.53	5019.81
	STDEV	0.031	0.032	0.210	0.212	239.08	169.44
Sandstone	**A.Mean**	2.304	2.409	10.503	11.749	3163.81	3208.29
	STDEV	0.037	0.029	1.019	1.276	171.64	145.33
Tuff	**A.Mean**	1.473	1.719	24.640	32.834	2026.69	1567.93
	STDEV	0.075	0.066	2.490	4.387	122.24	227.94

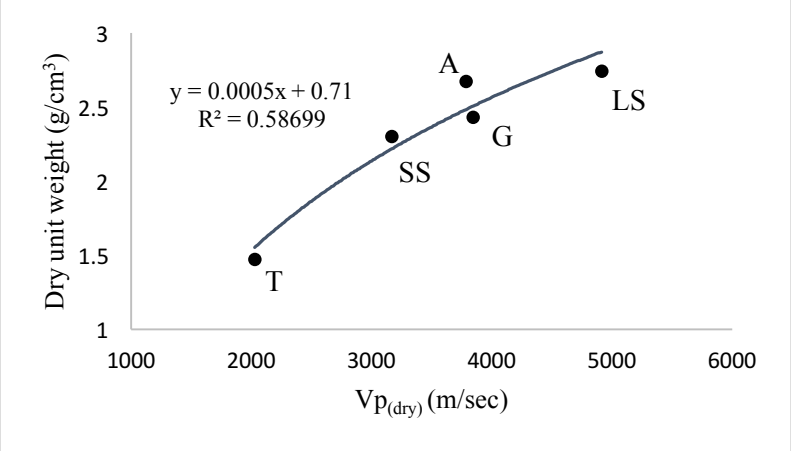

Figure 4.51 Graphical representation of Mean $Vp_{(dry)}$ to Mean dry unit weight trend

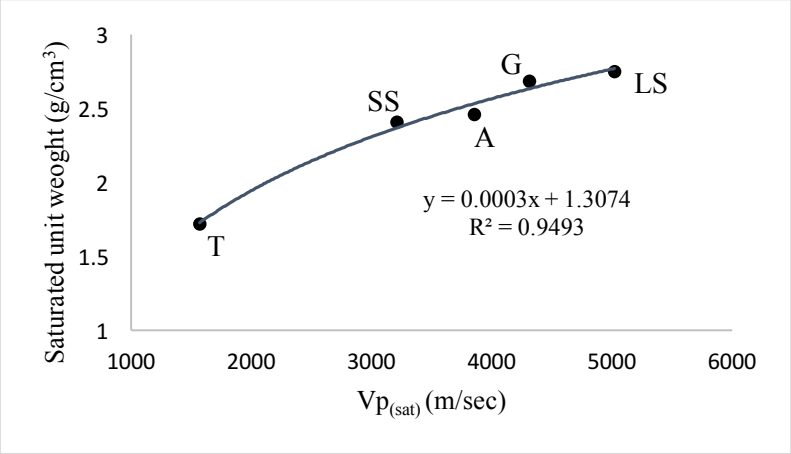

Figure 4.52 Graphical representation of Mean $Vp_{(sat)}$ to Mean saturated dry unit weight trend

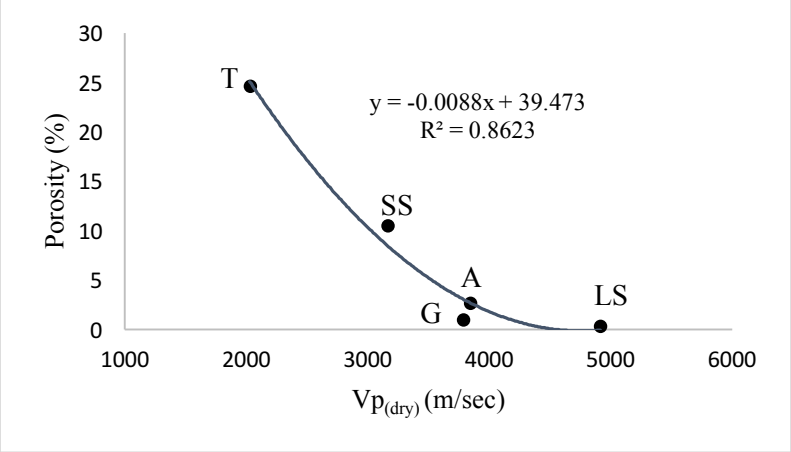

Figure 4.53 Graphical representation of Mean $Vp_{(dry)}$ to Mean porosity trend

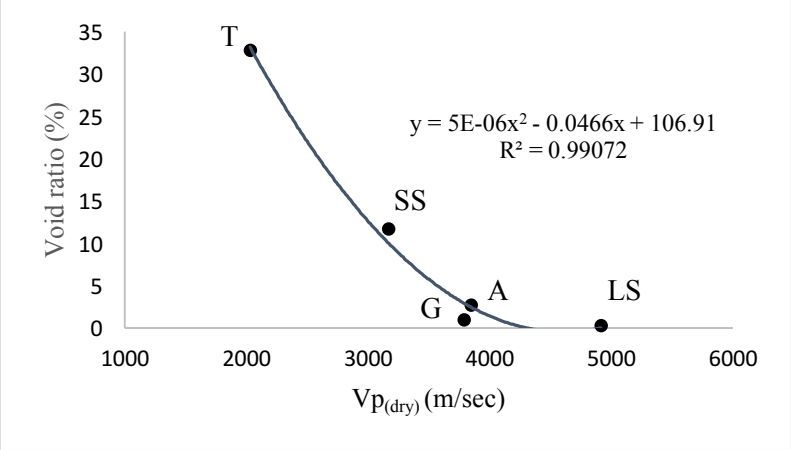

Figure 4.54 Graphical representation of Mean $Vp_{(dry)}$ to Mean void ratio trend

4.4 Time Average Equation

The time-average equation of Wyllie et al. (1956, 1958) has been used to obtain saturated velocity of rocks with porosities. Wyllie's time average equation calculates the velocity through a porous medium with a saturating fluid in its pore space (Wyllie et al., 1956, 1958). In water-saturated rock, the equation for P-wave velocity (Vp) is,

$$\frac{1}{V_p} = \frac{(1-n)}{V_m} + \frac{n}{V_w} \tag{4.1}$$

where " $\frac{1}{V_p}$ " is the seismic gap, "V_m" is the P-wave velocity in the rock matrix, "V_w" P-wave velocity in water that is 1500 m/s (Kahraman, 2007) and "n" is porosity.

4.4.1 Core Samples

Table 4.6 Estimated solid/matrix P-wave velocity and seismic gap for the core samples

S.No	Vw(m/s)	n	Vm (m/s)	1/Vp(sat) (s/m)
A-1	1500	0.02732	4174.03	0.000251
A-2	1500	0.02819	4137.43	0.000254
A-3	1500	0.02744	4241.28	0.000248
A-4	1500	0.02527	4264.49	0.000245
A-5	1500	0.02326	4240.26	0.000246
A.Mean		**0.0263**	**4211.50**	**0.000249**
STDEV		**0.00201**	**53.41**	**0.000004**
G-1	1500	0.0104	4660.70	0.000219
G-2	1500	0.01006	4574.72	0.000223
G-3	1500	0.01194	4502.15	0.000227
G-4	1500	0.01195	4460.60	0.000229
G-5	1500	0.01007	4488.21	0.000227
A.Mean		**0.01088**	**4537.28**	**0.000225**
STDEV		**0.00098**	**80.86**	**0.000004**
LS-1	1500	0.00086	5206.02	0.000192
LS-2	1500	0.00103	5198.17	0.000193
LS-3	1500	0.00812	5082.77	0.000201
LS-4	1500	0.00737	5081.45	0.000200
LS-5	1500	0.00405	5203.12	0.000194

Table 4.6 Continues

LS-6	1500	0.00076	5270.68	0.000190
A.Mean		**0.00370**	**5173.70**	**0.000195**
STDEV		**0.00338**	**75.75**	**0.000006**
SS-1	1500	0.010775	3411.84	0.000297
SS-2	1500	0.010353	3441.90	0.000294
SS-3	1500	0.012483	3280.13	0.000309
SS-4	1500	0.011447	3370.09	0.000301
SS-5	1500	0.011842	3165.27	0.000320
A.Mean		**0.01138**	**3333.85**	**0.000304**
STDEV		**0.00084**	**112.22**	**0.000010**
T-1	1500	0.025321	1341.26	0.000744
T-2	1500	0.022559	1480.29	0.000675
T-3	1500	0.02027	1186.20	0.000839
T-4	1500	0.02885	1614.35	0.000621
T-5	1500	0.0282	1844.46	0.000546
A.Mean		**0.00069**	**1493.32**	**0.000685**
STDEV		**0.00366**	**252.77**	**0.000113**

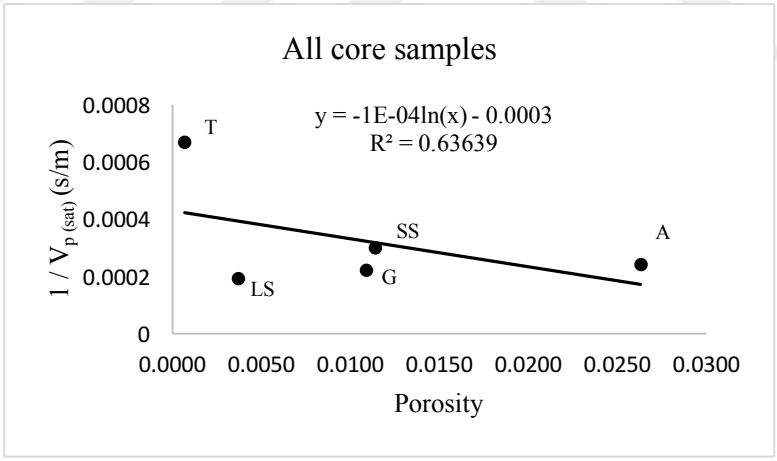

Figure 4.55 The calculated mean seismic gap value versus mean porosity for all core samples

4.4.2 Cube Samples

Table 4.7 Estimated solid/matrix P-wave velocity and seismic gap for the cube samples

S.No	Vw (m/s)	n	Vm (m/s)	1/Vp(sat) (s/m)
A-1	1500	0.05305	3798.51	0.000285
A-2	1500	0.03416	3703.97	0.000284
A-3	1500	0.0343	3917.61	0.000269
A-4	1500	0.05054	3697.94	0.000290
A-5	1500	0.05389	3749.93	0.000288
A.Mean		**0.04519**	**3773.59**	**0.000283**
STDEV		**0.01008**	**90.13**	**0.000008**
G-1	1500	0.00933	4125.71	0.000246
G-2	1500	0.00898	4141.63	0.000245
G-3	1500	0.00921	4124.66	0.000246
G-4	1500	0.00557	4107.32	0.000246
G-5	1500	0.00645	4321.20	0.000234
A.Mean		**0.00791**	**4164.10**	**0.000244**
STDEV		**0.00176**	**88.66**	**0.000005**
LS-1	1500	0.0038	4865.16	0.000207
LS-2	1500	0.00184	4904.19	0.000205
LS-3	1500	0.00202	4840.12	0.000208
LS-4	1500	0.00297	4907.68	0.000205
LS-5	1500	0.00341	4840.51	0.000208
A.Mean		**0.00281**	**4871.53**	**0.000207**
STDEV		**0.00086**	**33.03**	**0.000002**
SS-1	1500	0.010322	2993.45	0.000337
SS-2	1500	0.010341	3203.87	0.000316
SS-3	1500	0.011417	3070.27	0.000330
SS-4	1500	0.010271	3184.64	0.000318
A.Mean		**0.01059**	**3113.06**	**0.000325**
STDEV		**0.00055**	**99.18**	**0.000010**
T-1	1500	0.024249	1835.98	0.000548
T-2	1500	0.021778	1688.97	0.000594
T-3	1500	0.02333	1685.71	0.000595
T-4	1500	0.025557	1649.83	0.000608
T-5	1500	0.024914	1575.25	0.000636
T-6	1500	0.028017	2017.00	0.000501
A.Mean		**0.02464**	**1742.12**	**0.00058**
STDEV		**0.00212**	**159.21**	**0.00005**

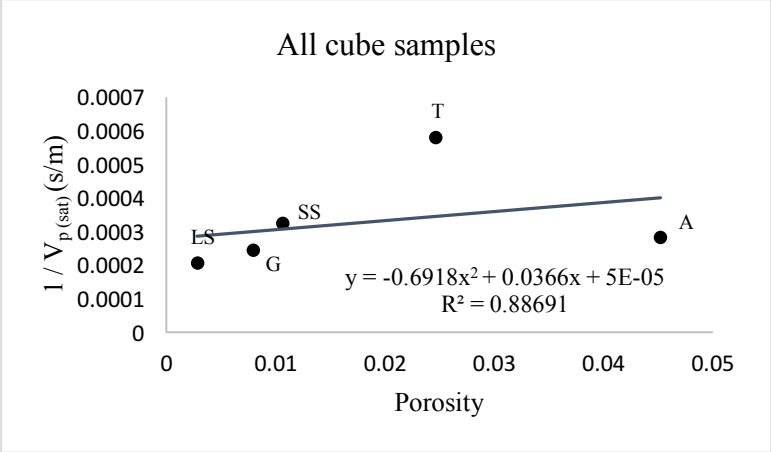

Figure 4.56 The calculated mean seismic gap value versus mean porosity for all cube samples

Table 4.8 Mean Estimated solid/matrix P-wave velocity and seismic gap for core and cube samples

Lithology		n	V_m (m/s)	$1/Vp_{(sat)}$ (s/m)
Andesite	**A.Mean**	0.0357	3992.55	0.000266
	STDEV	0.012	241.13	1.91137E-05
Granite	**A.Mean**	0.00940	4350.69	0.000234
	STDEV	0.002	212.33	0.000011
Limestone	**A.Mean**	0.00330	5036.35	0.000200
	STDEV	0.002	167.95	0.000007
Sandstone	**A.Mean**	0.01103	3235.72	0.000314
	STDEV	0.001	153.38	0.000015
Tuff	**A.Mean**	0.02482	1692.03	0.000628
	STDEV	0.003	234.76	0.000096

V_w = 1500 (m/s)

CHAPTER FIVE
MECHANICAL PROPERTIES OF CUBE ROCK SAMPLES

5.1 Compressive Strength Experiment

The compressive strength of the rocks is determined according to TS EN 1926 (TSE, 2013). The rocks were cut into 7x7x7 sized cubes as specified in the standard. Care has been taken to ensure that the upper and lower surfaces to be tested are parallel to one another and that there is no defect from the cut. The samples were then broken by 300 tones of press (Figures 5.1). The compressive strength (σ_c) of the rocks is calculated from the following equation.

$$\sigma_c = \frac{F}{Ar} \tag{5.1}$$

Ar: Cross-sectional area of pre-test sample (cm^2)

F: Fracture load (kgf)

σ_c**:** Uniaxial compressive strength of tested sample (kgf/cm^2)

Figure 5.1 Compressive strength test

Table 5.1 Compressive strength test results of cube samples

Sample No.	Length (cm)	Width (cm)	Height (cm)	Ar (cm^2)	F (kgf)	σ_c (kgf/cm^2)
A-1	6.980	7.280	6.892	50.81	56685	1115.53
A-2	7.066	7.284	7.020	51.47	49922	969.95
A-3	6.695	7.328	6.994	49.06	48850	995.70
A-4	6.698	7.327	6.998	49.08	51863	1056.78
A-5	7.309	6.689	7.012	48.89	48418	990.35
				Arithmetic mean		**1025.66**
				Standard deviation		**59.78**
G-1	7.091	7.00	6.974	49.64	71530	1441.06
G-2	7.075	7.068	7.075	50.01	72210	1444.02
G-3	7.054	7.151	7.054	50.44	75820	1503.08
G-4	7.179	6.943	7.020	49.84	83500	1675.23
G-5	7.12	7.087	7.055	50.46	73420	1455.03
				Arithmetic mean		**1503.69**
				Standard deviation		**99.09**
LS-1	7.022	6.968	6.994	48.86	110933	2270.47
LS-2	6.986	6.984	7.018	48.79	99735	2044.15
LS-3	7.010	7.120	7.014	49.84	78066	1566.33
LS-4	7.10	7.022	6.988	49.70	73361	1476.08
LS-5	6.912	7.012	6.978	48.37	109111	2255.76
				Arithmetic mean		**1922.56**
				Standard deviation		**378.51**
SS-1	7.012	7.120	7.012	49.77	25200	506.32
SS-2	6.980	7.054	7.008	49.21	23800	483.65
SS-3	7.022	6.964	7.062	48.86	27000	552.61
SS-4	6.956	7.012	6.988	48.93	25500	521.17
SS-5	6.968	6.948	6.996	48.30	24800	513.43
				Arithmetic mean		**515.44**
				Standard deviation		**25.06**
T-1	6.964	6.984	6.686	48.64	8220	169.01
T-2	6.97	7.004	7.002	48.82	7750	158.75
T-3	6.948	7.006	7.012	48.68	7590	155.92
T-4	7.018	6.984	7l050	49.01	8510	173.62
T-5	7.051	6.958	6.988	49.06	7720	157.36
				Arithmetic mean		**162.93**
				Standard deviation		**7.89**

5.2 Bending Strength Experiment

The bending strengths of rocks under intense load are determined according to TS EN 12372 (TSE, 2013)

As stated in the standard of rocks; it was prepared by cutting in 3 times thickness and 6 times thickness. It was then placed on two cylindrical supports to break the sample with gradually increasing load (Figures 5.2 and Figure 5.3). The bending strength of rocks under intense load is calculated from the following equation.

$$\sigma_b = \frac{3Fl}{2bh^2} \tag{5.2}$$

The result is expressed in kgf/cm^2 approx. 1 MPa.

σ_b: Bending strength under heavy load (kgf/cm^2)

F: Fracture load (kgf)

l: Distance between support rollers (cm)

b: Width adjacent to the fracture plane of the sample (cm)

H: The thickness of the sample adjacent to the plane of fracture (cm)

h: Total length of the sample (cm)

Figure 5.2 Practice of bending strength under heavy load

Figure 5.3 Bending strength test

Table 5.2 Bending strength experiment results of cube samples

S. No	h (cm)	b (cm)	H (cm)	l (cm)	F (kgf)	σ_b (kgf/cm^2)
A-1	30	15.50	5.13	25	1335	122.82
A-2	30	15.44	5.23	25	1208	107.27
A-3	30	15.20	5.33	25	1081	94.05
A-4	30	15.29	5.26	25	1304	115.73
A-5	30	15.45	5.17	25	1113	101.20
					Arithmetic mean	**108.21**
					Standard deviation	**10.20**
G-1	30	15.12	4.93	25	1049	107.29
G-2	30	15.75	5.01	25	1113	105.56
G-3	30	15.13	5.01	25	1177	116.21
G-4	30	15.18	4.92	25	954	97.35
G-5	30	15.19	4.95	25	954	96.11
					Arithmetic mean	**104.50**
					Standard deviation	**7.32**
LS-1	30	15.02	5.05	25	1844	180.54
LS-2	30	15.02	5.18	25	827	76.93
LS-3	30	15.10	5.11	25	1749	166.32
LS-4	30	15.10	5.03	25	1335	131.08
LS-5	30	15.02	5.14	25	1430	135.25
					Arithmetic mean	**138.02**
					Standard deviation	**39.99**
SS-1	30	15.01	5.03	25	890.29	87.91
SS-2	30	14.99	5.12	25	826.69	78.89
SS-3	30	15.1	5.03	25	794.90	78.02
SS-4	30	151	5.03	25	635.92	62.42
SS-5	30	15.016	5.08	25	731.31	70.77
					Arithmetic mean	**75.60**
					Standard deviation	**9.56**
T-1	30	15.16	5.13	25	268	25.15
T-2	30	15.30	5.05	25	260	24.98
T-3	30	15.14	5.11	25	271	25.72
T-4	30	15.13	5,08	25	323	31.02
					Arithmetic mean	**26.72**
					Standard deviation	**2.88**

5.3 Abrasion Resistance Experiment

The abrasion resistances of the rocks were made according to the methods specified in TS EN 14157 (TSE, 2005) standard both in the "Böhme Experiment" and "Wide Wheel Experiments".

5.3.1 Wide Disc Abrasion Experiment

This experiment is based on the principle of measuring the size of the cavity (mm) formed on a rotating discrete stone surface. The experiment was carried out on rock samples cut into 5x10x10 cm^3. After the rock specimens were placed in the large disc test apparatus, the White fused alumina (5 liters) was supplied as an abrasive between the rotating disc and the specimen surface, and the disc was completed with 75 revolutions in total. The size of the cavity formed with the abrasive powder on the surface of the rocks was calculated from 3 points (Figure 5.4).

Figure 5.4 Abrasion resistance test with large disc

Table 5.3 Wide disc abrasion experiment results of cube samples

S. No	1st measurement (mm)	2nd measurement (mm)	3rd measurement (mm)	Arithmetic mean of the groove
A-1	15.93	16.72	17.64	16.76
A-2	17.15	18.04	18.85	18.01
A-3	17.42	16.96	17.93	17.44
			Arithmetic mean	**17.40**
			Standard deviation	**0.63**
G-1	16.06	16.01	16.73	16.27
G-2	16.01	16.74	16.74	16.50
G-3	14.75	14.75	15.63	15.04
			Arithmetic mean	**15.94**
			Standard deviation	**0.781**
LS-1	17.84	18.2	19.15	18.40
LS-2	17.4	18.2	19.15	18.25
LS-3	17.4	18.2	19.15	18.25
			Arithmetic mean	**18.30**
			Standard deviation	**0.07**
SS-1	26.61	26.62	26.62	26,62
SS-2	26.43	26.51	26.75	26,56
SS-3	28.71	27.17	27.06	27,65
			Arithmetic mean	**26.94**
			Standard deviation	**0.61**
T-1	32.33	33.66	32.19	32.73
T-2	36.56	36.67	36.6	36.61
T-3	38.26	38.66	38.71	38.54
			Arithmetic mean	**35.96**
			Standard deviation	**2.96**

5.3.2 Böhme Abrasion Test

The rock samples cut at 7x7x7 cm^3 are placed on a disk rotating under a load of 294 newtons (Figure 5.5) and twenty-two turns were provided using 20 g of abrasive material (artificial corundum) and this was repeated 16 times according to the TS EN 14157 (TSE, 2005). Resistance against erosion of 352 turns in total is calculated as volume reduction in mm^3.

The average loss (Δv) in the sample volume is the abrasion caused by the abrasive material after 16 cycles;

$$\Delta V = \frac{\Delta m}{Pb} \tag{5.3}$$

where;

ΔV : volume loss after 16 cycles (mm^3) to the nearest mm^3

Δm : (mi-m1) mass loss after 16 cycles (gr) to the nearest 0.1 gr

Pb **:** The apparent density of the sample or the apparent density of the wearing layer in the case of multi-layered samples (gr/mm^3).

Figure 5.5 Böhme abrasion test

Table 5.4 Böhme abrasion test results of cube samples

S. No	V_0 (mm^3)	V_1 (mm^3)	V (mm^3)
A-1	354588	339455	15134
A-2	355647	342306	13341
A-3	349782	330978	18804
		Arithmetic mean	**15760**
		Standard deviation	**2785**
G-1	353430	349820	3610
G-2	345180	341210	3972
G-3	354410	350730	3680
		Arithmetic mean	**3754**
		Standard deviation	**192**
LS-1	345340	337880	7460
LS-2	345140	337580	7560
LS-3	348390	341140	7250
		Arithmetic mean	**7423**
		Standard deviation	**158**
SS-1	373470	338290	35180
SS-2	376180	329050	47130
SS-3	375410	337180	38230
		Arithmetic mean	**40180**
		Standard deviation	**6209**
T-1	339210	311600	27610
T-2	339430	313680	25750
T-3	339480	316400	23080
		Arithmetic mean	**25480**
		Standard deviation	**2277**

5.4 Relationship Between P-Wave Velocity and Mechanical Properties of Cube Samples

Mechanical properties have a great effect on the velocity of P-waves. Compressive strength is one of the most important mechanical property of rock.

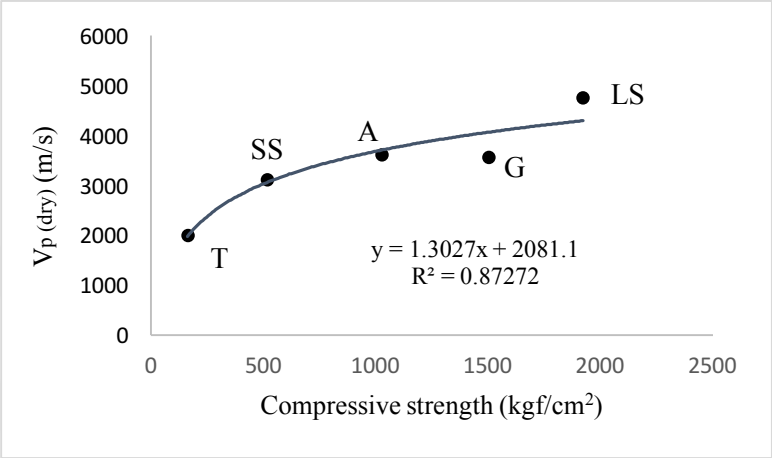

Figure 5.6 Graphical representation of dry Vp to compressive strength trend of all cube samples

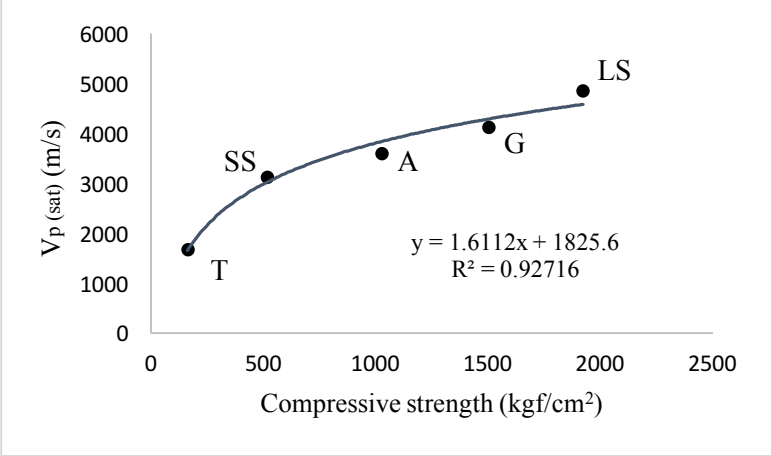

Figure 5.7 Graphical representation of saturated Vp to compressive strength trend of all cube samples

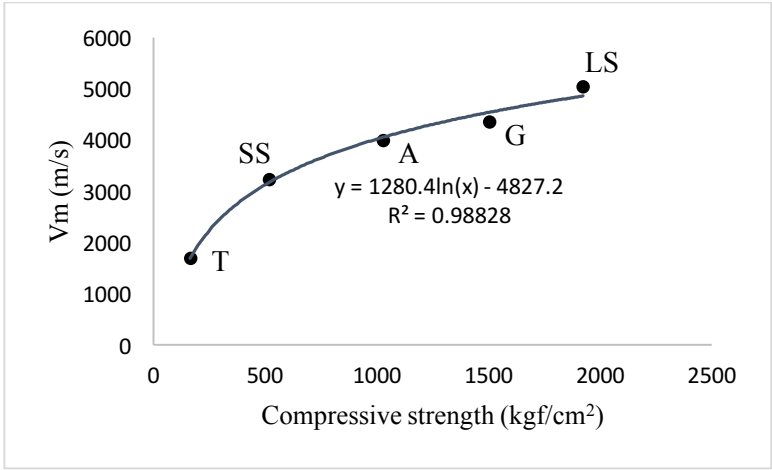

Figure 5.8 Graphical representation of Vm to compressive strength trend of all cube samples

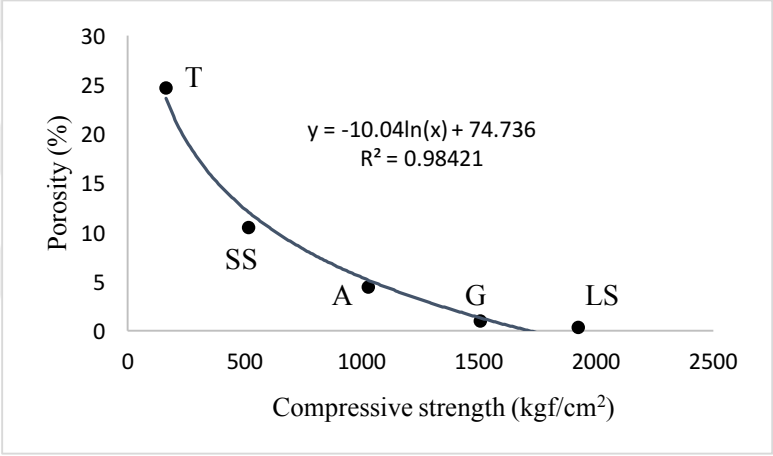

Figure 5.9 Graphical representation of porosity to compressive strength trend of all cube samples

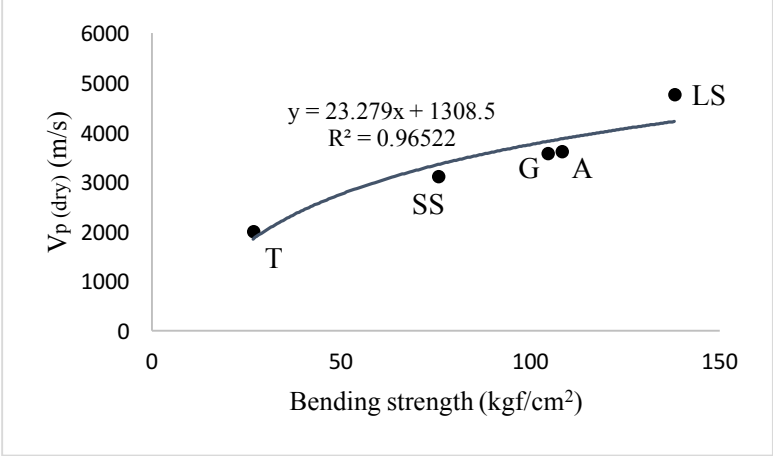

Figure 5.10 Graphical representation of dry Vp to bending strength trend of all cube samples

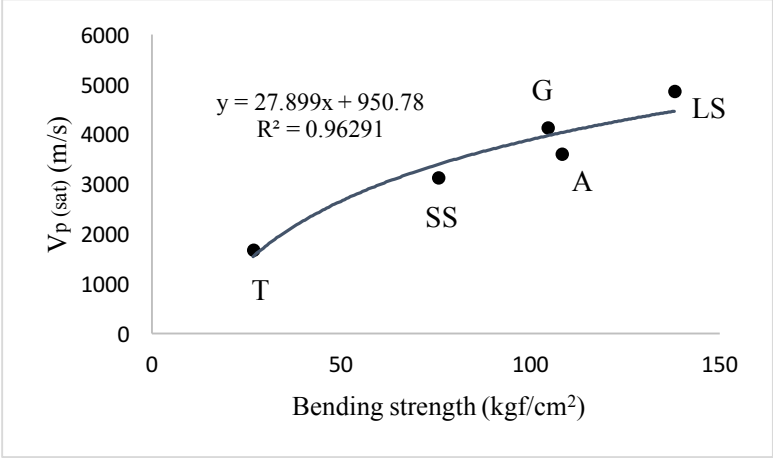

Figure 5.11 Graphical representation of saturated Vp to bending strength trend of all cube samples

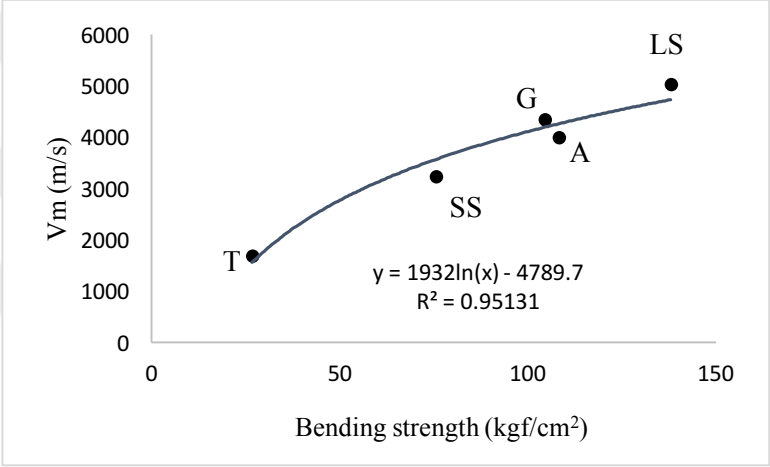

Figure 5.12 Graphical representation of Vm to bending strength trend of all cube samples

Experiments done on cube samples in the laboratory showed that the cube samples with more compressive and bending strength had more P-wave velocity value. Limestone cube samples which were dolomitic in nature, had the highest compressive and bending strength among all other four types of rocks samples which resulted in the highest P-wave velocity in limestone cube samples than all other rock samples. Tuff cube sample's compressive and bending strength was the least among all the cube samples due to which the P-wave velocity was least too.

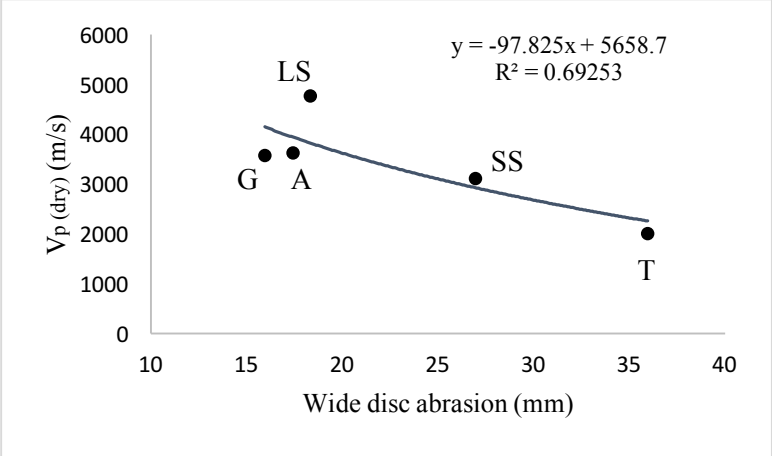

Figure 5.13 Graphical representation of dry Vp to wide disc abrasion trend of all cube samples

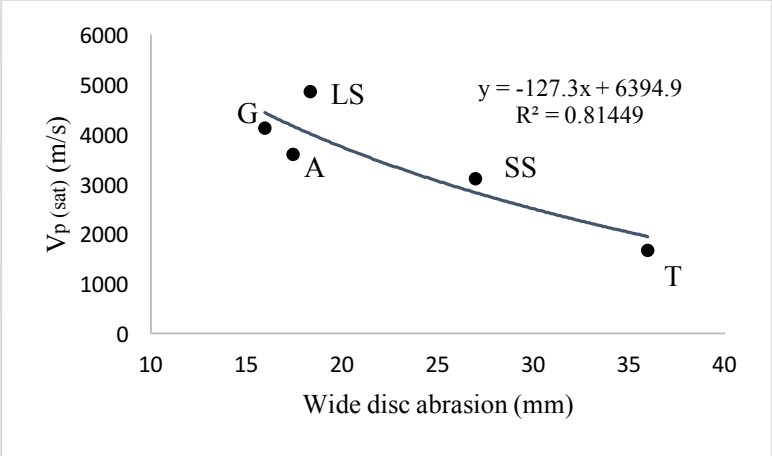

Figure 5.14 Graphical representation of saturated Vp to wide disc abrasion trend of all cube samples

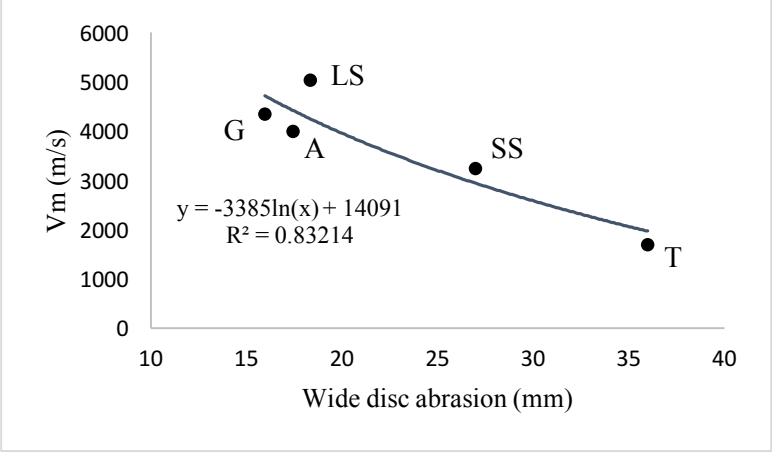

Figure 5.15 Graphical representation of Vm to wide disc abrasion trend of all cube samples

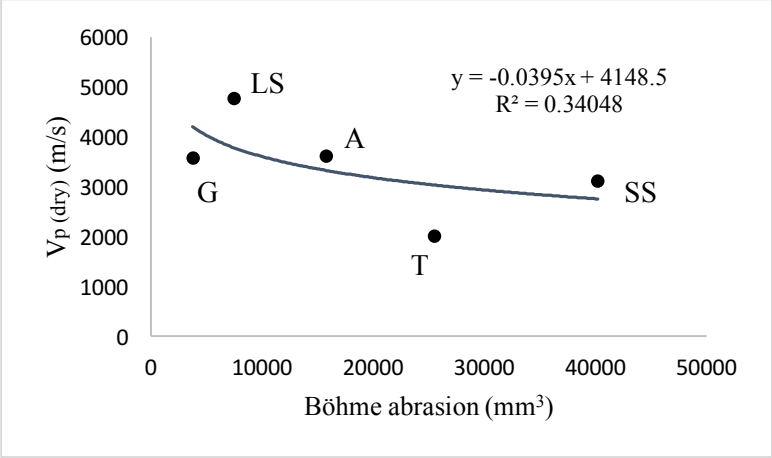

Figure 5.16 Graphical representation of dry Vp to Böhme abrasion trend of all cube samples

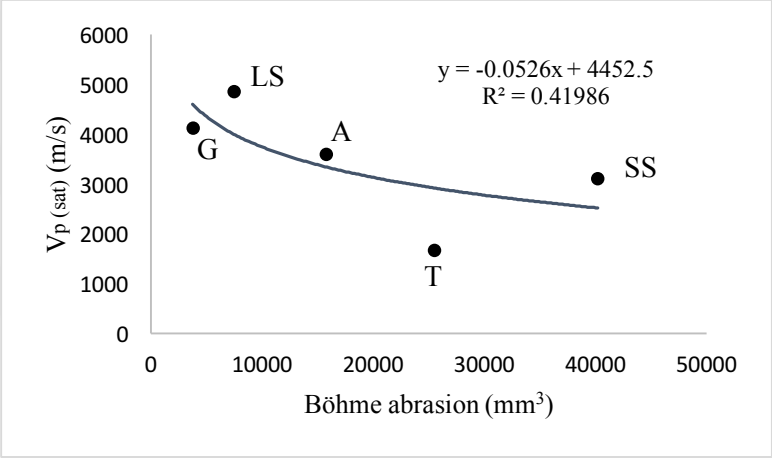

Figure 5.17 Graphical representation of saturated Vp to Böhme abrasion trend of all cube samples

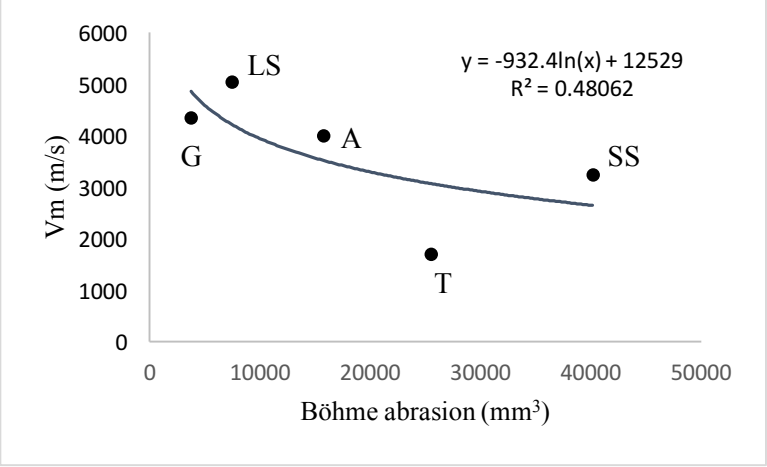

Figure 5.18 Graphical representation of Vm to Böhme abrasion trend of all cube samples

Two different types of abrasion resistance experiments were performed during the study, wide disc abrasion experiment and Böhme abrasion experiment. Both experiments were performed on cube rock samples. The results showed that the P-wave velocity has inverse relation with abrasion.

CHAPTER SIX
PHYSICAL PROPERTIES OF AGGREGATE SAMPLES

6.1 Size and shape of Granular Samples Used in This Study

Particle shape and size are very important characteristics of granular materials. The structure of particles show their mechanical behavior. Structure mainly depends on the size, shape and arrangement of particles. Particle shape is scale dependent.

Table 6.1 Methods for Particle Shape Characterization from Hawkins (1993), Santamarina et al. (2001), and Bowman et al. (2001)

Method	Definition
Morphology–Sphere	
Sphericity 1	$\frac{\text{Diameter of a sphere of equal volume}}{\text{Diameter of circumscribing sphere}}$
Sphericity 2	$\frac{\text{Particle volume}}{\text{Volume of circumscribing sphere}}$
Sphericity 3	
Projection sphericity	$\frac{\text{Area of particle outline}}{\text{Area of a circle with diameter equal to the longest length of outline}}$
Inscribed circle sphericity	$\frac{\text{Diameter of the largest inscribed circle}}{\text{Diameter of the smallese inscribed circle}}$
Morphology–Ellipse	
Eccentricity	δ_p/R_{ap}, where the ellipse is characterized by $R_p+\delta_p cos2\theta$ in polar coordinates
Elongation	$\frac{\text{Smallest diameter}}{\text{Diameter perpendicular to the smallest diameter}}$
Slenderness	$\frac{\text{Maximum dimension}}{\text{Minimum dimension}}$
Texture–Roundness	
Roundness 1	$\frac{\text{Average of radius of curveture of surface features, } \left(\sum r_i\right)/N}{\text{Radius of the maximum sphere that can be inscribed, } r_{max}}$
Roundness 2	$\frac{\text{Radius of curveture of the most convex part}}{\text{0.5 (longest diameter through the most convex part)}}$
Roundness 3	$\frac{\text{Radius of curveture of the most convex part}}{\text{Mean radius}}$
Morphology/Texture	
Fourier method	Eq. (4.3), first and second harmonics characterize sphericity, whereas higher harmonics (around 10^{th}) characterize roundness. Surface texture is characterized by much higher harmonics.
Fourier descriptor method	More flexible that the Fourier method by using the complex plane (Bowman et al., 2001). Lower harmonics give shape characteristics such as elongation, triangularity, squareness, and asymmetry. Higher harmonics (larger than 8^{th}) give textural features.
Fractal analysis	Use as a measure of texture (Vallejo, 1995; Santamarina et al. 2001).

At smaller scale, texture which explains the roundness of corners, asperities and surface smoothness were being study. At larger scale, it is called particle morphology which explains sphericity, bulkiness, elongation and roundness of the particle itself. Roundness and sphericity of grains defined by Powers in 1953.

6.1.1 Andesite

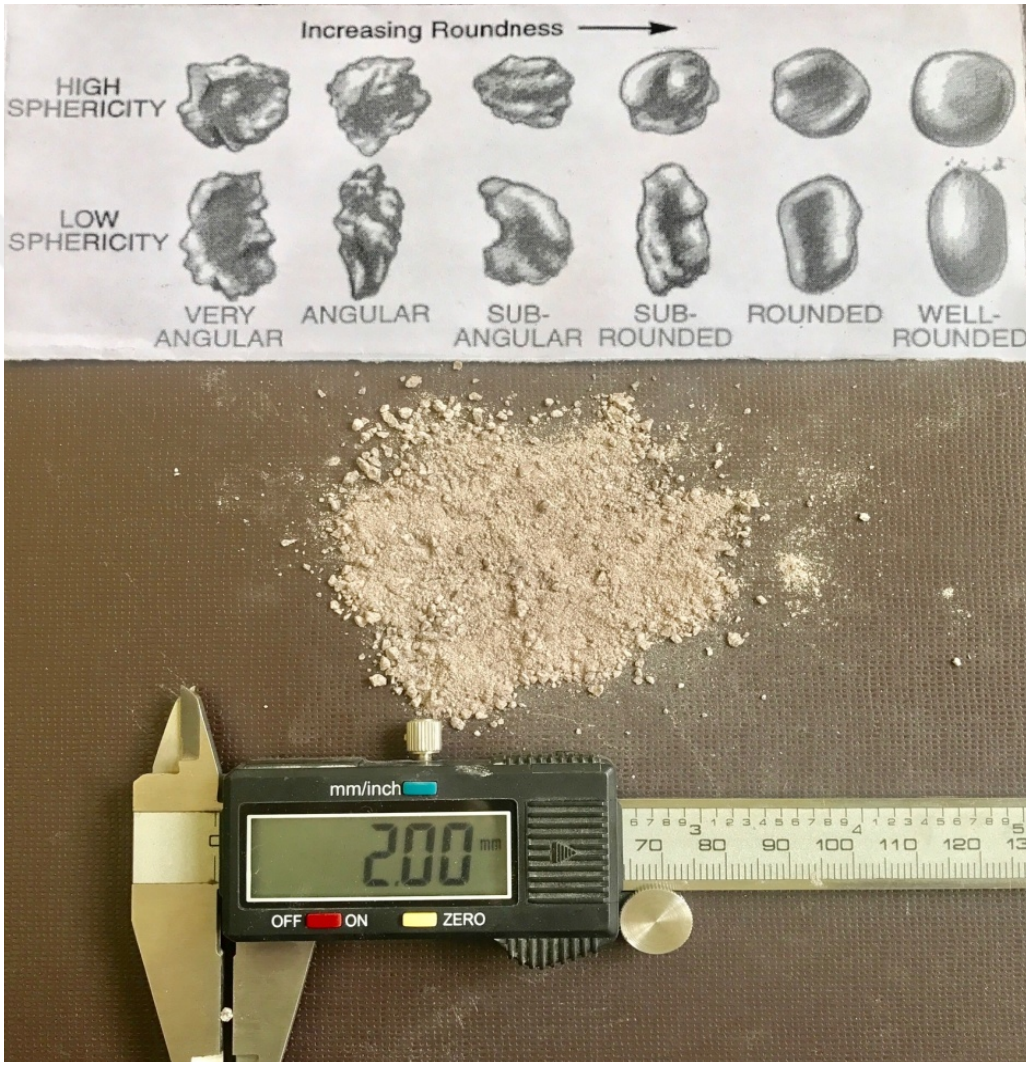

Figure 6.1 Andesite aggregate with 0-2 mm grain size (Personal archive, 2017)

Lithology	Grain size	Roundness	Sphericity
Andesite	0-2 mm	Rounded to sub rounded	Low sphericity

Figure 6.2 Andesite aggregate with 2-4 mm grain size (Personal archive, 2017)

Lithology	**Grain size**	**Roundness**	**Sphericity**
Andesite	2-4 mm	Sub-rounded to sub-angular	Low sphericity

Figure 6.3 Andesite aggregate with 4-8 mm grain size (Personal archive, 2017)

Lithology	**Grain size**	**Roundness**	**Sphericity**
Andesite	4-8 mm	Rounded to sub-rounded	Low sphericity

Figure 6.4 Andesite aggregate with 8-10 mm grain size (Personal archive, 2017)

Lithology	**Grain size**	**Roundness**	**Sphericity**
Andesite	8-10 mm	Rounded to sub-rounded	Low sphericity

6.1.2 Granite

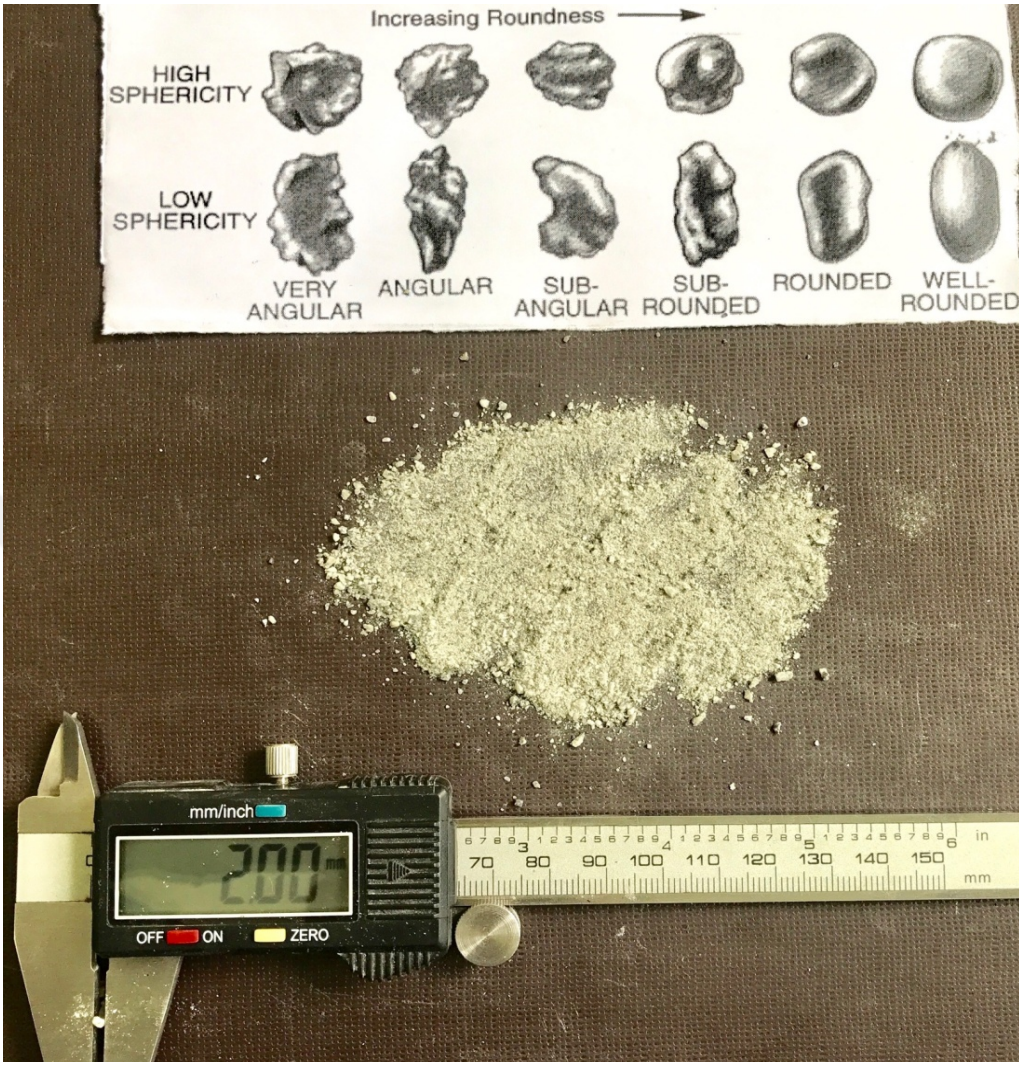

Figure 6.5 Granite aggregate with 0-2 mm grain size (Personal archive, 2017)

Lithology	Grain size	Roundness	Sphericity
Granite	0-2 mm	Rounded to sub-rounded	Low sphericity

Figure 6.6 Granite aggregate with 2-4 mm grain size (Personal archive, 2017)

Lithology	**Grain size**	**Roundness**	**Sphericity**
Granite	2-4 mm	Sub-rounded to sub-angular	Low sphericity

Figure 6.7 Granite aggregate with 4-8 mm grain size (Personal archive, 2017)

Lithology	**Grain size**	**Roundness**	**Sphericity**
Granite	4-8 mm	Rounded to sub-rounded	Low sphericity

Figure 6.8 Granite aggregate with 8-10 mm grain size (Personal archive, 2017)

Lithology	**Grain size**	**Roundness**	**Sphericity**
Granite	8-10 mm	Sub-rounded to sub-angular	Low sphericity

6.1.3 Limestone

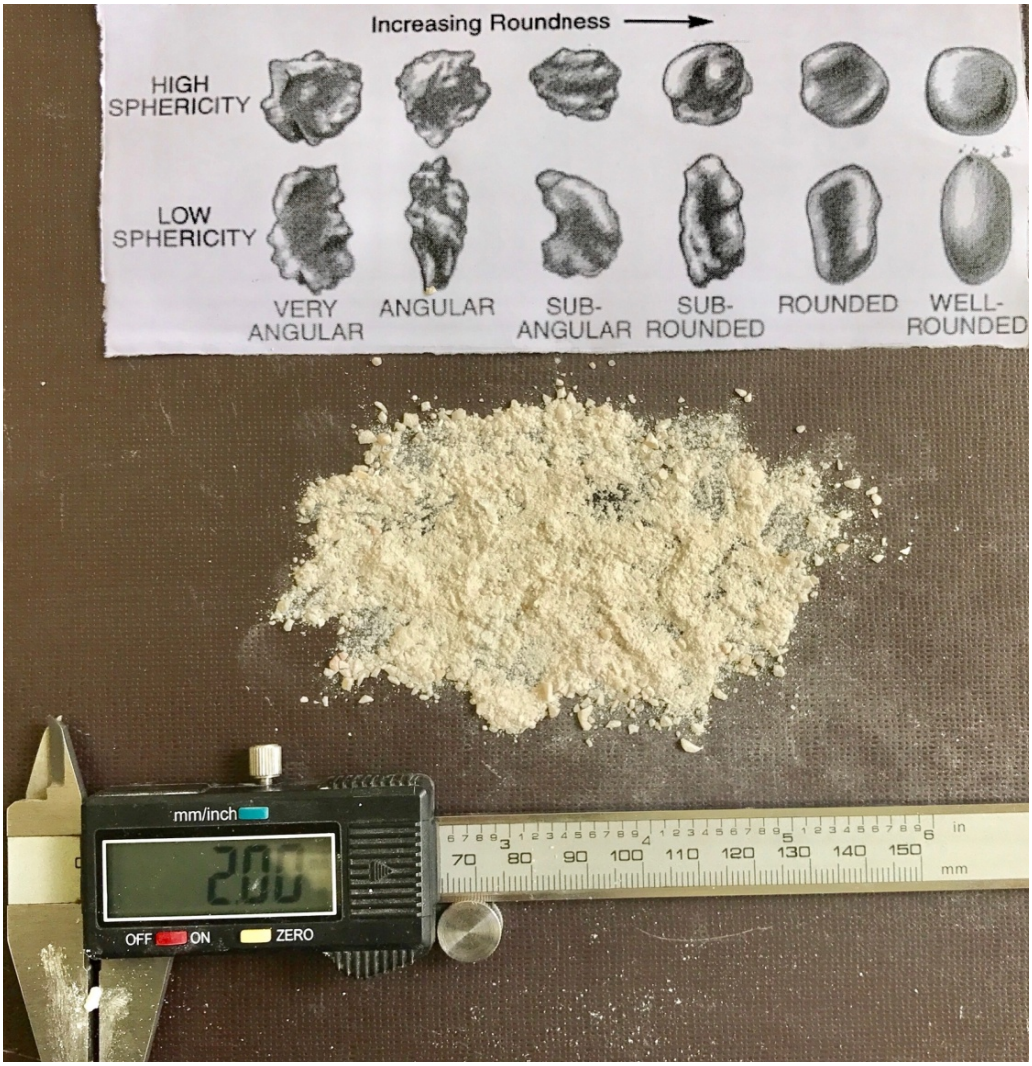

Figure 6.9 Limestone aggregate with 0-2 mm grain size (Personal archive, 2017)

Lithology	**Grain size**	**Roundness**	**Sphericity**
Limestone	0-2 mm	Sub-rounded to sub-angular	Low sphericity

Figure 6.10 Limestone aggregate with 2-4 mm grain size (Personal archive, 2017)

Lithology	**grain size**	**Roundness**	**Sphericity**
Limestone	2-4 mm	Sub- angular to Angular	Low sphericity

Figure 6.11 Limestone aggregate with 4-8 mm grain size (Personal archive, 2017)

Lithology	**Grain size**	**Roundness**	**Sphericity**
Limestone	4-8 mm	Sub-rounded to Sub-angular	Low sphericity

Figure 6.12 Limestone aggregate with 8-10 mm grain size (Personal archive, 2017)

Lithology	**Grain size**	**Roundness**	**Sphericity**
Limestone	8-10 mm	Sub-rounded to Sub-angular	Low sphericity

6.1.4 Sandstone

Figure 6.13 Sandstone aggregate with 0-2 mm grain size (Personal archive, 2017)

Lithology	**Grain size**	**Roundness**	**Sphericity**
Sandstone	0-2 mm	Rounded to Sub-rounded	Low sphericity

Figure 6.14 Sandstone aggregate with 2-4 mm grain size (Personal archive, 2017)

Lithology	**Grain size**	**Roundness**	**Sphericity**
Sandstone	2-4 mm	Sub-rounded to Sub-angular	Low sphericity

Figure 6.15 Sandstone aggregate with 4-8 mm grain size (Personal archive, 2017)

Lithology	**Grain size**	**Roundness**	**Sphericity**
Sandstone	4-8 mm	Rounded to Sub-rounded	Low sphericity

Figure 6.16 Sandstone aggregate with 8-10 mm grain size (Personal archive, 2017)

Lithology	**Grain size**	**Roundness**	**Sphericity**
Sandstone	8-10 mm	Rounded to Sub-rounded	Low sphericity

6.1.5 Tuff

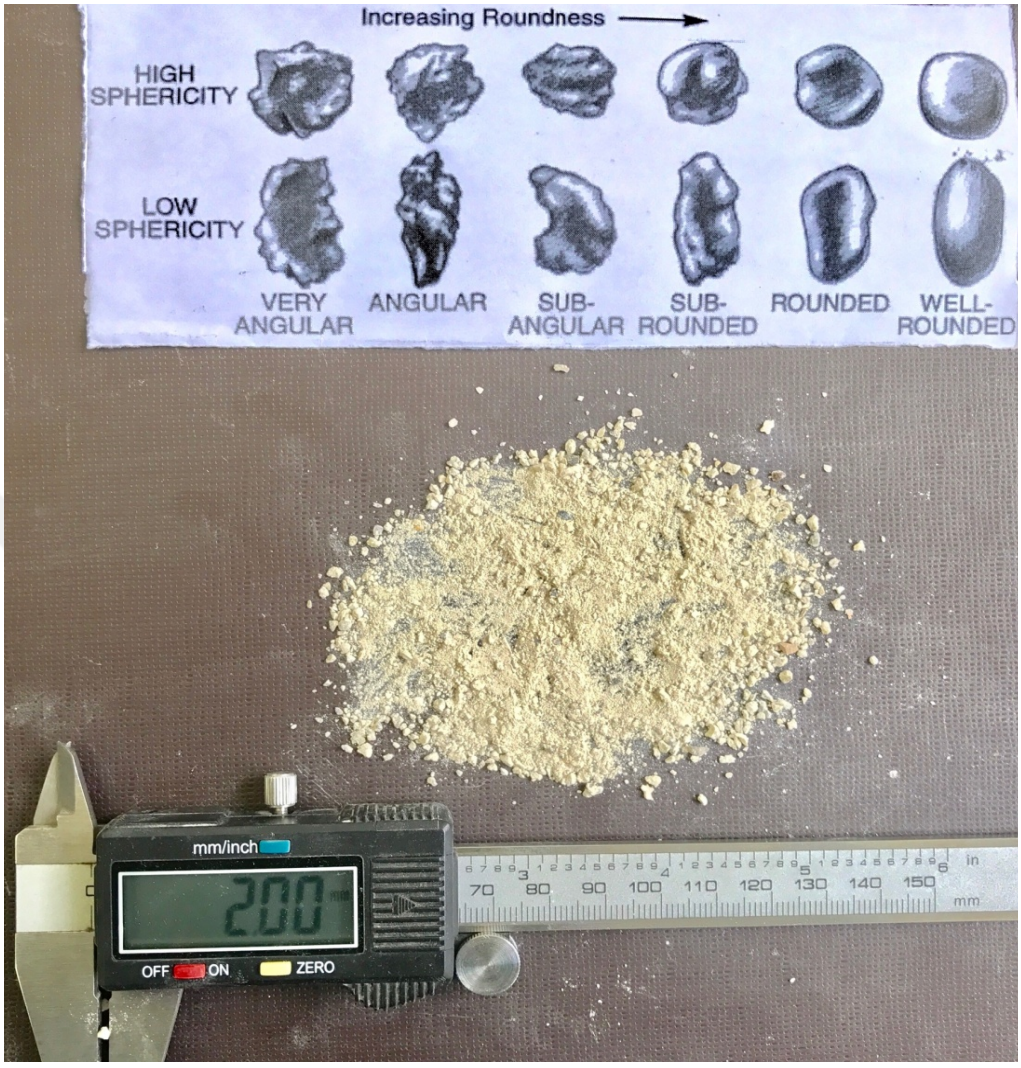

Figure 6.17 Tuff aggregate with 0-2 mm grain size (Personal archive, 2017)

Lithology	**Grain size**	**Roundness**	**Sphericity**
Tuff	0-2 mm	Rounded to Sub-rounded	Low sphericity

Figure 6.18 Tuff aggregate with 2-4 mm grain size (Personal archive, 2017)

Lithology	**Grain size**	**Roundness**	**Sphericity**
Tuff	2-4 mm	Sub-rounded to Sub-angular	Low sphericity

Figure 6.19 Tuff aggregate with 4-8 mm grain size (Personal archive, 2017)

Lithology	**Grain size**	**Roundness**	**Sphericity**
Tuff	4-8 mm	Sub-rounded to Sub-angular	Low sphericity

Figure 6.20 Tuff aggregate with 8-10 mm grain size (Personal archive, 2017)

Lithology	**Grain size**	**Roundness**	**Sphericity**
Tuff	8-10 mm	Sub-rounded to Sub-angular	Low sphericity

Table 6.2 Size and shape of aggregates used in this study

Lithology	Grain size	Roundness	Sphericity
Andesite	0-2 mm	Rounded to sub-rounded	Low sphericity
	2-4 mm	Sub-rounded to sub-angular	Low sphericity
	4-8 mm	Rounded to sub-rounded	Low sphericity
	8-10 mm	Rounded to sub-rounded	Low sphericity
Granite	0-2 mm	Rounded to sub-rounded	Low sphericity
	2-4 mm	Sub-rounded to sub-angular	Low sphericity
	4-8 mm	Rounded to sub-rounded	Low sphericity
	8-10 mm	Sub-rounded to sub-angular	Low sphericity
Limestone	0-2 mm	Sub-rounded to sub-angular	Low sphericity
	2-4 mm	Sub- angular to Angular	Low sphericity
	4-8 mm	Sub-rounded to Sub-angular	Low sphericity
	8-10 mm	Sub-rounded to Sub-angular	Low sphericity
Sandstone	0-2 mm	Rounded to sub-rounded	Low sphericity
	2-4 mm	Sub-rounded to sub-angular	Low sphericity
	4-8 mm	Rounded to sub-rounded	Low sphericity
	8-10 mm	Rounded to sub-rounded	Low sphericity
Tuff	0-2 mm	Sub-rounded to Sub-angular	Low sphericity
	2-4 mm	Sub-rounded to Sub-angular	Low sphericity
	4-8 mm	Sub-rounded to Sub-angular	Low sphericity
	8-10 mm	Sub-rounded to Sub-angular	Low sphericity

6.2 Dry and Saturated Bulk Density of Aggregates

Dry and saturated bulk densities are determined following TS EN 1097-3 (TSE, 1999). All aggregate samples were measured for grain densities in both dry and water-saturated conditions. A cylindrical plastic container with a diameter of 50 mm and a length of 100 mm was used for this work. Samples of each size were weighed and filled into the vessel. The bulk density of the aggregates were calculated by dividing the volume of the container by the loose bulk density of each sample.

Figure 6.21 Dry and saturated bulk density measurement (Personal archive, 2017)

6.3 Determination of Particle Density and Water Absorption of Aggregates by Wire Basket Method

First, the aggregates were placed in the water for 24 hours. Aggregates that were saturated with water were weighed in water with the help of wire basket containing the aggregate samples (M2). Subsequently, the aggregates removed from the water were laid on a dry cloth, surface dried aggregates were still saturated and weighed (M1). Finally, the aggregates were placed in the oven at 105 ° C for 24 hours to get their dry weight (M4).

The wire basket method was used to calculate particle density and water absorption of 4-8 mm and 8-10 mm aggregate samples.

Particle density and water absorption were calculated according to the following formulas:

Visible particle density = pa = pw (M4) / M4- (M2-M3) (6.1)

Flux dried particle density = prd = pw (M4) / M1- (M2-M3) (6.2)

Saturated and surface dried particle density = pssd = pw (M4) / M4 - (M2 - M3) (6.3)

Water absorption = 100 x (M1 - M4) / M4 (6.4)

Void ratio = (M1 - M4) / (M4 – M2) x 100 (6.5)

Porosity = (M1 – M4) / (M1 – M2) x 100 (6.6)

M1 = mass of air saturated and surface dried aggregate, in grams.
M2 = apparent mass of the basket containing the saturated aggregate sample in grams.
M3 = apparent mass in grams of empty basket in grams.
M4 = gram of air-dried test piece in the air.

Void (%) = $\rho_{rd} - \rho_{bulk\ (loose)} / \rho_{rd} \times 100$ (6.7)

ρ_{rd} = Oven-dried particle density

$\rho_{bulk\ (loose)}$ = Loose bulk density

Table 6.3 Particle density and water absorption of 4-8 mm aggregate samples

Lithology	Grain size	M2 (g)	M1 (g)	M4 (g)	ρ_{water} (g/cm^3)	ρ_a (g/cm^3)	ρ_{rd} (g/cm^3)	ρ_{ssd} (g/cm^3)	WA_{24} (%)
Andesite	4-8 mm	144.22	236.9	234.49	0.998	2.592	2.525	2.551	1.028
		157.15	255.95	253.35	0.998	2.628	2.559	2.585	1.026
		169.22	276.11	273.33	0.998	2.620	2.552	2.578	1.017
		156.15	255.85	253.35	0.998	2.601	2.536	2.561	0.987
		170.22	276.11	273.33	0.998	2.646	2.576	2.602	1.017
					A.Mean	**2.618**	**2.550**	**2.576**	**1.015**
					STDEV	**0.021**	**0.020**	**0.020**	**0.017**
Granite	4-8 mm	158.95	253.65	252.65	0.998	2.691	2.663	2.673	0.396
		151.14	245.41	244.41	0.998	2.615	2.587	2.598	0.409
		142.14	230.1	229.09	0.998	2.629	2.599	2.611	0.441
		151.11	245.41	244.41	0.998	2.614	2.587	2.597	0.409
		142.15	230.1	229.09	0.998	2.630	2.600	2.611	0.441
					A.Mean	**2.636**	**2.607**	**2.618**	**0.419**
					STDEV	**0.032**	**0.032**	**0.031**	**0.021**
Limestone	4-8 mm	170.78	269.02	268.74	0.998	2.738	2.730	2.733	0.104
		189.96	298.68	298.25	0.998	2.749	2.738	2.742	0.144
		180.27	288.8	288.47	0.998	2.661	2.653	2.656	0.114
		170.78	268.95	268.74	0.998	2.738	2.732	2.734	0.078
		189.96	298.56	298.25	0.998	2.749	2.741	2.744	0.104
					A.Mean	**2.727**	**2.719**	**2.722**	**0.109**
					STDEV	**0.037**	**0.037**	**0.037**	**0.024**
Sandstone	4-8 mm	161.2	266.5	256.34	0.998	2.689	2.430	2.526	3.963
		165.04	272.81	262.99	0.998	2.680	2.435	2.526	3.734
		153.1	253.2	243.88	0.998	2.681	2.431	2.524	3.822
		165.04	272.91	262.99	0.998	2.680	2.433	2.525	3.772
		153.1	253.87	243.88	0.998	2.681	2.415	2.514	4.096
					A.Mean	**2.682**	**2.429**	**2.523**	**3.877**
					STDEV	**0.004**	**0.008**	**0.005**	**0.150**
Tuff	4-8 mm	76.04	154.04	135.07	0.998	2.284	1.728	1.971	14.045
		72.55	150.03	130.52	0.998	2.247	1.681	1.932	14.948
		82	166.09	145.4	0.998	2.289	1.726	1.971	14.230
		76.04	154.44	135.07	0.998	2.284	1.719	1.966	14.341
		72.55	150.65	130.52	0.998	2.247	1.668	1.925	15.423
					A.Mean	**2.270**	**1.704**	**1.953**	**14.597**
					STDEV	**0.021**	**0.028**	**0.022**	**0.573**

ρ_{water} = Density of water at 20 ^{0}C

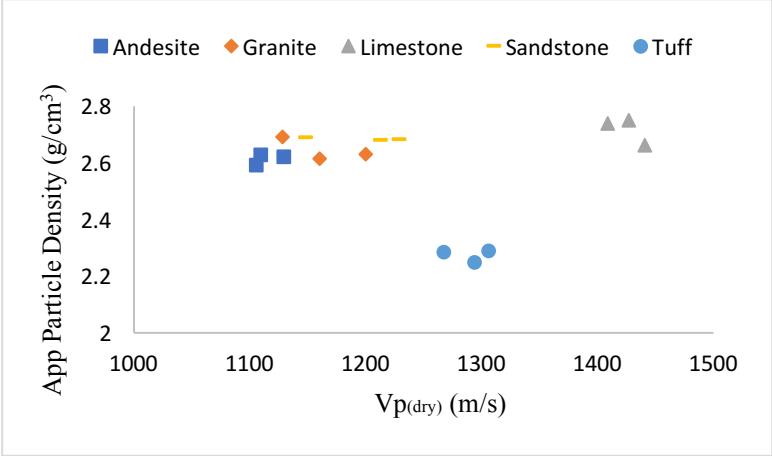

Figure 6.22 Graphical representation of dry Vp to apparent particle density of 4-8 mm aggregates

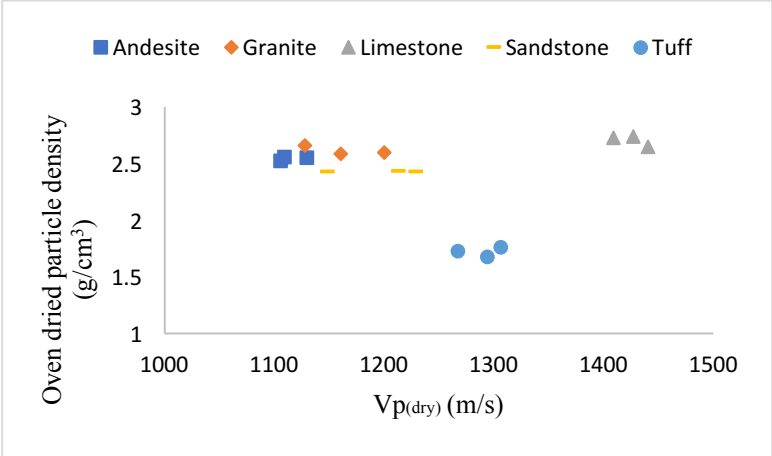

Figure 6.23 Graphical representation of dry Vp to oven dried particle density of 4-8 mm aggregates

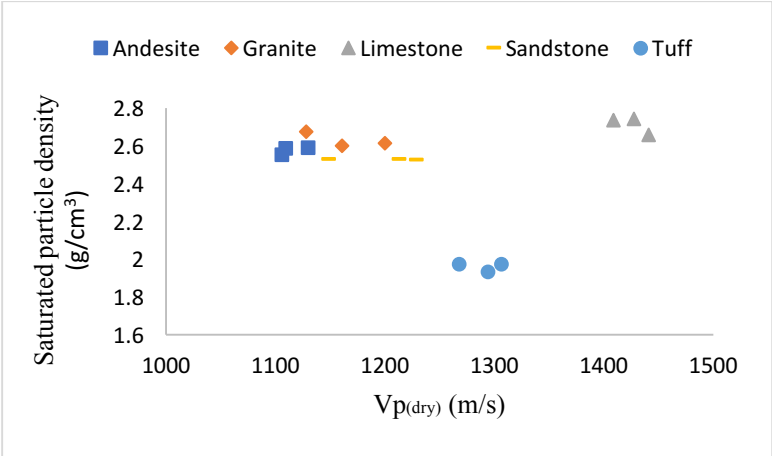

Figure 6.24 Graphical representation of dry Vp to saturated particle density of 4-8 mm aggregates

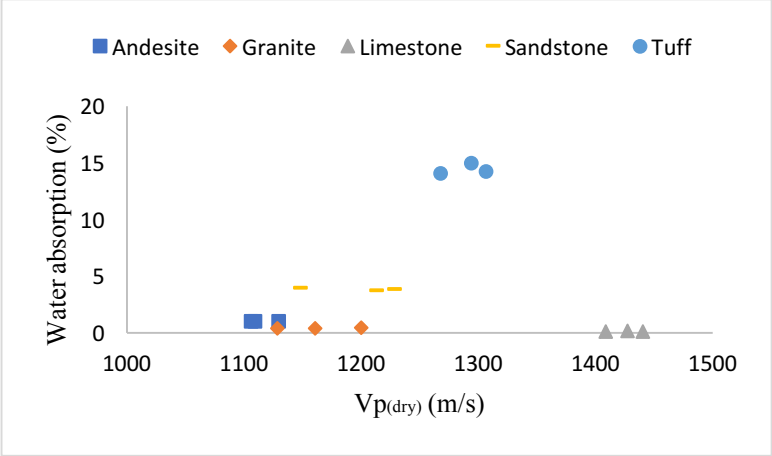

Figure 6.25 Graphical representation of dry Vp to water absorption of 4-8 mm aggregates

Table 6.4 Porosity and void ratio of 4-8 mm aggregate samples

Lithology	Grain size	M2 (g)	M1 (g)	M4 (g)	ρ_{water} (g/cm^3)	ρ_{bulk} (loose)	n (%)	e (%)	Void %
Andesite	4-8 mm	144.22	236.9	234.49	0.998	1.168	2.600	2.670	53.743
		157.15	255.95	253.35	0.998	1.168	2.632	2.703	54.360
		169.22	276.11	273.33	0.998	1.168	2.601	2.670	54.232
		156.15	255.85	253.35	0.998	1.168	2.508	2.572	53.944
		170.22	276.11	273.33	0.998	1.168	2.625	2.696	54.660
					A.Mean	**1.168**	**2.593**	**2.662**	**54.188**
					STDEV	**0.000**	**0.050**	**0.053**	**0.358**
Granite	4-8 mm	158.95	253.65	252.65	0.998	1.201	1.056	1.067	54.893
		151.14	245.41	244.41	0.998	1.201	1.061	1.072	53.584
		142.14	230.1	229.09	0.998	1.201	1.148	1.162	53.795
		151.11	245.41	244.41	0.998	1.201	1.060	1.072	53.569
		142.15	230.1	229.09	0.998	1.201	1.148	1.162	53.800
					A.Mean	**1.201**	**1.095**	**1.107**	**53.928**
					STDEV	**0.000**	**0.049**	**0.050**	**0.551**
Limestone	4-8 mm	170.78	269.02	268.74	0.998	1.266	0.285	0.286	53.628
		189.96	298.68	298.25	0.998	1.266	0.396	0.397	53.758
		180.27	288.8	288.47	0.998	1.266	0.304	0.305	52.274
		170.78	268.95	268.74	0.998	1.266	0.214	0.214	53.661
		189.96	298.56	298.25	0.998	1.266	0.285	0.286	53.810
					A.Mean	**1.266**	**0.297**	**0.298**	**53.426**
					STDEV	**0.000**	**0.065**	**0.065**	**0.648**
Sandstone	4-8 mm	161.2	266.5	256.34	0.998	1.124	9.649	10.68	53.736
		165.04	272.81	262.99	0.998	1.124	9.112	10.03	53.848
		153.1	253.2	243.88	0.998	1.124	9.311	10.27	53.773
		165.04	272.91	262.99	0.998	1.124	9.196	10.13	53.805
		153.1	253.87	243.88	0.998	1.124	9.914	11.01	53.464
					A.Mean	**1.124**	**9.436**	**10.42**	**53.725**
					STDEV	**0.000**	**0.336**	**0.410**	**0.152**
Tuff	4-8 mm	76.04	154.04	135.07	0.998	0.728	24.32	32.14	57.875
		72.55	150.03	130.52	0.998	0.728	25.18	33.66	56.697
		82	166.09	145.4	0.998	0.728	24.61	32.63	57.813
		76.04	154.44	135.07	0.998	0.728	24.71	32.81	57.659
		72.55	150.65	130.52	0.998	0.728	25.78	34.73	56.351
					A.Mean	**0.728**	**24.92**	**33.19**	**57.279**
					STDEV	**0.000**	**0.571**	**1.017**	**0.704**

ρ_{water} = Density of water at 20 ^{0}C

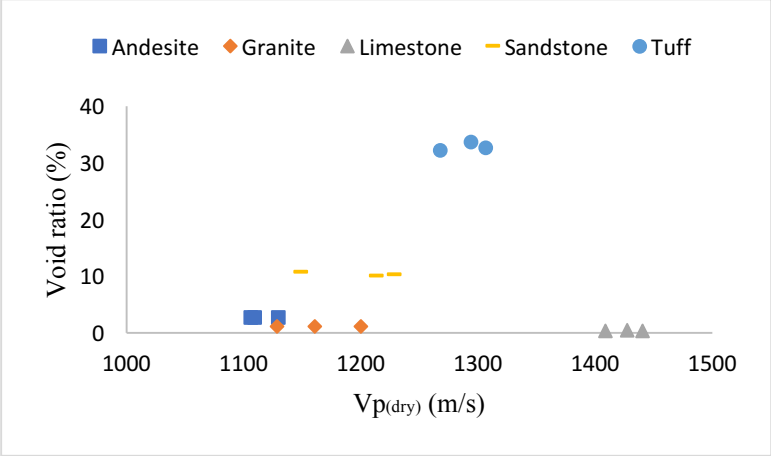

Figure 6.26 Graphical representation of dry Vp to void ratio 4-8 mm aggregates

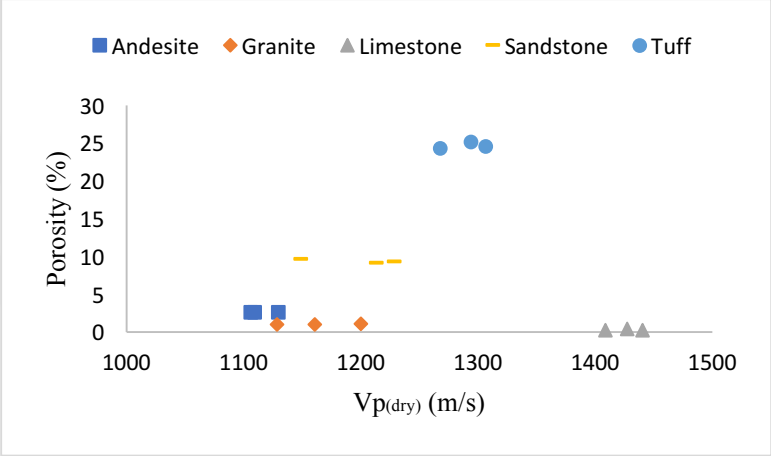

Figure 6.27 Graphical representation of dry Vp to porosity 4-8 mm aggregates

Table 6.5 Particle density and water absorption of 8-10 mm aggregate samples

Lithology	Grain size	M2 (g)	M1 (g)	M4 (g)	ρ_{water} (g/cm^3)	ρ_a (g/cm^3)	ρ_{rd} (g/cm^3)	ρ_{ssd} (g/cm^3)	WA_{24} (%)
Andesite	8-10 mm	159.13	259.98	257.37	0.998	2.615	2.547	2.573	1.014
		164.65	273.69	270.87	0.998	2.545	2.479	2.505	1.041
		169.3	276.4	273.72	0.998	2.616	2.551	2.576	0.979
		164.65	273.69	270.87	0.998	2.545	2.479	2.505	1.041
		169.6	276.42	273.72	0.998	2.624	2.557	2.583	0.986
					A.Mean	**2.589**	**2.523**	**2.548**	**1.012**
					STDEV	**0.040**	**0.040**	**0.040**	**0.029**
Granite	8-10 mm	177.85	282.61	281.61	0.998	2.709	2.683	2.692	0.355
		139.05	225.68	224.76	0.998	2.617	2.589	2.600	0.409
		167.15	265.84	264.78	0.998	2.707	2.678	2.688	0.400
		139.05	225.69	224.76	0.998	2.617	2.589	2.600	0.414
		167.15	265.8	264.78	0.998	2.707	2.679	2.689	0.385
					A.Mean	**2.671**	**2.643**	**2.654**	**0.393**
					STDEV	**0.049**	**0.050**	**0.049**	**0.024**
Limestone	8-10 mm	163.17	272.3	271.99	0.998	2.494	2.487	2.490	0.114
		148.97	241.22	240.95	0.998	2.614	2.607	2.610	0.112
		153.59	241.55	241.29	0.998	2.746	2.738	2.741	0.108
		148.97	241.18	240.95	0.998	2.614	2.608	2.610	0.097
		153.59	241.54	241.29	0.998	2.746	2.738	2.741	0.104
					A.Mean	**2.643**	**2.636**	**2.638**	**0.107**
					STDEV	**0.106**	**0.105**	**0.106**	**0.007**
Sandstone	8-10 mm	103.8	173.38	166.88	0.998	2.640	2.394	2.487	3.895
		156.04	259.45	249.81	0.998	2.659	2.411	2.504	3.859
		209.37	349.73	336.62	0.998	2.640	2.393	2.487	3.895
		156.04	259.25	249.81	0.998	2.659	2.416	2.507	3.779
		209.37	349.15	336.62	0.998	2.640	2.403	2.493	3.722
					A.Mean	**2.648**	**2.403**	**2.495**	**3.830**
					STDEV	**0.010**	**0.010**	**0.009**	**0.077**
Tuff	8-10 mm	100.04	206.21	180.79	0.998	2.234	1.699	1.938	14.061
		73.28	149.08	131.11	0.998	2.263	1.726	1.963	13.706
		88.14	181.26	158.66	0.998	2.245	1.700	1.943	14.244
		73.28	150.08	131.11	0.998	2.263	1.704	1.950	14.469
		88.14	181.26	158.66	0.998	2.245	1.700	1.943	14.244
					A.Mean	**2.250**	**1.706**	**1.947**	**14.145**
					STDEV	**0.012**	**0.011**	**0.010**	**0.285**

ρ_{water} = Density of water at 20 ^{0}C

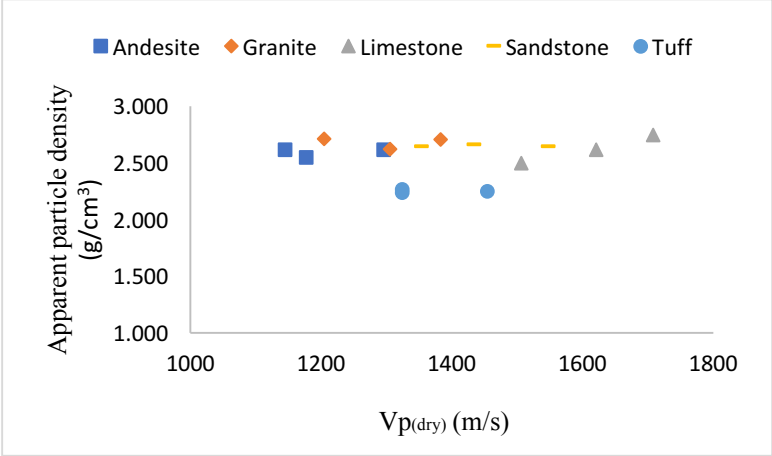

Figure 6.28 Graphical representation of dry Vp to apparent particle density of 8-10 mm aggregates

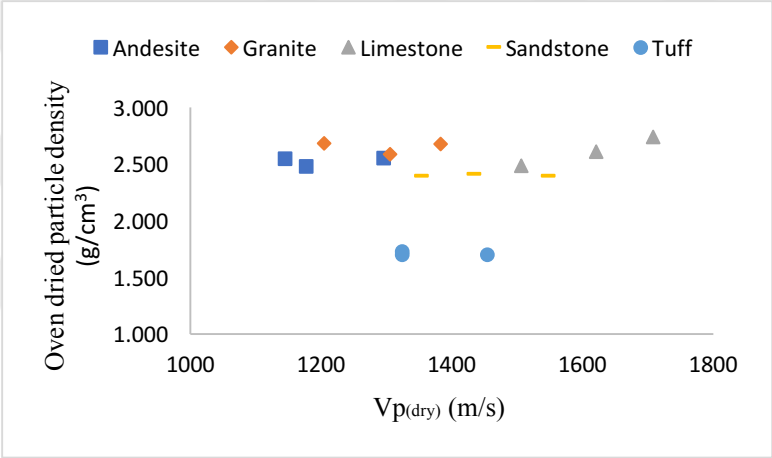

Figure 6.29 Graphical representation of dry Vp to oven dried particle of 8-10 mm aggregates

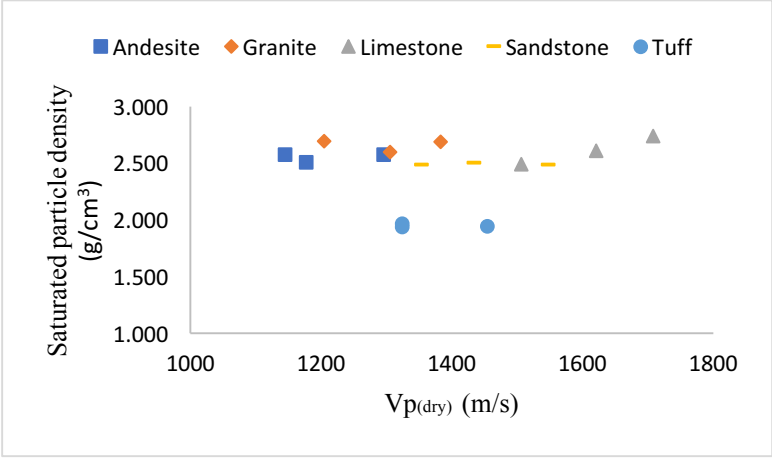

Figure 6.30 Graphical representation of dry Vp to saturated particle density of 8-10 mm aggregates

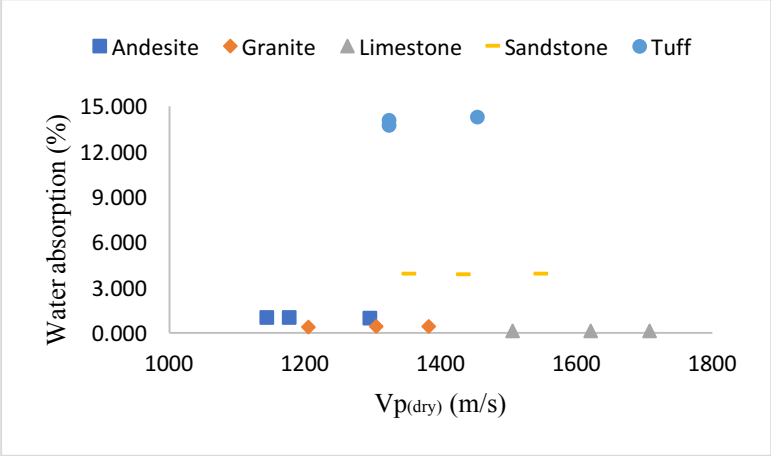

Figure 6.31 Graphical representation of dry Vp to water absorption of 8-10 mm aggregates

Table 6.6 Porosity and void ratio of 8-10 mm aggregate samples

Lithology	Grain size	M2	M1	M4	ρ_{water} (g/cm^3)	ρ_{bulk} (loose)	n (%)	e (%)	Void %
Andesite	8-10 mm	159.13	259.98	257.37	0.998	1.168	2.588	2.657	54.140
		164.65	273.69	270.87	0.998	1.168	2.586	2.655	49.742
		169.3	276.4	273.72	0.998	1.168	2.502	2.567	50.821
		164.65	273.69	270.87	0.998	1.168	2.586	2.655	50.821
		169.6	276.42	273.72	0.998	1.168	2.528	2.593	50.821
					A.Mean	**1.168**	**2.558**	**2.625**	**51.269**
					STDEV	**0.000**	**0.040**	**0.042**	**1.672**
Granite	8-10 mm	177.85	282.61	281.61	0.998	1.168	0.955	0.964	56.463
		139.05	225.68	224.76	0.998	1.168	1.062	1.073	54.891
		167.15	265.84	264.78	0.998	1.168	1.074	1.086	56.379
		139.05	225.69	224.76	0.998	1.168	1.073	1.085	54.886
		167.15	265.8	264.78	0.998	1.168	1.034	1.045	56.396
					A.Mean	**1.168**	**1.040**	**1.051**	**55.803**
					STDEV	**0.000**	**0.050**	**0.051**	**0.835**
Limestone	8-10 mm	163.17	272.3	271.99	0.998	1.168	0.284	0.285	53.043
		148.97	241.22	240.95	0.998	1.168	0.293	0.294	55.192
		153.59	241.55	241.29	0.998	1.168	0.296	0.296	57.336
		148.97	241.18	240.95	0.998	1.168	0.253	0.253	55.210
		153.59	241.54	241.29	0.998	1.168	0.284	0.285	57.341
					A.Mean	**1.168**	**0.282**	**0.283**	**55.625**
					STDEV	**0.000**	**0.017**	**0.017**	**1.796**
Sandstone	8-10 mm	103.8	173.38	166.88	0.998	1.168	9.342	10.30	52.402
		156.04	259.45	249.81	0.998	1.168	9.322	10.28	52.309
		209.37	349.73	336.62	0.998	1.168	9.340	10.30	52.402
		156.04	259.25	249.81	0.998	1.168	9.146	10.07	52.103
		209.37	349.15	336.62	0.998	1.168	8.964	9.847	51.967
					A.Mean	**1.168**	**9.223**	**10.16**	**52.237**
					STDEV	**0.000**	**0.166**	**0.202**	**0.194**
Tuff	8-10 mm	100.04	206.21	180.79	0.998	1.168	23.94	31.48	53.514
		73.28	149.08	131.11	0.998	0.722	23.70	31.07	53.209
		88.14	181.26	158.66	0.998	0.722	24.27	32.05	52.980
		73.28	150.08	131.11	0.998		24.70	32.80	52.602
		88.14	181.26	158.66	0.998		24.27	32.05	52.516
					A.Mean	**0.871**	**24.18**	**31.89**	**52.964**
					STDEV	**0.257**	**0.376**	**0.655**	**0.417**

ρ_{water} = Density of water at 20 ^{0}C

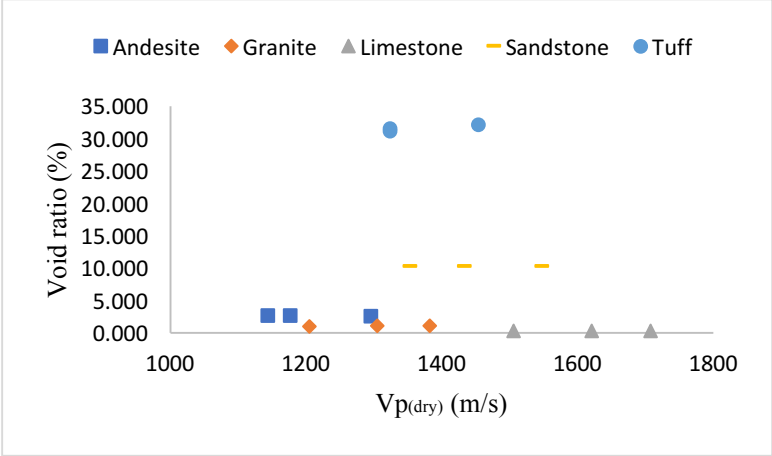

Figure 6.32 Graphical representation of dry Vp to void ratio of 8-10 mm aggregates

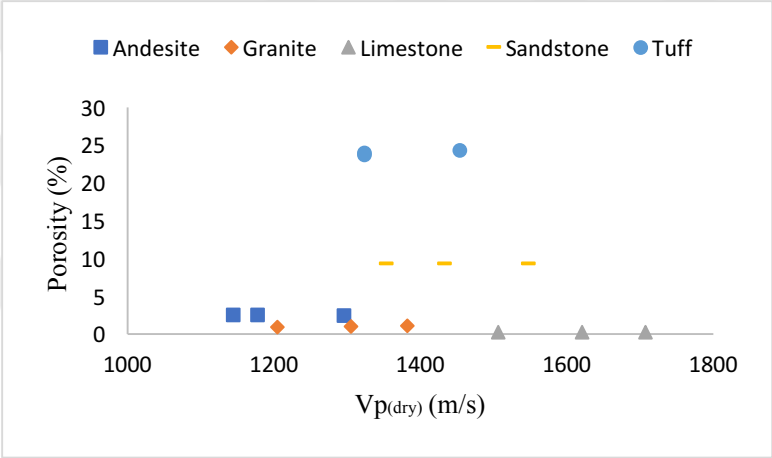

Figure 6.33 Graphical representation of dry Vp to porosity of 8-10 mm aggregates

6.4 Ultrasonic P-wave Velocity Measurements of Aggregate Specimens

Five different lithologies of selected rocks were broken with jaw type crushers laboratory. Samples were then sieved to prepare aggregate samples at 4 different sizes ranging from 0-2, 2-4, 4-8, 8-10 mm. Measurements of the sound velocity of the prepared samples were measured in both dry and saturated condition.

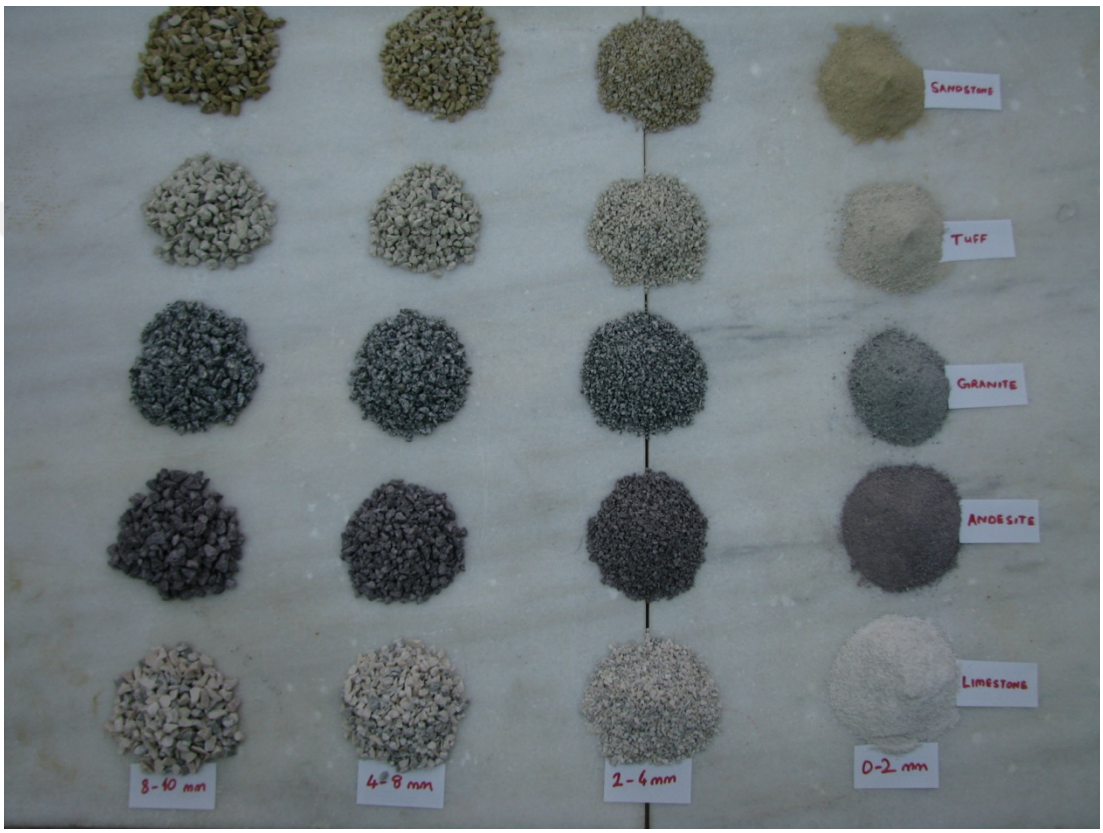

Figure 6.34 Four different grain sizes of five different lithologies

Laboratory setup in Figure 6.37 was used for ultrasonic testing of granular materials. Aggregate specimens were filled into a cylindrical transparent plastic tube with a diameter of 52 mm and a length of 130 mm. The pundit probes were also inserted into this cylindrical pipe to make contact with the aggregates. However, the sound velocity of aggregate samples could not be measured directly. When these loose aggregates (Figure 6.35 and Figure 6.36) were compiled they could be read from the pundit. A 100 kgf press was used to compress the aggregate samples. After each

sample was compressed at a load of 100 kgf, the pundit device was operated and the readings were taken (Figure 6.37).

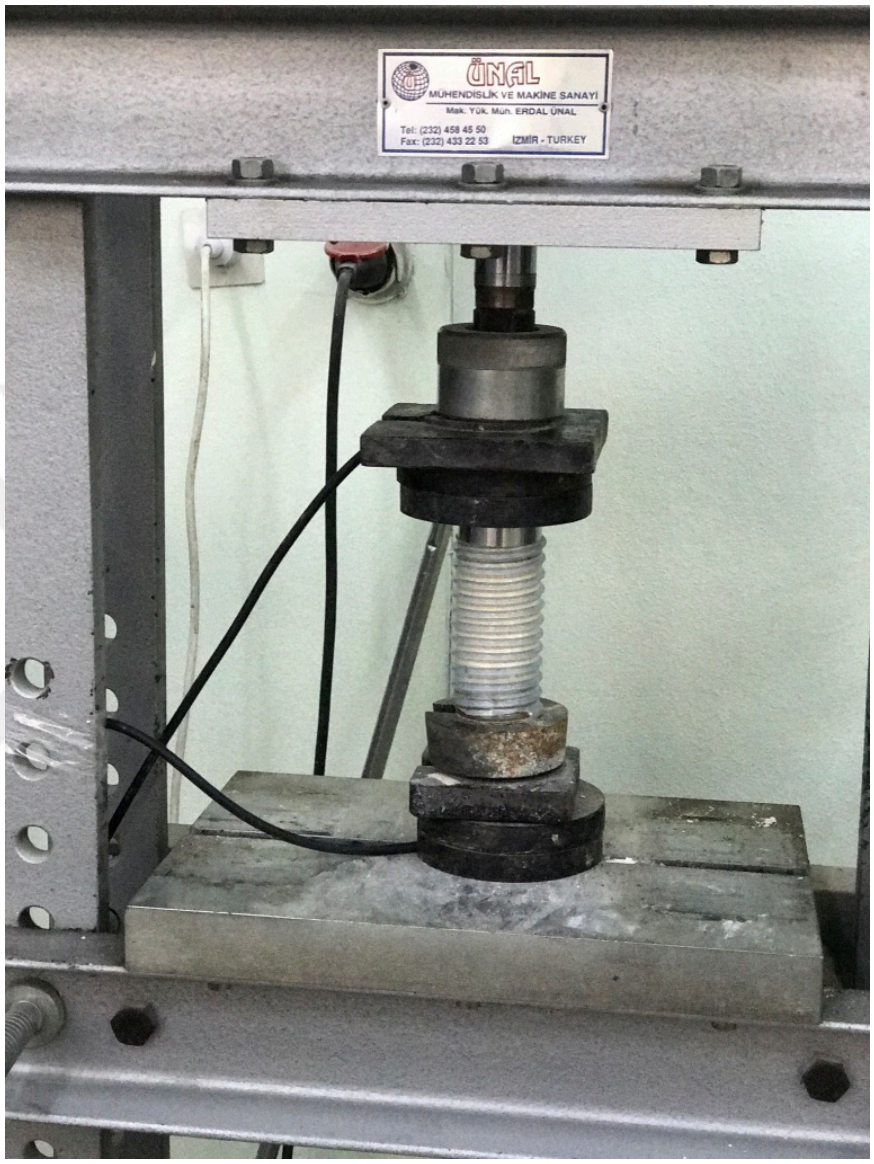

Figure 6.35 Compressing Tuff aggregate sample for ultrasonic test (Personal archive, 2017)

Figure 6.36 Andesite granular material inside the tube with ultrasonic probes at both ends (Personal archive, 2017)

Figure 6.37 Laboratory setup for ultrasonic testing of granular materials (Personal archive, 2017)

Table 6.7 Bulk density and Vp of dry aggregates

Lithology	Grain size (mm)	S. No	md (g)	V (cm^3)	$\rho_{bulk(dry)}$ (g/cm^3)	L (mm)	t_{dry} (µs)	F (kgf)	Vp (dry) (m/s)
Andesite	0-2	1	275.44	196.25	1.404	54.83	82.3	100	666.221
		2	272.05	196.25	1.386	59.95	86.9	100	689.873
		3	269.14	196.25	1.371	55.91	78.8	100	709.518
			A.Mean		**1.387**				**688.537**
			STDEV		**0.017**				**21.679**
	2-4	1	222.71	196.25	1.135	63.84	69.2	100	922.543
		2	217.48	196.25	1.108	55.64	60.1	100	925.790
		3	220.08	196.25	1.121	59.65	61	100	977.869
			A.Mean		**1.121**				**942.067**
			STDEV		**0.014**				**31.048**
	4-8	1	224.23	196.25	1.143	69.66	63	100	1105.714
		2	234.02	196.25	1.192	70	63.1	100	1109.350
		3	229.45	196.25	1.169	69.12	61.2	100	1129.412
			A.Mean		**1.168**				**1114.825**
			STDEV		**0.025**				**12.763**
	8-10	1	224.4	196.25	1.143	73.45	64.2	100	1144.081
		2	225.2	196.25	1.148	66.15	56.2	100	1177.046
		3	227.36	196.25	1.159	63.2	48.8	100	1295.082
			A.Mean		**1.15**				**1205.403**
			STDEV		**0.008**				**79.394**
Granite	0-2	1	291.53	196.25	1.486	54.44	87.8	100	620.046
		2	289.88	196.25	1.477	53.42	85.1	100	627.732
		3	288.67	196.25	1.471	52.93	80.7	100	655.886
			A.Mean		**1.478**				**634.555**
			STDEV		**0.008**				**18.869**
	2-4	1	244.97	196.25	1.248	60.18	68.7	100	875.983
		2	245.2	196.25	1.249	61.94	69.9	100	886.123
		3	249.49	196.25	1.271	64.81	72.1	100	898.890
			A.Mean		**1.256**				**886.999**
			STDEV		**0.013**				**11.479**
	4-8	1	238.02	196.25	1.213	65.43	58	100	1128.103
		2	237.66	196.25	1.211	58.02	50	100	1160.400
		3	231.45	196.25	1.179	57.6	48	100	1200.00

Table 6.7 Continues

			A.Mean		**1.201**				**1162.834**
			STDEV		**0.019**				**36.01**
	8-10	1	245.2	196.25	1.249	68.54	56.9	100	1204.569
		2	249.23	196.25	1.270	64.48	49.4	100	1305.263
		3	242.66	196.25	1.236	62.89	45.5	100	1382.198
			A.Mean		**1.252**				**1297.343**
			STDEV		**0.017**				**89.079**
Limestone	0-2	1	295.85	196.25	1.508	58.84	75.8	100	776.253
		2	286.64	196.25	1.461	59.76	76.4	100	782.199
		3	282.78	196.25	1.441	60.98	76.3	100	799.214
			A.Mean		**1.47**				**785.889**
			STDEV		**0.034**				**11.917**
	2-4	1	249.24	196.25	1.270	65.26	59.6	100	1094.966
		2	246.13	196.25	1.254	62.51	56.8	100	1100.528
		3	243.9	196.25	1.243	63.77	57	100	1118.772
			A.Mean		**1.256**				**1104.775**
			STDEV		**0.014**				**12.453**
	4-8	1	242.59	196.25	1.236	71.85	51	100	1408.824
		2	247.18	196.25	1.260	70.65	49.5	100	1427.273
		3	255.54	196.25	1.302	70.3	48.8	100	1440.574
			A.Mean		**1.266**				**1425.557**
			STDEV		**0.033**				**15.994**
	8-10	1	252.21	196.25	1.285	78.15	51.9	100	1505.780
		2	256.25	196.25	1.306	76.99	47.5	100	1620.842
		3	259.05	196.25	1.320	71.88	42.1	100	1707.363
			A.Mean		**1.304**				**1611.328**
			STDEV		**0.018**				**101.128**
Sandstone	0-2	1	249.61	196.25	1.272	56.9	76	100	748.684
		2	249.5	196.25	1.271	63.39	78	100	812.692
		3	252.93	196.25	1.289	63.05	77.3	100	815.653
			A.Mean		**1.277**				**792.343**
			STDEV		**0.010**				**37.839**
	2-4	1	202.53	196.25	1.032	59.55	63.4	100	939.274
		2	212.28	196.25	1.082	61.02	56	100	1089.643
		3	207.62	196.25	1.058	68.78	61.3	100	1122.023

Table 6.7 Continues

			A.Mean		**1.057**				**1050.313**
			STDEV		**0.025**				**97.516**
	4-8	1	220.1	196.25	1.122	76.13	66.3	100	1148.265
		2	216.31	196.25	1.102	81.5	67.2	100	1212.798
		3	225.52	196.25	1.149	72.73	59.2	100	1228.547
			A.Mean		**1.124**				**1196.537**
			STDEV		**0.024**				**42.540**
	8-10	1	210.95	196.25	1.075	63.6	47	100	1353.191
		2	207.87	196.25	1.059	69.5	48.5	100	1432.990
		3	212.69	196.25	1.084	68.84	44.5	100	1546.966
			A.Mean		**1.072**				**1444.382**
			STDEV		**0.013**				**97.389**
Tuff	0-2	1	169.47	196.25	0.864	62.86	84.7	100	742.149
		2	169.99	196.25	0.866	60.87	80	100	760.875
		3	171.59	196.25	0.874	57.3	72	100	795.833
			A.Mean		**0.868**				**766.286**
			STDEV		**0.005**				**27.248**
	2-4	1	138.89	196.25	0.708	61.99	60.7	100	1021.252
		2	141.25	196.25	0.720	62.56	60.1	100	1040.932
		3	138.43	196.25	0.705	64.22	60.8	100	1056.250
			A.Mean		**0.711**				**1039.478**
			STDEV		**0.008**				**17.554**
	4-8	1	144.71	196.25	0.737	56.15	44.3	100	1267.494
		2	141.31	196.25	0.720	58.62	45.3	100	1294.040
		3	142.73	196.25	0.727	59.7	45.7	100	1306.346
			A.Mean		**0.728**				**1289.293**
			STDEV		**0.009**				**19.856**
	8-10	1	141.74	196.25	0.722	71.59	54.1	100	1323.290
		2	142.92	196.25	0.728	63.93	48.3	100	1323.602
		3	140.57	196.25	0.716	65.14	44.8	100	1454.018
			A.Mean		**0.722**				**1366.970**
			STDEV		**0.006**				**75.386**

Table 6.8 Bulk density and Vp of saturated aggregates

Lithology	Grain size (mm)	S. No	ms (g)	V (cm^3)	$\rho_{bulk\ (sat)}$ (g/cm^3)	L (mm)	t_{sat} (µs)	F (kgf)	Vp (sat) (m/s)
Andesite	0-2	1	238.9	196.25	1.217	72.9	89.9	100	810.901
		2	233.38	196.25	1.189	70.16	86.5	100	811.098
		3	240.01	196.25	1.223	70.51	84.4	100	835.427
			A.Mean		**1.210**				**819.142**
			STDEV		**0.018**				**14.104**
	2-4	1	222.66	196.25	1.135	79.51	89.7	100	886.399
		2	226.03	196.25	1.152	78.25	85.8	100	912.005
		3	224.72	196.25	1.145	78.89	85.5	100	922.690
			A.Mean		**1.144**				**907.031**
			STDEV		**0.009**				**18.650**
	4-8	1	237.65	196.25	1.211	74.96	63	100	1189.841
		2	241.2	196.25	1.229	78.27	64.3	100	1217.263
		3	242.82	196.25	1.237	70.89	57.5	100	1232.870
			A.Mean		**1.226**				**1213.325**
			STDEV		**0.013**				**21.783**
	8-10	1	239.03	196.25	1.218	73.91	58.1	100	1272.117
		2	236.41	196.25	1.205	71.03	55.8	100	1272.939
		3	237.85	196.25	1.212	69.86	51.3	100	1361.793
			A.Mean		**1.212**				**1302.283**
			STDEV		**0.007**				**51.539**
Granite	0-2	1	246.92	196.25	1.258	67.02	91.8	100	730.065
		2	240.53	196.25	1.226	67.53	89.7	100	752.843
		3	236.26	196.25	1.204	72.58	93.9	100	772.950
			A.Mean		**1.229**				**751.953**
			STDEV		**0.027**				**21.456**
	2-4	1	234.38	196.25	1.194	74.16	80.3	100	923.537
		2	236.98	196.25	1.208	72.04	78	100	923.590
		3	234.25	196.25	1.194	70.08	74	100	947.027
			A.Mean		**1.199**				**931.385**
			STDEV		**0.008**				**13.547**
	4-8	1	245.58	196.25	1.251	71.23	69.8	100	1020.487
		2	248.96	196.25	1.269	68.57	61.3	100	1118.597
		3	247.86	196.25	1.263	69.88	62.4	100	1119.872

Table 6.8 Continues

			A.Mean		**1.261**				**1086.319**
			STDEV		**0.009**				**57.015**
	8-10	1	258.9	196.25	1.319	69.11	51.1	100	1352.446
		2	257.2	196.25	1.311	66.41	46.9	100	1415.991
		3	259.4	196.25	1.322	67.68	44.6	100	1517.489
			A.Mean		**1.317**				**1428.642**
			STDEV		**0.006**				**23.246**
Limestone	0-2	1	255.89	196.25	1.304	72.76	72	100	1010.556
		2	260.46	196.25	1.327	72	70.8	100	1016.949
		3	260.94	196.25	1.330	69.25	67.3	100	1028.975
			A.Mean		**1.320**				**1018.827**
			STDEV		**0.014**				**9.352**
	2-4	1	246.88	196.25	1.258	74.35	70	100	1062.143
		2	246.74	196.25	1.257	72.15	65.3	100	1104.900
		3	238.02	196.25	1.213	73	62	100	1177.419
			A.Mean		**1.243**				**1114.821**
			STDEV		**0.026**				**58.275**
	4-8	1	260.3	196.25	1.326	74.21	56.2	100	1320.463
		2	260.54	196.25	1.328	75.61	53.1	100	1423.917
		3	271.37	196.25	1.383	68.8	46.5	100	1479.570
			A.Mean		**1.346**				**1407.983**
			STDEV		**0.032**				**80.741**
	8-10	1	258.6	196.25	1.318	69.81	47	100	1485.319
		2	268.89	196.25	1.370	70.79	47	100	1506.170
		3	262.9	196.25	1.340	72.17	47.7	100	1512.998
			A.Mean		**1.343**				**1501.496**
			STDEV		**0.026**				**14.419**
Sandstone	0-2	1	241.14	196.25	1.229	61.91	62.5	100	990.560
		2	240.19	196.25	1.224	59.54	60.1	100	990.682
		3	238.6	196.25	1.216	57.79	58	100	996.379
			A.Mean		**1.223**				**992.540**
			STDEV		**0.006**				**3.325**
	2-4	1	231.05	196.25	1.177	71.74	68.3	100	1050.366
		2	218.21	196.25	1.112	67.95	58.8	100	1155.612
		3	212.2	196.25	1.081	61.99	53.2	100	1165.226

Table 6.8 Continues

			A.Mean		**1.123**				**1123.735**
			STDEV		**0.049**				**63.721**
	4-8	1	232.09	196.25	1.183	68.83	51.6	100	1333.915
		2	229.26	196.25	1.168	67	49.8	100	1345.382
		3	231.25	196.25	1.178	79.6	55.8	100	1426.523
			A.Mean		**1.176**				**1368.607**
			STDEV		**0.008**				**50.484**
	8-10	1	231.61	196.25	1.180	69.77	45.5	100	1533.407
		2	230.18	196.25	1.173	66.98	43.3	100	1546.882
		3	228.72	196.25	1.165	69.74	44.2	100	1577.828
			A.Mean		**1.173**				**1552.706**
			STDEV		**0.008**				**22.776**
Tuff	0-2	1	192.4	196.25	0.980	62.53	87	100	718.736
		2	188.05	196.25	0.958	61.48	79.3	100	775.284
		3	197.41	196.25	1.006	64	81	100	790.123
			A.Mean		**0.981**				**761.381**
			STDEV		**0.024**				**37.670**
	2-4	1	160.27	196.25	0.817	63.71	69.5	100	916.691
		2	161.67	196.25	0.824	59.48	60.8	100	978.289
		3	161.96	196.25	0.825	59.83	59.9	100	998.831
			A.Mean		**0.822**				**964.604**
			STDEV		**0.004**				**42.746**
	4-8	1	176.46	196.25	0.899	66.56	61	100	1091.148
		2	178.42	196.25	0.909	61.72	52.4	100	1177.863
		3	177.37	196.25	0.904	61.4	50.4	100	1218.254
			A.Mean		**0.904**				**1162.422**
			STDEV		**0.005**				**64.945**
	8-10	1	174.4	196.25	0.889	61.76	50.3	100	1227.833
		2	175.98	196.25	0.897	61.41	49.2	100	1248.171
		3	172.64	196.25	0.880	60.11	47.5	100	1265.474
			A.Mean		**0.889**				**1247.159**
			STDEV		**0.009**				**18.841**

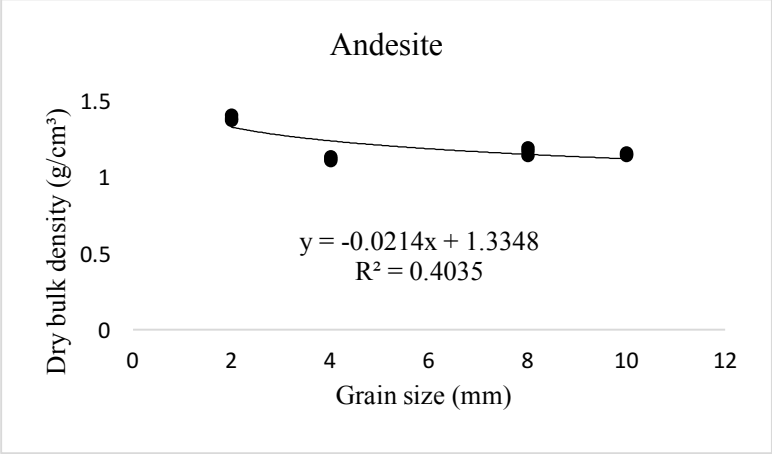

Figure 6.38 Graphical representation of grain size to dry bulk density for Andesite (aggregate)

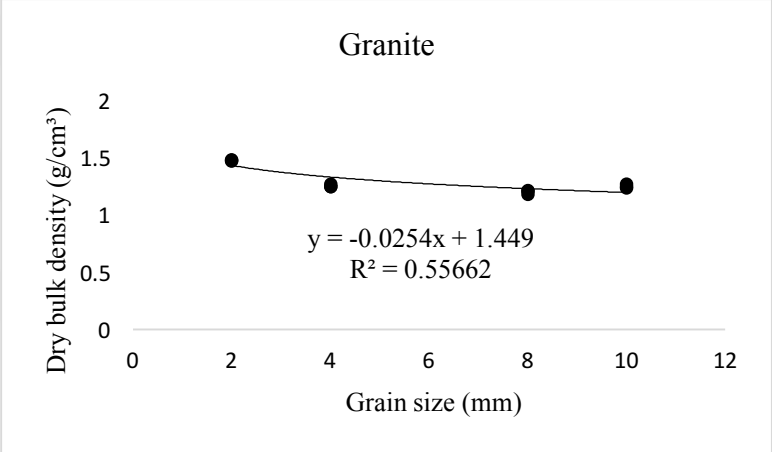

Figure 6.39 Graphical representation of grain size to dry bulk density for Granite (aggregate)

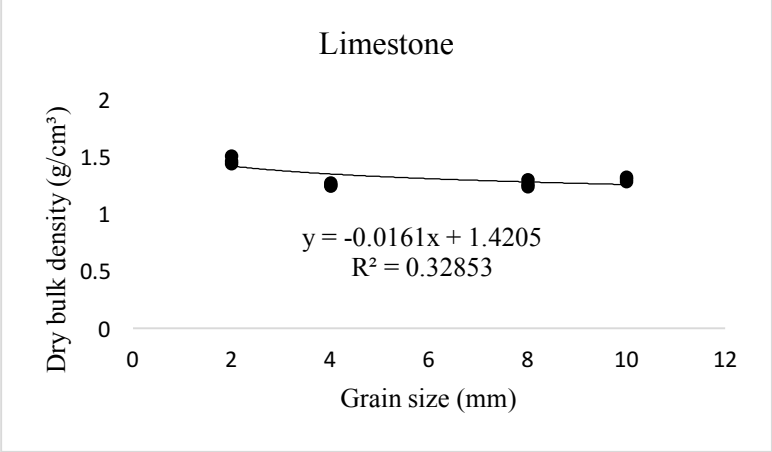

Figure 6.40 Graphical representation of grain size to dry bulk density for Limestone (aggregate)

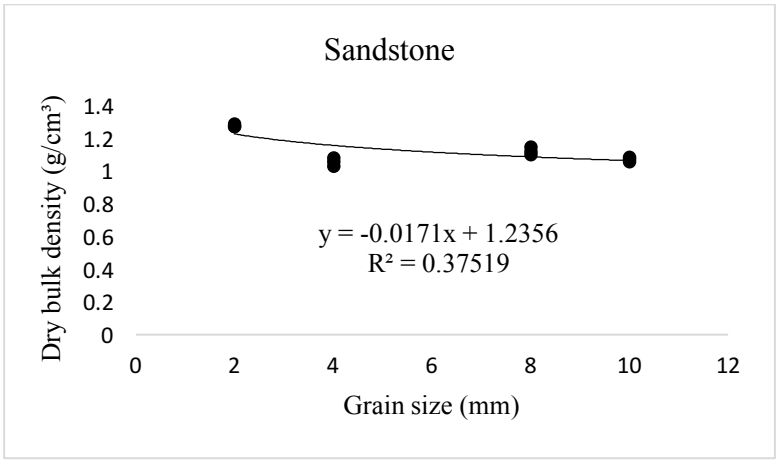

Figure 6.41 Graphical representation of grain size to dry bulk density for Sandstone (aggregate)

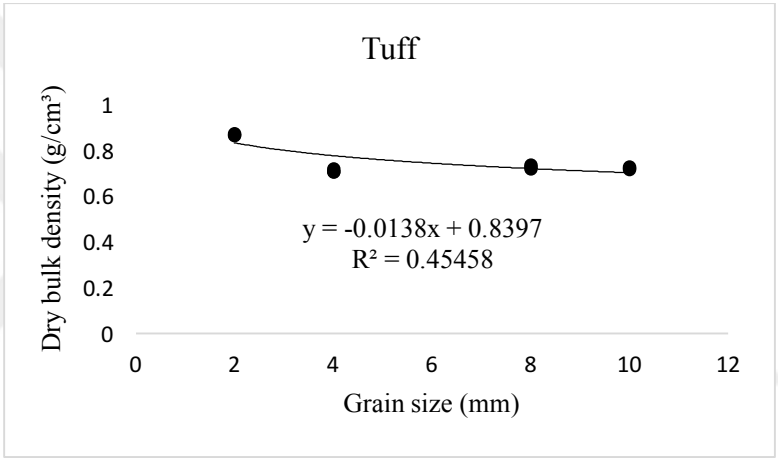

Figure 6.42 Graphical representation of grain size to dry bulk density for Tuff (aggregate)

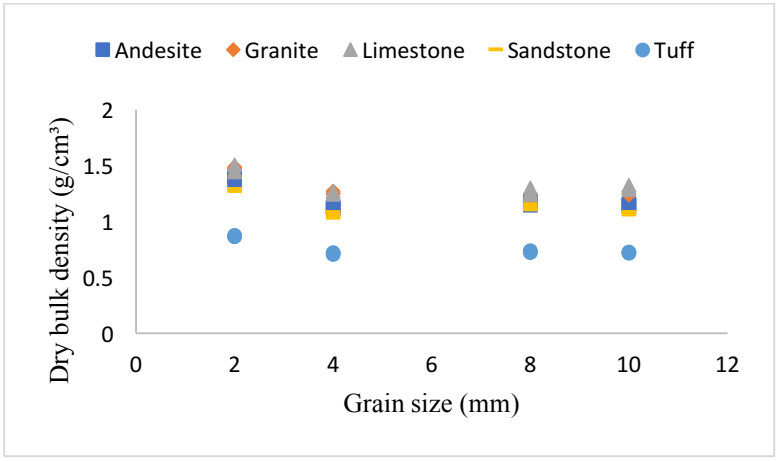

Figure 6.43 Graphical representation of grain size to dry bulk density for all granular samples

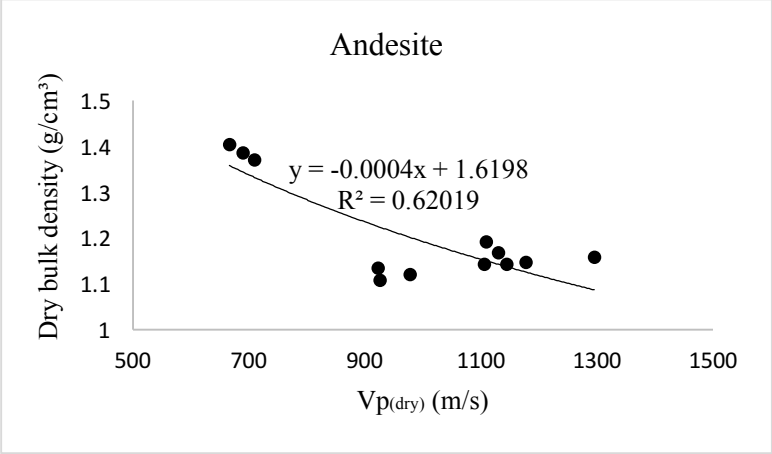

Figure 6.44 Graphical representation of dry Vp to dry bulk density for Andesite (aggregate)

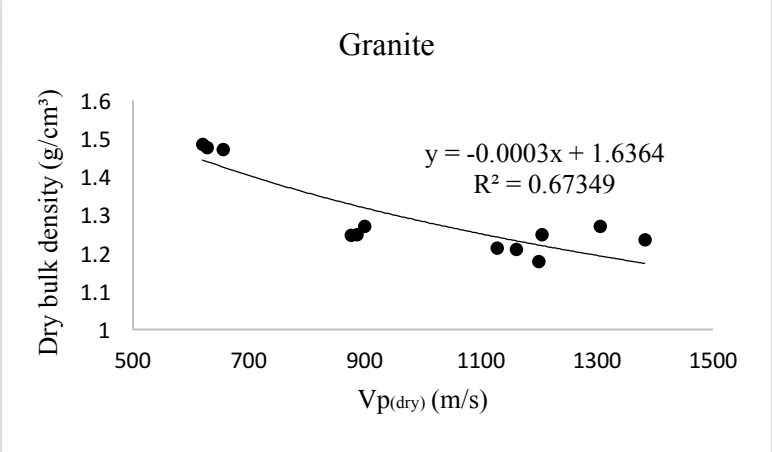

Figure 6.45 Graphical representation of dry Vp to dry bulk density for Granite (aggregate)

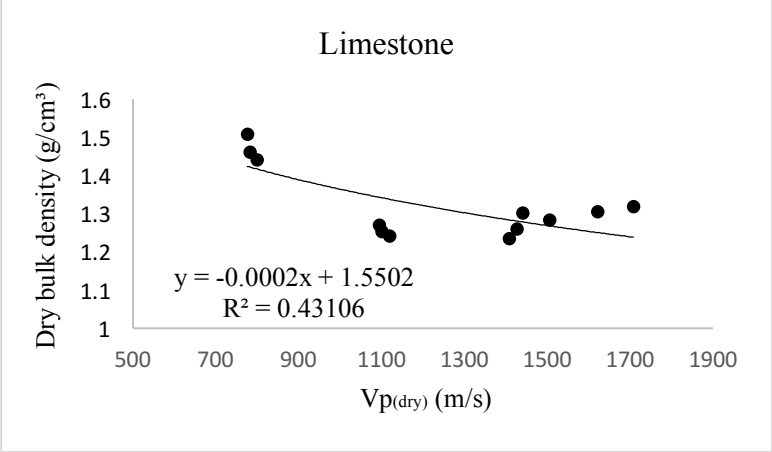

Figure 6.46 Graphical representation of dry Vp to dry bulk density for Limestone (aggregate)

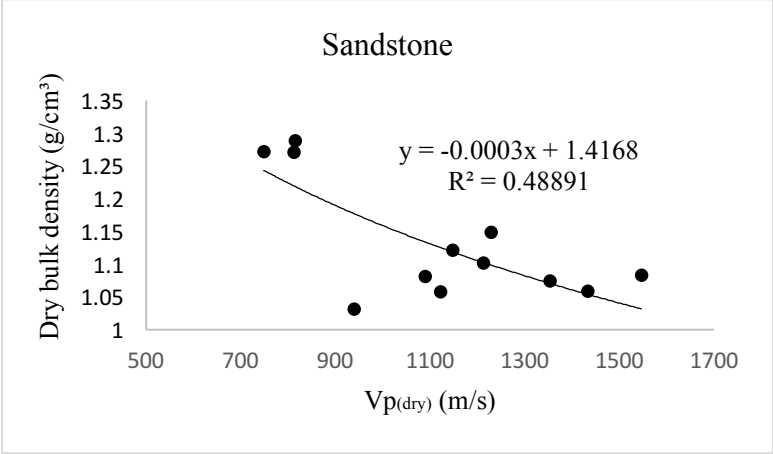

Figure 6.47 Graphical representation of dry Vp to dry bulk density for Sandstone (aggregate)

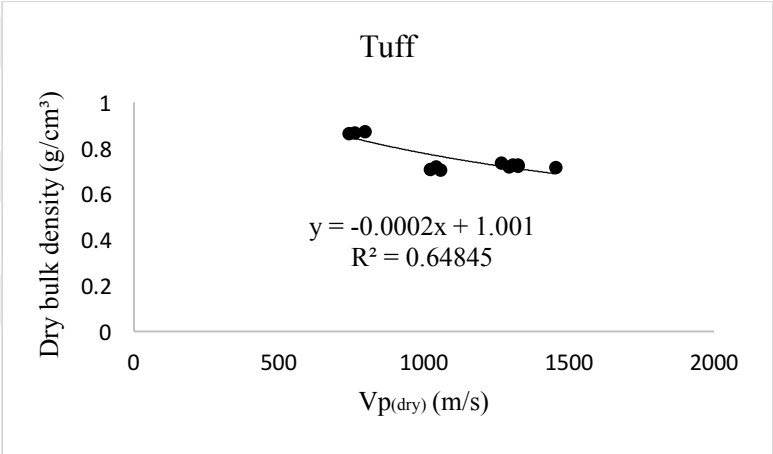

Figure 6.48 Graphical representation of dry Vp to dry bulk density for Tuff (aggregate)

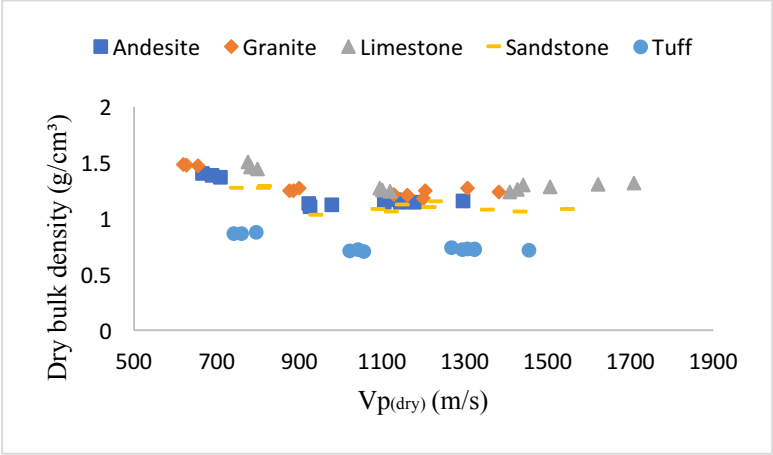

Figure 6.49 Graphical representation of dry Vp to dry bulk density for all granular samples

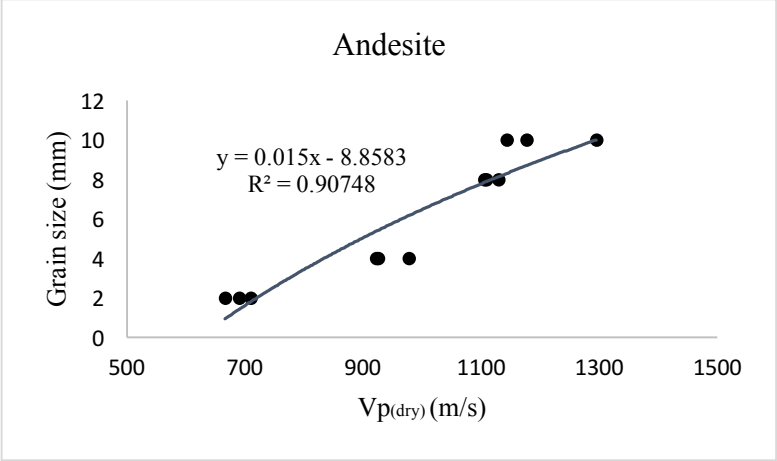

Figure 6.50 Graphical representation of dry Vp to grain size for Andesite (aggregate)

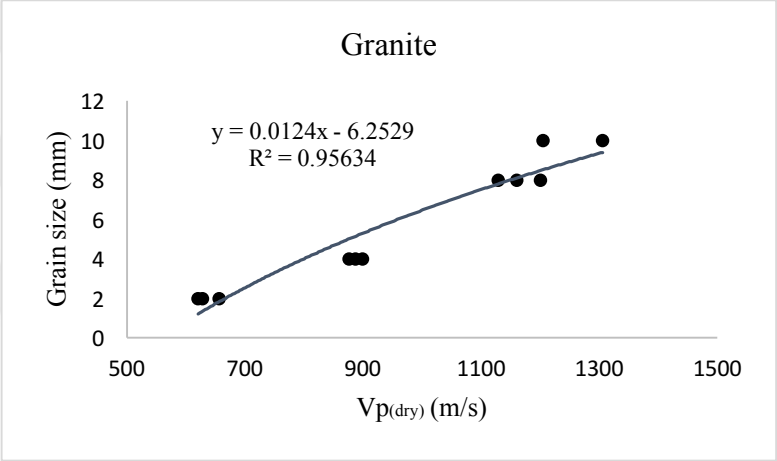

Figure 6.51 Graphical representation of dry Vp to grain size for Granite (aggregate)

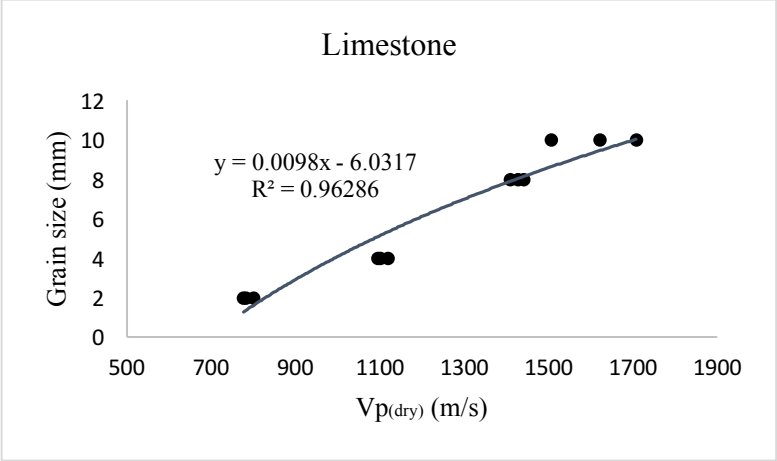

Figure 6.52 Graphical representation of dry Vp to grain size for Limestone (aggregate)

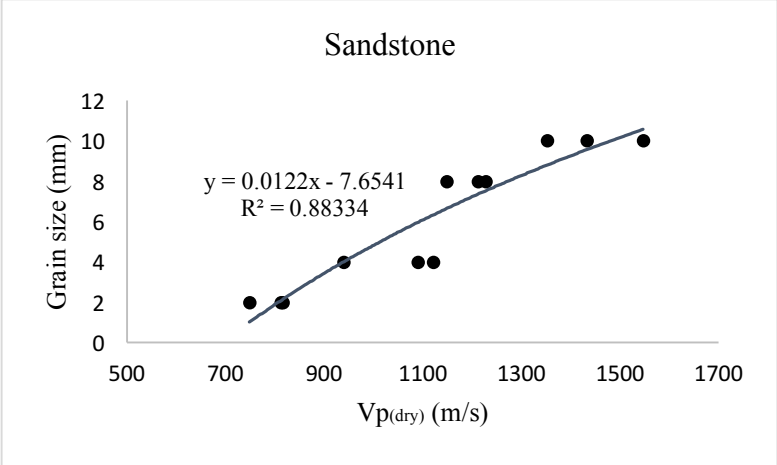

Figure 6.53 Graphical representation of dry Vp to grain size for Sandstone (aggregate)

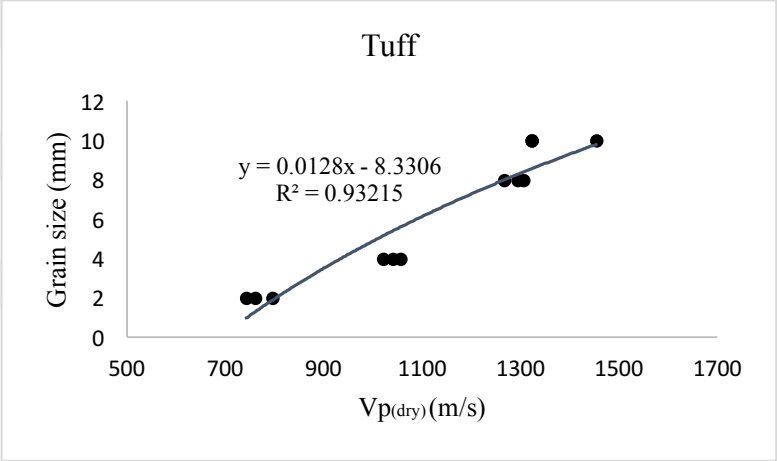

Figure 6.54 Graphical representation of dry Vp to grain size for Tuff (aggregate)

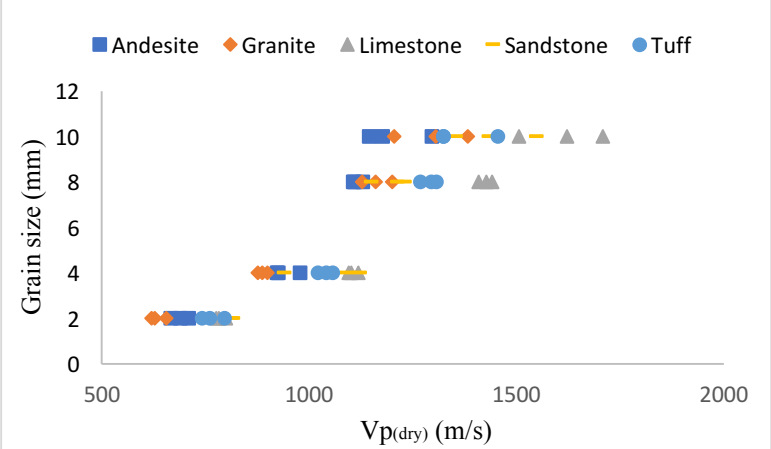

Figure 6.55 Graphical representation of dry Vp to grain size for all granular samples

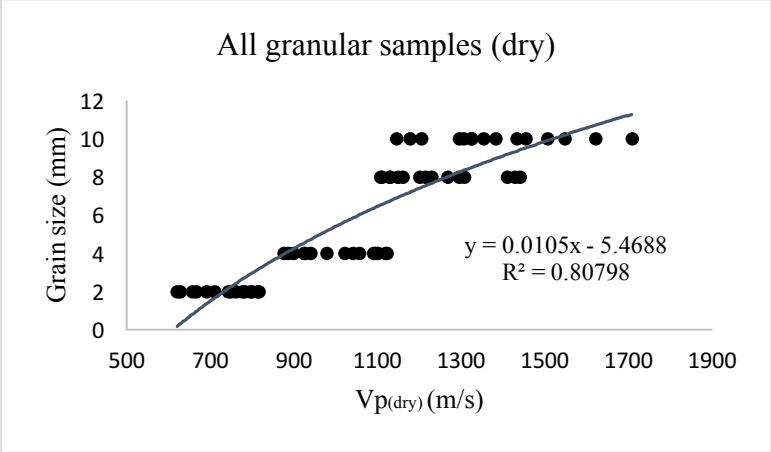

Figure 6.56 Graphical representation of dry Vp to grain size trend for all granular samples

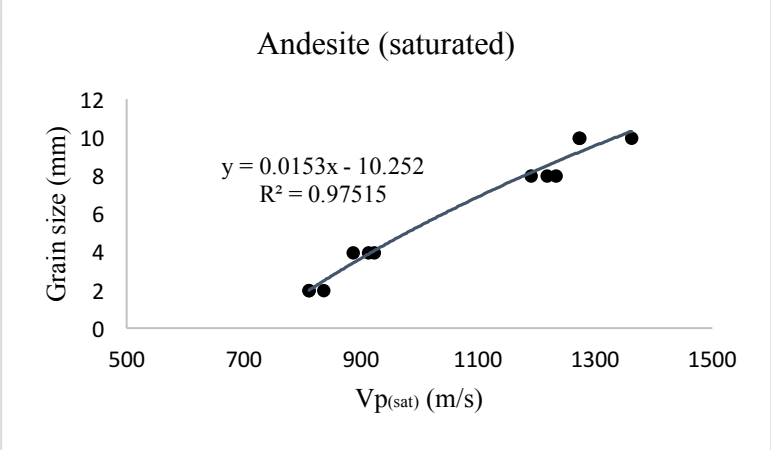

Figure 6.57 Graphical representation of saturated Vp to grain size for Andesite (saturated aggregate)

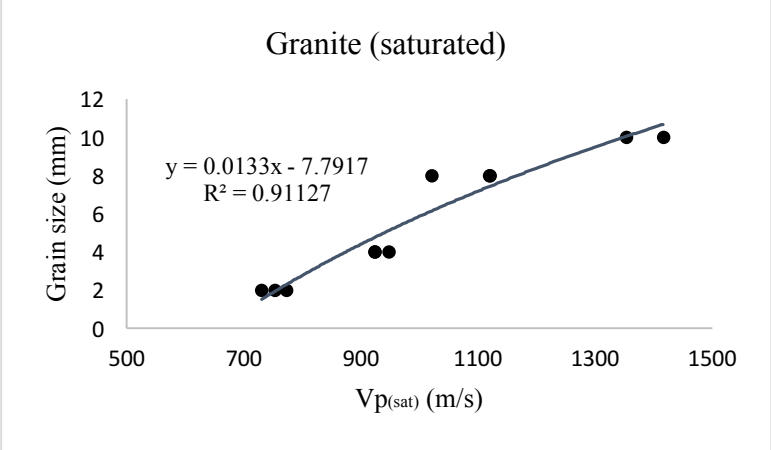

Figure 6.58 Graphical representation of saturated Vp to grain size for Granite (saturated aggregate)

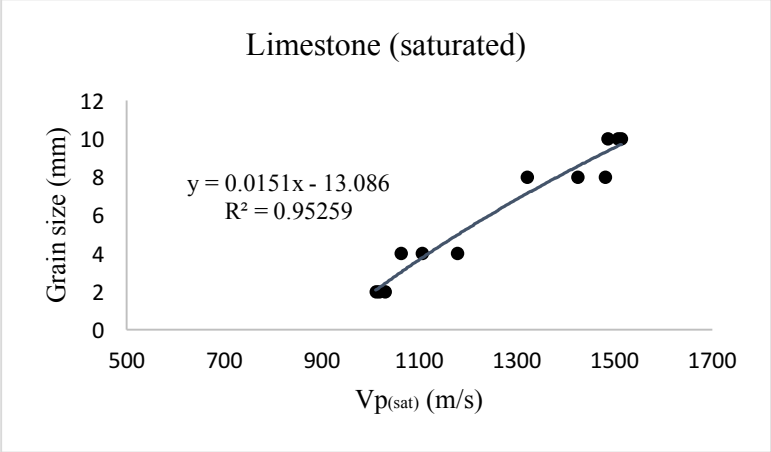

Figure 6.59 Graphical representation of saturated Vp to grain size for Limestone (saturated aggregate)

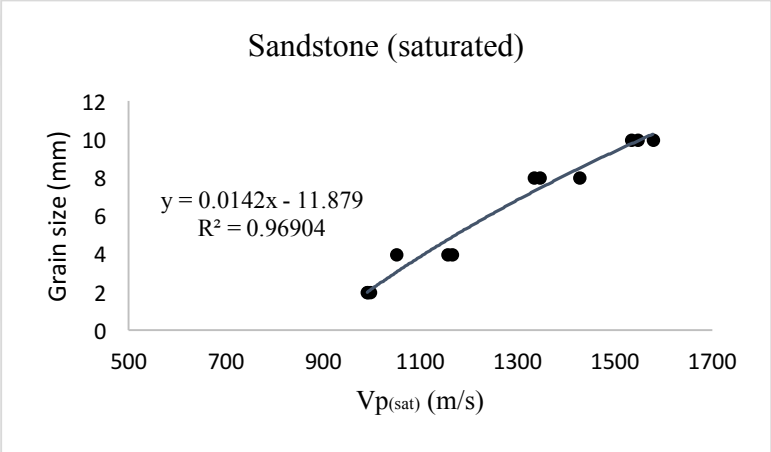

Figure 6.60 Graphical representation of saturated Vp to grain size for Sandstone (saturated aggregate)

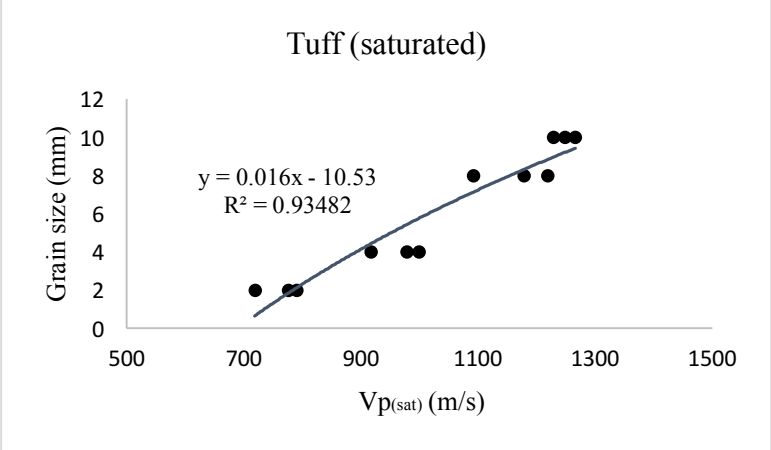

Figure 6.61 Graphical representation of saturated Vp to grain size for Tuff (saturated aggregate)

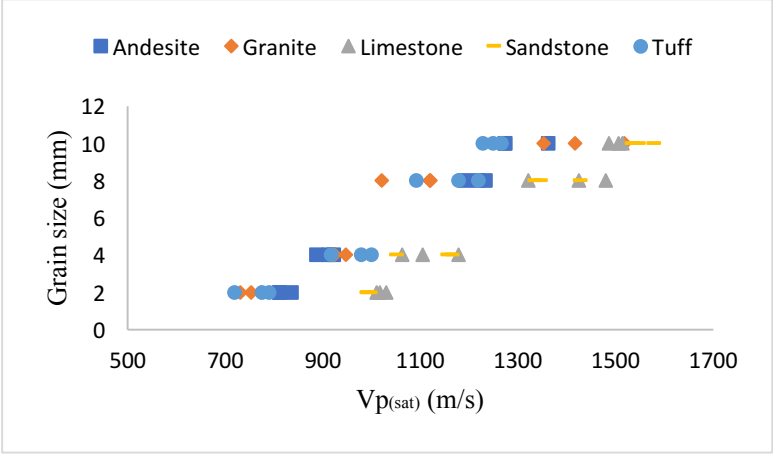

Figure 6.62 Graphical representation of saturated Vp to grain size for all saturated granular samples

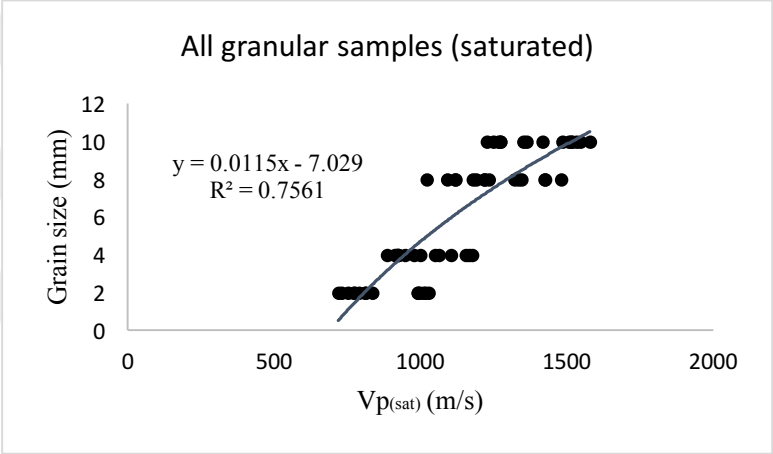

Figure 6.63 Graphical representation of saturated Vp to grain size trend for all saturated granular samples

6.4 Intergranular porosity

The porosity between the grains is known as intergranular porosity. To find the intergranular porosity between the grains first the total volume of the transparent plastic tube in which aggregate samples were placed and compressed was determined by the following formula,

$$V_T = \pi r^2 h \tag{6.8}$$

where,

"V_T" is the total volume of the transparent plastic tube
"r" is the radius of the transparent plastic tube
"h" is the length of the transparent plastic tube

The volume of the aggregate samples was found by the following equation.

$$V_{Agr} = \frac{W_{Agr}}{\gamma} \tag{6.9}$$

where,

"W_{Agr}" is the weight of aggregates
"γ" is the unit weight of intact rock
By using equation (6.8) and (6.9), intergranular porosity was determined.

$$n = \frac{V_T - V_{Agr}}{V_T} \tag{6.10}$$

Table 6.9 Intergranular porosity of dry aggregate samples

Lithology	Grain size (mm)	V_T (cm^3)	W_{Agr} (g)	γ_{dry} (g/cm^3)	V_{Agr} (cm^3)	n (%) (intergranular)	e (%)
Andesite	0-2	255.125	272.21	2.392	113.800	55.4	1.24
	2-4	255.125	220.09	2.392	92.011	63.9	1.77
	4-8	255.125	229.23	2.392	95.832	62.4	1.66
	8-10	255.125	225.65	2.392	94.335	63.0	1.70
				A.Mean	**98.995**	**61.2**	**1.59**
				STDEV	**9.995**	**3.9**	**0.24**
Granite	0-2	255.125	290.03	2.677	108.341	57.5	1.35
	2-4	255.125	246.55	2.677	92.099	63.9	1.77
	4-8	255.125	235.71	2.677	88.050	65.5	1.90
	8-10	255.125	245.7	2.677	91.782	64.0	1.78
				A.Mean	**95.068**	**62.7**	**1.7**
				STDEV	**9.038**	**3.6**	**0.24**
Limestone	0-2	255.125	288.42	2.746	105.033	58.8	1.43
	2-4	255.125	246.42	2.746	89.738	64.8	1.84
	4-8	255.125	248.43	2.746	90.470	64.5	1.82
	8-10	255.125	255.83	2.746	93.165	63.5	1.74
				A.Mean	**94.602**	**62.9**	**1.71**
				STDEV	**7.109**	**2.8**	**0.19**
Sandstone	0-2	255.125	250.68	2.304	108.802	57.4	1.35
	2-4	255.125	207.48	2.304	90.052	64.7	1.83
	4-8	255.125	220.64	2.304	95.764	62.5	1.67
	8-10	255.125	210.5	2.304	91.363	64.2	1.79
				A.Mean	**96.495**	**62.2**	**1.66**
				STDEV	**8.560**	**3.3**	**0.22**
Tuff	0-2	255.125	170.35	2.74	115.648	54.7	1.21
	2-4	255.125	139.52	2.74	94.718	62.9	1.70
	4-8	255.125	142.91	2.74	97.020	62.0	1.63
	8-10	255.125	141.74	2.74	96.225	62.3	1.65
				A.Mean	**100.903**	**60.5**	**1.55**
				STDEV	**9.876**	**3.9**	**0.23**

Table 6.10 Intergranular porosity of Saturated aggregate samples

Lithology	Grain size (mm)	V_T (cm^3)	W_{Agr} (g)	γ_{sat} (g/cm^3)	V_{Agr} (cm^3)	n (%) (intergranular)	e (%)
Andesite	0-2	255.125	237.43	2.436	97.467	61.8	1.62
	2-4	255.125	224.47	2.436	92.147	63.9	1.77
	4-8	255.125	240.56	2.436	98.751	61.3	1.58
	8-10	255.125	237.76	2.436	97.604	61.7	1.61
				A.Mean	**96.492**	**62.2**	**1.65**
				STDEV	**2.953**	**1.2**	**0.08**
Granite	0-2	255.125	241.24	2.687	89.799	64.8	1.84
	2-4	255.125	235.20	2.687	87.534	65.7	1.92
	4-8	255.125	247.47	2.687	92.098	63.9	1.77
	8-10	255.125	258.5	2.687	96.204	62.3	1.65
				A.Mean	**91.409**	**64.2**	**1.79**
				STDEV	**3.700**	**1.5**	**0.11**
Limestone	0-2	255.125	259.10	2.749	94.251	63.1	1.71
	2-4	255.125	243.88	2.749	88.716	65.2	1.87
	4-8	255.125	264.07	2.749	96.060	62.3	1.65
	8-10	255.125	263.46	2.749	95.840	62.4	1.66
				A.Mean	**93.711**	**63.3**	**1.72**
				STDEV	**3.430**	**1.3**	**0.10**
Sandstone	0-2	255.125	239.98	2.409	99.617	61.0	1.56
	2-4	255.125	220.49	2.409	91.526	64.1	1.79
	4-8	255.125	230.87	2.409	95.835	62.4	1.66
	8-10	255.125	230.17	2.409	95.546	62.5	1.67
				A.Mean	**95.631**	**62.5**	**1.67**
				STDEV	**3.306**	**1.3**	**0.09**
Tuff	0-2	255.125	192.62	1.719	112.054	56.1	1.28
	2-4	255.125	161.3	1.719	93.834	63.2	1.72
	4-8	255.125	177.42	1.719	103.209	59.5	1.47
	8-10	255.125	174.34	1.719	101.419	60.2	1.51
				A.Mean	**102.629**	**59.8**	**1.49**
				STDEV	**7.483**	**2.9**	**0.18**

CHAPTER SEVEN
DISCUSSION AND CONCLUSION

This study was carried out to observe compressional wave velocities (Vp) of different rock cores and cubes but most importantly in granular materials produced from these rocks both in dry and saturated condition. In addition, bulk density, porosity were also determined for all the samples. Four different grain sized aggregates (ranging from 0-10 mm) of Andesite, Granite, Limestone, Sandstone and Tuff were used in tests. Pundit Lab^{+} ultrasonic instrument was used to determine the Vp. First the length of specimen was measured and then arrival time was recorded by the Pundit Lab^{+}. Two probes, one act as a transducer and other as a receiver, used to pass the P-waves through the sample. Based on the observations, results and experience gained from the laboratory work during study, this chapter summarizes the main findings.

In this thesis, initially the P-wave velocity measuring technique has been described and relevant literature reviewed. In laboratory, different test arrangements were examined and a suitable testing method was developed to meet the aim of measuring P-wave velocity in granular media. A testing method was established using cylindrical transparent plastic tube with a diameter of 52 mm and a length of 130 mm to measure both dry and saturated granular samples. From a laboratory point of view the selected size of the cylindrical transparent plastic tube was sufficiently large to enable granular samples of a suitable quality to be made, i.e. placed and compacted well and uniformly. In terms of mixing and compacting the granular samples, it was practically acceptable, but there were limitations from the ultrasonic experimentation point of view. The system and equipment reliability performance were checked, prior to the granular samples being tested.

At least five core and cube samples of five same lithologies as well as their granular materials were used to determine their compressional (P) wave velocity. The diameter of all the core samples was 50 mm and the diameter of cube sample was 70 mm. P-wave velocity of both dry and water saturated samples was measured.

Table 7.1 Mean results of different tests performed in the thesis

Intact Rock Samples								Aggregate Samples						
Lithology	**γ_{dry} (g/cm^3)**	**γ_{sat} (g/cm^3)**	**n (%)**	**e (%)**	**$V_{p(dry)}$ (m/sec)**	**$V_{p(sat)}$ (m/sec)**	**V_m (m/sec)**	**Grain size (mm)**	**$\rho_{bulk(dry)}$ (g/cm³)**	**$\rho_{bulk(sat)}$ (g/cm³)**	**n (%)**	**e (%)**	**$V_{p(dry)}$ (m/sec)**	**$V_{p(sat)}$ (m/sec)**
Andesite	2.435	2.462	2.636	2.708	3842.21	3852.06	3715.61	0-2	1.387	1.210	-	-	688.537	819.142
								2-4	1.121	1.144	-	-	942.067	907.031
								4-8	1.168	1.226	2.593	2.662	1114.825	1213.325
								8-10	1.15	1.212	2.558	2.625	1205.403	1302.283
Granite	2.677	2.687	1.001	1.011	3782.76	4309.57	4255.58	0-2	1.478	1.229	-	-	634.555	751.953
								2-4	1.256	1.199	-	-	886.999	931.385
								4-8	1.201	1.261	1.095	1.107	1162.834	1086.319
								8-10	1.252	1.317	1.040	1.051	1297.343	1428.642
Limestone	2.746	2.749	0.350	0.352	4912.53	5019.81	4992.05	0-2	1.47	1.320	-	-	785.889	1018.827
								2-4	1.256	1.243	-	-	1104.775	1114.821
								4-8	1.266	1.346	0.297	0.298	1425.557	1407.983
								8-10	1.304	1.343	0.282	0.283	1611.328	1501.496
Sandstone	2.304	2.409	10.503	11.749	3163.81	3208.29	3174.43	0-2	1.277	1.223	-	-	792.343	992.540
								2-4	1.057	1.123	-	-	1050.313	1123.735
								4-8	1.124	1.176	9.436	10.42	1196.537	1368.607
								8-10	1.072	1.173	9.223	10.16	1444.382	1552.706
Tuff	1.473	1.719	24.640	32.834	2026.69	1567.93	1593.05	0-2	0.868	0.981	-	-	766.286	761.381
								2-4	0.711	0.822	-	-	1039.478	964.604
								4-8	0.728	0.904	24.92	33.19	1289.293	1162.422
								8-10	0.722	0.889	24.18	31.89	1366.970	1247.159

Ultrasonic tests performed in the lab showed a consistency with cores and cube samples in regards to an overall decrease in P-wave velocity with an increase in porosity while on the other hand the increase in dry unit weight and saturated unit weight of core and cube samples increased the P-wave velocity in those same samples.

Experiments done on cube samples in the laboratory showed that the cube samples with more compressive and bending strength had more P-wave velocity value. Abrasion resistance experiments performed on cube rock samples showed that the P-wave velocity has inverse relation with abrasion.

It was observed that without any pressure, the ultrasonic lab instrument was not recording the travel time in granular samples. For all granular samples, 100 kgf of force was taken as a standard and when this force was applied to the aggregates, the P-wave velocities were calculated. The behavior of compressional (P) waves was studied in granular media under different scenarios like dry granular material and saturated granular material. These experiments demonstrated that compressional (P) waves were sensitive to the presence of water. Compressional wave velocities (Vp) in dry samples were lower as compared to saturated samples but not all the times (Table 7.1).

Increase in bulk density was observed when going from dry to saturated granular samples. Compaction was one of the most important characteristic to determine the P-wave velocity (Vp) in granular material. Lab experiments showed that the P-wave velocity (Vp) increased with the increase in grain size both in dry and saturated samples (Figure 7.1).

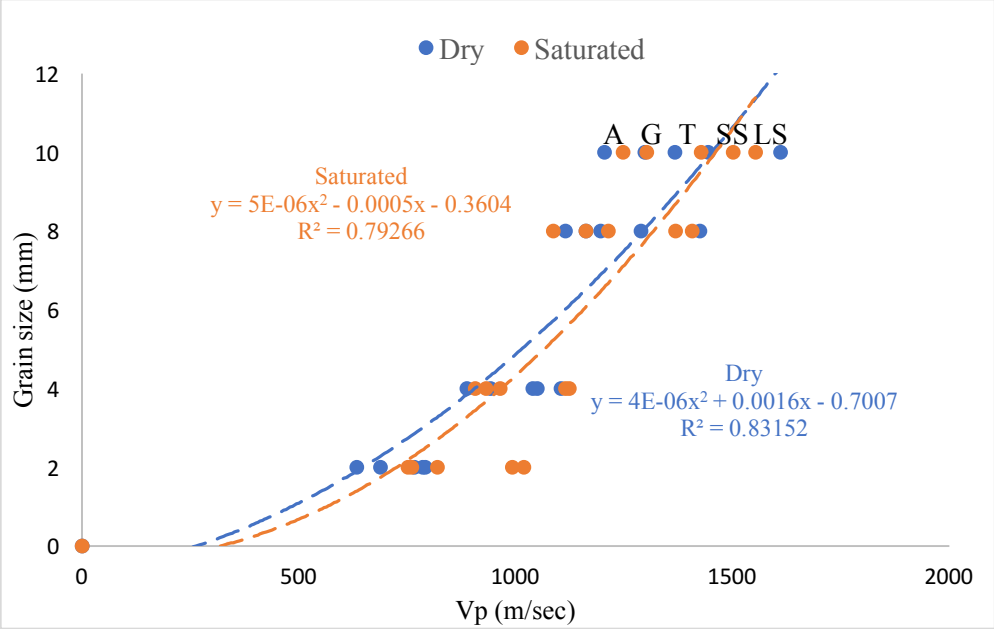

Figure 7.1 Graphical representation of dry and saturated Vp to grain size for all granular samples (mean values taken from Table 7.1)

7.1 Recommendations for Future Research

It would be beneficial to conduct shear wave (S) velocity tests to validate the seismic surface wave results. This was also an intention of this research, but due to repeated equipment malfunctions, only P-wave velocity tests were performed and the project's objectives achieved without S-wave velocity measurement.

Note: Some graphs showed very low R^2 value due to scattered data taken from different tests performed during this study. Further research would be useful to overcome the limitations faced during the research work.

REFERENCES

Akal, C., & Helvaci, C. (1999). Mafic Microgranular Enclaves in the Kozak Granodiorite, Western Anatolia. *Turkish Journal of Earth Sciences, 8,* 1–17.

Altunkaynak, S., & Yılmaz, Y. (1998). The Mount Kozak magmatic complex, Western Anatolia. *Journal of Volcanology and Geothermal Research, 85,* 211–231.

Ben-Dor, G., Britan, A., Elperin, T., Igra, O., & Jiang, J. (1997). Experimental investigation of the interaction between weak shock waves and granular layers. *Experiments in Fluids 22,* 432–443.

Bonner, B. P., Berge, P. A., Aracne-Ruddle, C. M., Bertete-Aguirre, H., Wildenschild, D., Trombino, C.N., et al. (2002). Linear and Nonlinear Ultrasonic Properties of Granular Soils. *Materials Research Society Meeting San Francisco, CA. UCRL-JC-136207,* 1–8.

Bowman, E. T., Soga, K., & Drummond, T. W. (2001). Particle shape characterization using Fourier descriptor analysis. *Geotechnique, 51* (6), 545–554.

Duffy, J., & Mindlin, R. (1957). Stress-strain relations and vibrations of a granular medium. *ASME Journal of Applied Mechanics, 24,* 585–593.

Erdoğan, B. (1990). İzmir – Ankara Zonu ile Karaburun Kuşağının Tektonik İlişkisi, *MTA Dergisi, 110,* 1–15.

Fountain, D. M. (1980). Influence of porosity and water saturation on the compressional-wave velocities of basalts from the North Philippine Sea. *Department of Geology, University of Montana, Missoula, Montana,* 935–940.

Goddard, J. (1990). Nonlinear elasticity and pressure-dependent wave speeds in granular media. *Proceedings of the Royal Society of London, 430,* 105–131.

Griffiths, S., Rescaglio, A., & Mel, F. (2010). Ultrasound propagation in wet and airless non-tylerconsolidated granular materials. *Ultrasonics, 50,* 139–144.

Hamada, G. M. (2004). Reservoir Fluids Identification Using Vp/Vs Ratio. *Oil & Gas Science and Technology, 59* (6), 649–654.

Han, D. H., Nur, A., & Morgani, D. (1986). Effects of porosity and clay content on wave velocities in sandstones. *Geophysics, 51* (11), 2093–2107.

Hardin, B., & Richart, F. (1963). Elastic wave velocities in granular soils. *ASCE Journal of the Soil Mechanics and Foundations Division, 89,* 33–65.

Hawkins, A. E. (1993). The Shape of Powder-Particle Outlines. *Wiley, New York.*

Jia, X., Caroli, C., & Velicky, B. (1999). Ultrasound propagation in externally stressed granular media. *Physical Review Letters, 82* (9), 1863–1866.

Kahraman, S. (2007). The correlations between the saturated and dry P-wave velocity of rocks. *Ultrasonics, 46,* 341–348.

Knuth, M., Harold, J., & Marone, C. (2013). Evolution of ultrasonic velocity and dynamic elastic moduli with shear strain in granular layers. *Granular Matter,* 1–17.

Liu, C., & Nagel, S. R. (1993). Sound in a granular material: Disorder and nonlinearity. *Physical Review B, 48* (21), 646–650.

Mahdevari, S., & Maarefvand, P. (2017). Applying ultrasonic waves to evaluate the volumetric block proportion of bimrocks. *Arabian Journal Geosciences, 10* (204), 1–12.

Makse, H. A., Gland, N., Johnson, D., & Schwartz, L. (1999). Why effective medium theory fails in granular materials. *Physical Review Letters, 83* (24), 5070–5073.

Mandal, T., Tinjum, J., & Edil, T. (2014). Non-destructive testing of cementitiously stabilized materials using ultrasonic pulse velocity test. *TRB 2014 Annual Meeting,* 1–20.

Marwah, I. A. I. (2017). *On the Relationship between Compressional Wave Velocity of Saturated Porous Rocks and Density: Theory and Application (Thesis).* Department of Earth, Atmospheric, and Planetary Sciences in partial fulfillment of the requirements for the degree of Master of Science in Earth and Planetary Sciences, 1–98.

Powers, M. C. (1953). A new roundness scale for sedimentary particles. *Journal of Sedimentary Petrology, 23* (2), 117–119.

Santamarina, J. C., Klein, K. A., & Fam, M. A. (2001). *Soils and waves - Particulate materials behavior, characterization and process monitoring, Wiley, Chichester, England.*

Sikora, J., & Turkiewicz, J. (2010). Sound absorption coefficients of granular materials. *Mechanics and Control 29* (3), 149–157.

Sun, Z., Stephen, R. S., & Brown, R. J. (1991). Borehole velocity-prediction models and estimation of fluid saturation effects. *Journal of Canadian Petroleum Technology, 43* (10), 274–290.

Terlemez, İ., & Yılmaz, A. (1980). Ünye - Ordu - Koyulhisar - Reşadiye Arasında Kalan Yörenin Stratigrafisi (Stratigraphy of the area between Ünye—Ordu—Koyulhisar—Reşadiye). *Bulletin of the Geological Society of Turkey, V. 23,* 179–191.

TS EN 1097-3, (TSE 1999). Tests for mechanical and physical properties of aggregates- Part 3: *Determination of loose bulk density and voids.*

TS EN 14157, (TSE 2005). Natural stones - *Determination of abrasion resistance.*

TS EN 1926, TSE (2013). Natural stone test methods - *Determination of uniaxial compressive strength.*

TS EN 12372, (TSE 2013). Natural stone test methods - *Determination of flexural strength under concentrated load*.

TS EN 1097-6, (TSE 2013). Tests for mechanical and physical properties of aggregates - Part 6: *Determination of particle density and water absorption*.

Tyler, T. J., Hill, R., & Lai. E. (2004). Friction generated ultrasound from geotechnical materials. *Ultrasonics, 42*, 169–172.

Vallejo, L. E. (1995). Fractal analysis of granular materials. *Geotechnique, 45* (l), 159-163.

Verwer, K., & Braaksma, H. (2009). Data report: petrophysical properties of "young" carbonate rocks (Tahiti Reef Tract, French Polynesia). *Camoin, G.F., Iryu, VP., McInroy, D.B., and the Expedition 310 Scientists Proceedings of the Integrated Ocean Drilling Program, 310,* 1–23.

Wang, Z., Wang, R., Weger, R. J., Li, T., & Wang, F. (2015). Pore-scale modeling of elastic wave propagation in carbonate rocks. *Geophysics, 80* (1), 51-63.

Wyllie, M. R. J., Gregory, A. R., & Gardner, G. H. F. (1956). Elastic wave velocities in heterogeneous porous media. *Geophysics, 21* (1), 41–70.

Wyllie, M. R. J., Gregory, A. R., & Gardner, G. H. F. (1958). An experimental investigation of factors affecting elastic wave velocities in porous media. *Geophysics, 23* (3), 459–493.

Wyllie, M. R. J. (1960). Log interpretation in sandstone reservoirs. *Geophysics, 25* (4), 748–778.

Yavuz, A. B. (2012). Durability assessment of the Alaçatı tuff (İzmir) in western Turkey. *Environmental Earth Sciences, 67,* 1909–1925.

APPENDICES

A = Andesite

G = Granite

LS = Limestone

SS = Sandstone

T = Tuff

Ar = Cross-sectional area of pre-test sample

A.Mean = Arithmetic Mean

b = Width adjacent to the fracture plane of the sample

e = Void ratio

F = Fracture load/Force

H = The thickness of the sample adjacent to the plane of fracture

h = Total length of the sample

l = Distance between support rollers

M1 = mass of air saturated and surface dried aggregate, in grams.

M2 = apparent mass of the basket containing the saturated aggregate sample in grams.

M3 = apparent mass in grams of empty basket in grams.

M4 = gram of air-dried test piece in the air.

me = Mass of ground and dried sample

md = Mass of dry sample

mh = Mass of sample immersed in water

ms = Mass of the saturated sample

Δm = (mi-m1) mass loss after 16 cycles (gr) to the nearest 0.1 gr

n = Porosity

pb = Apparent density of the sample

r = radius of the transparent plastic tube

STDEV = Standard deviation

T = Temperature

t_{dry} = Wave travel time in dry sample

t_{sat} = Wave travel time in water saturated sample

V = Volume of intact rock sample

V_w = P-wave velocity in water

V_{Agr} = Volume of the aggregate

V_T = Total volume of the transparent plastic tube

Vp = Compressional wave velocity

$V_{p\ (dry)}$ = Compressional wave velocity in dry sample

$V_{p\ (sat)}$ = Compressional wave velocity in water saturated sample

ΔV = volume loss after 16 cycles (mm^3) to the nearest mm^3

WA_{24} = Water absorption

W_{Agr} = Weight of aggregates

σ_c = Uniaxial compressive strength of tested sample

σ_b = Bending strength under heavy load

ρ_a = Apparent particle density

ρ_{rd} = Oven-dried particle density

ρ_{ssd} = Saturated and surface-dried particle density

$\rho_{bulk\ (loose)}$ = Loose bulk density

$\rho_{bulk\ (sat)}$ = Saturated bulk density

$\rho_{bulk\ (dry)}$ = Dry bulk density

γ = Unit weight

γ_{dry} = Dry unit weight

γ_{sat} = Saturated unit weight